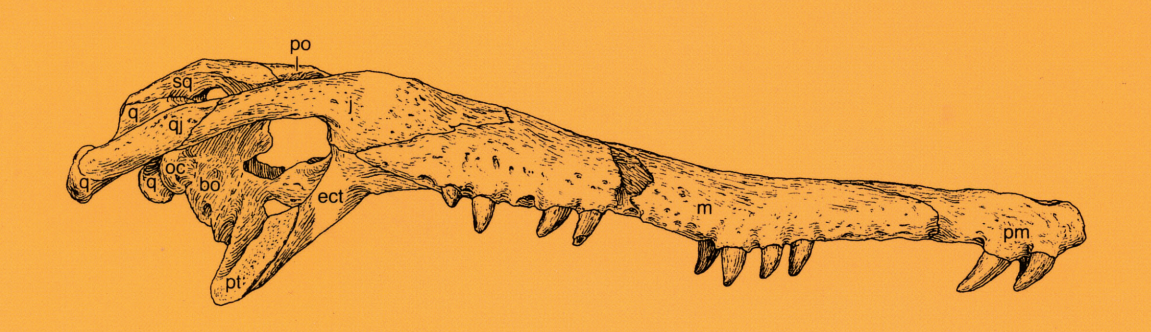
ANATOMY OF A JAPANESE TOMISTOMINE CROCODYLIAN, TOYOTAMAPHIMEIA MACHIKANENSIS (KAMEI ET MATSUMOTO, 1965), FROM THE MIDDLE PLEISTOCENE OF OSAKA PREFECTURE: THE REASSESSMENT OF ITS PHYLOGENETIC STATUS WITHIN CROCODYLIA

Yoshitsugu Kobayashi
Yukimitsu Tomida
Tadao Kamei
and Taro Eguchi



National Science Museum, Tokyo March, 2006

NATIONAL SCIENCE MUSEUM MONOGRAPHS

NO. 35



Frontispiece: Reconstruction of preserved skeletal elements of *Toyotamaphimeia machikanensis* holotype. Hindlimb and pes elements are originally preserved on the right side, although they are drawn on the left.

ANATOMY OF A JAPANESE TOMISTOMINE CROCODYLIAN, TOYOTAMAPHIMEIA MACHIKANENSIS (KAMEI ET MATSUMOTO, 1965), FROM THE MIDDLE PLEISTOCENE OF OSAKA PREFECTURE: THE REASSESSMENT OF ITS PHYLOGENETIC STATUS WITHIN CROCODYLIA

Yoshitsugu Kobayashi¹⁾
Yukimitsu Tomida²⁾
Tadao Kamei³⁾
and Taro Eguchi⁴⁾

¹⁾Hokkaido University Museum, Hokkaido University, Sapporo, Hokkaido 060-0810, Japan

²⁾Department of Geology and Paleontology, National Science Museum, Shinjuku-ku, Tokyo 169-0073, Japan

> ³⁾Professor Emeritus, Department of Geology and Mineralogy, Kyoto University, Kyoto 606-8502, Japan

> > ⁴⁾Museum of Osaka University, Osaka University, Toyonaka, Osaka 560-0043, Japan

National Science Museum, Tokyo
March, 2006

Editorial Board

Satoshi Matsubara, Department of Geology and Paleontology, Editor in Chief Naoki Kohno, Department of Geology and Paleontology

Masatsune Takeda, Department of Zoology

Hiroshi Saito, Department of Zoology

Masahiro Katou, Department of Botany

Taiju Kitayama, Department of Botany

Hisao Baba, Department of Anthropology

Yuji Mizoguchi, Department of Anthropology

Katsuhiro Sasaki, Department of Science & Engineering

Fumitaka Wakabayashi, Department of Science & Engineering

National Science Museum Ueno Park, Tokyo 110-8718 Japan

Copyright ©2006 National Science Museum, Tokyo Published on March 30, 2006 Printed by Gakujutsu-tosho Co., Ltd., Tokyo ISSN 1342-9574 ISBN 4-87803-020-8

Cover illustration: Skull of Toyotamaphimeia machikanensis in right lateral view (see Figure 9 for further information).

CONTENTS

Abstract	.vii
INTRODUCTION	1
GEOLOGY	
SYSTEMATIC PALEONTOLOGY	
DESCRIPTION	
Skull	
Mandible	
Dentition	
Axial Skeleton	
Pectoral Girdle	
Forelimb	
Pelvic Girdle	
Hindlimb	
Osteoderms	
DISCUSSION	
Phylogenetic Analyses	
Comments on "Toyotamaphimeia machikanensis", Another Tomistomine from	
the Osaka Group, from Kishiwada City of Osaka Prefecture	102
ACKNOWLEDGMENTS	
REFERENCES CITED	
APPENDICES	
Appendix 1. Character Descriptions Used for the Phylogenetic Analyses in This Study	
Appendix 2. Data Matrix Used for the Phylogenetic Analysis in This Study.	

Abstract

The holotype of *Toyotamaphimeia machikanensis*, discovered from the Middle Pleistocene sediments of the Osaka Group in Osaka Prefecture of Japan, is redescribed in details in this study. Phylogenetic analysis is conducted with 165 characters for 48 taxa (two outgroups). The analysis produces 323 most parsimonious trees of 420 steps. The strict consensus tree suggests that *Toyotamaphimeia* is deeply nested within the clade Tomistominae and is a sister taxon to the only extant tomistomine crocodylian, *Tomistoma schlegelii*. The topology of the phylogenetic trees implies that tomistomines originated in Europe as previously suggested and the clade of *Toyotamaphimeia machikanensis* plus *Tomistoma schlegelii* dispersed into eastern Asia by or prior to 400 thoudsand years ago.

Diagnoses of *Toyotamaphimeia machikanensis* are also revised. Although previous studies stated that maxillary tooth 7 was the largest in *Toyotamaphimeia*, maxillary teeth twelfth and thirteenth maxillary teeth are actually larger than the seventh. Maxillary teeth posterior to the seventh are more closely placed than anterior ones. Maxillary teeth eighth to twelfth are placed lateral to the dentary teeth in occlusion, whereas maxillary teeth thirteenth to sixteenth meet with corresponding dentary teeth, suggesting that posterior teeth of the maxilla and dentary may have been used for crushing. A tomistomine crocodylian from the Kishiwada Town, previously referred to *Toyotamaphimeia machikanensis*, is not comparable with the holotype of *Toyotamaphimeia* and considered here as a different taxon, possibly more primitive than *Toyotamaphimeia machikanensis*.

要約

中期更新統の大阪層群から発見されたマチカネワニ(Toyotamaphimeia machikanensis)の模式標本について、本論文で詳細な再記載を行った。系統解析は、48分類群(2外群)の165形質を使って行った。その結果、420ステップで323個の最節約樹が得られた。厳密合意樹は、マチカネワニが明らかにマレーガビアル亜科(Tomistominae)に含まれることと、同亜科の唯一の現生種(マレーガビアル Tomistoma schlegelii)の姉妹群であることを示している。さらに、系統樹の樹形は、マレーガビアル亜科がヨーロッパで起源したあとマチカネワニとマレーガビアルの分岐群が40万年前までに東アジアに拡散してきたことを支持し、これまでの研究と整合性を持つ。

マチカネワニの定義についても改定した。従来は上顎の最大の歯は7番目と言われていたが、実際には12、13番目の方が7番目より大きい。上顎の7番より後方の歯はそれより前方の歯に比べてより密に並ぶ。上顎の8番から12番の歯は、かみ合ったときに下顎の歯の外側に位置するが、13番から16番の歯は対応する下顎歯と噛みあうことから、後方の歯は破砕の用途に使われたと考えられる。岸和田市から発見された類似のマレーガビアル亜科のワニ化石は、以前にはマチカネワニと考えられていたが、マチカネワニとは異なる分類群で、より原始的な種の可能性がある。

INTRODUCTION

In 1964, a nearly complete skeleton of a crocodylian was discovered from the Middle Pleistocene deposits of the Kasuri Tuff (approximately 0.4 Ma) of the Osaka Group at the campus of the Osaka University in Machikane-yama, Toyonaka City, Osaka Prefecture, Japan (Figs. 1, 2) (Kobatake et al., 1965). Although this skeleton is missing most caudal vertebrae and portions of lower jaws and limb elements, it was the most complete crocodylian skeleton from Japan then and is now still one of the best crocodylian specimens from this country (Fig. 3). This crocodylian was described and named as a new species of an extant genus, "Tomistoma machikanense" (Kobatake et al., 1965; Kobatake and Kamei, 1966). Eighteen years after the original description, Aoki (1983) redescribed the skull of this crocodylian and erected a new genus for it, Toyotamaphimeia machikanensis. The most recent study focused on the paleopathology of Toyotamaphimeia machikanensis and discussed the implications to the behavior of this animal (Katsura, 2004).

The studies by Kobatake et al. (1965) and Kobatake and Kamei (1966) emphasized the elongated and narrow skull, and the taxonomic assessment of "Tomistoma machikanense" as a new taxon was based on comparisons with modern crocodylians (especially Tomistoma schlegelii and Crocodylus cataphractus) and some fossil species of Tomistoma. The similarities of "Tomistoma machikanense" and Tomistoma schlegelii, proposed in these studies are the exclusion of the nasal from the external narial opening, the alignment of the premaxilla-premaxilla suture matched to the sagittal plane, the "W"-shaped suture of the premaxilla and maxilla in dorsal view, the upper dental formula (five premaxillary and 16 maxillary teeth), and the possible length of the symphesis (extending to the level of the fourteenth or fifteenth dentary tooth). They distinguished "Tomistoma machikanense" from other fossil species of Tomistoma in having different shapes of the orbits, supratemporal fenestrae, and suborbital fenestrae. However, the diagnosis of "Tomistoma machikanense" was not specified in these papers.

In 1983, Aoki redescribed "Tomistoma machikanense" with emphasis on skull features and argued that the features (associated with the elongation of the snout) on which Kobatake et al. (1965) considered "Tomistoma machikanense" as a member of Tomistoma are most likely convergent features seen in other longirostral crocodylians. Therefore, he argued that "Tomistoma machikanense" could not be referred to Tomistoma and, instead, represents a different genus, Toyotamaphimeia machinensis, which was diagnosed by a new set of characters: leptolongirostral crocodylid; premaxillae contacting nasal, nasals failing to reach external nares; mandibular symphysis long, extending to level of diastema between the thirteenth and fourteenth dentary teeth (anterior two-thirds of the symphysis missing); dental formula (pm-5 + m-16)/(d-10 +); seventh maxillary tooth large, snout constricted posteriorly at diastema between the ninth and tenth maxillary teeth; perforation or emargination for first mandibular tooth absent in anterior plate of premaxilla; orbitae subcircular; supratemporal fenestrae large, subequal to

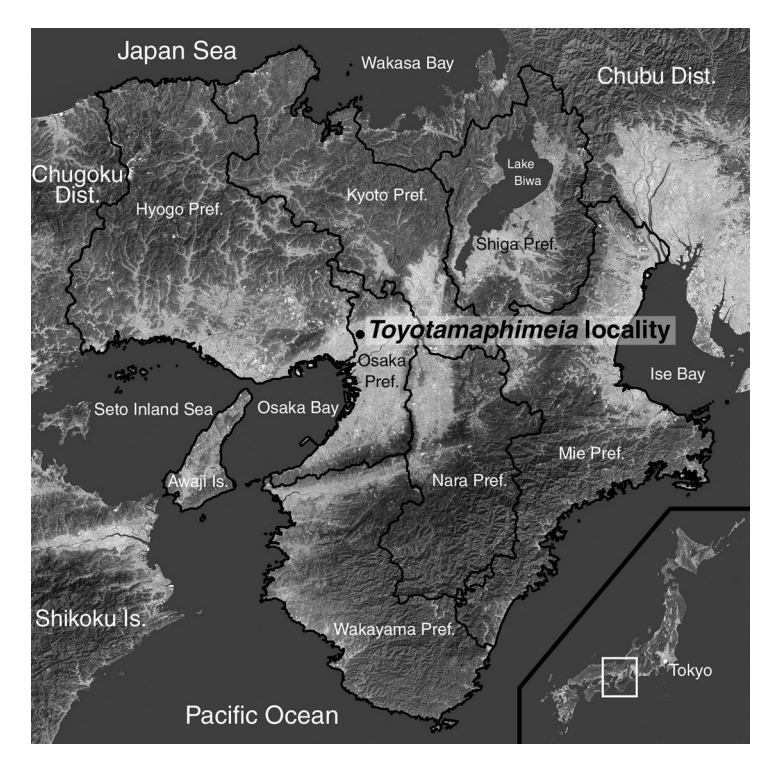


Fig. 1. Locality map of *Toyotamaphimeia machikanensis*, Machikane-yama, Toyonaka City, Osaka Prefecure, Kinki District.

the orbits in size; basioccipital tubera little developed; choana key-hole (as in key-hole neck-line) shaped, postchoanal ridge absent; axis of jaw articulation inclined posteromedially and ventromedially; and distortion of retroarticular process ventromedially.

Aoki (1983) stated the largest maxillary tooth 7 as a unique character of *Toyotamaphimeia machikanensis*. He also emphasized the shape of the retroarticular process (ventromedial distortion) as a similar condition seen in "derived crocodylians" such as *Crocodylus porosus* but unlike longirostrine crocodylians (e.g., *Tomistoma schlegelii. Crocodylus cataphractus*, and *Gavialis gangeticus*), indicating poor affinities between *Toyotamaphimeia machikanensis* and longirostrine crocodylians. Despite of the similarity with *Crocodylus porosus*, Aoki suggested that *Toyotamaphimeia machikanensis* was more primitive than *Crocodylus* because of plesiomorphic conditions of two characters in *Toyotamaphimeia machikanensis* (short interorbital distance and thin-walled and steep anterior plate of the premaxilla).

Katsura (2004) described pathological features of *Toyotamaphimeia machikanensis* in dentaries (missing anterior portion), tibia and fibula (fractured), and osteoderm (bite marks) with healing structures and suggested that these injuries occurred multiple times and *Toyotamaphimeia machikanensis* survived these injuries for a certain time. He also suggested that these injuries made by attacks of other individuals of the same taxon and the specimen *Toyotamaphimeia machikanensis* from the Osaka University may be a male because most



Fig. 2. Photographs of *Toyotamaphimeia machikanensis* site (in front of a building on the ride side) (A) and the excavated skull of *Toyotamaphimeia machikanensis* in 1964 (B).

intraspecific fighting is between males.

The geographic distribution of Japanese crocodylians during the Pliocene and Pleistocene is summarized by Taruno (1999). The northern most occurrence reaches to Iwate Prefecture (northern part of the Honshu Island), and southern most to Nagasaki Prefecture (the Kyushu Island) (Fig. 4). Although most discoveries are of fragmentary specimens or footprints, these records indicate the wide distribution of crocodylians in Japan. Aoki (1983) suggested that *Tomistoma taiwanicus* from Taiwan is *Toyotamaphimeia machikanensis*, and the geographic distribution of *Toyotamaphimeia* could be much larger and extend into Taiwan (Shikama, 1972; Aoki, 1983). Taruno (1999) described another crocodylian specimen from the Pleistocene of Osaka Prefecture, called the Kishiwada crocodylian, and referred to *Toyotamaphimeia machikanensis*.

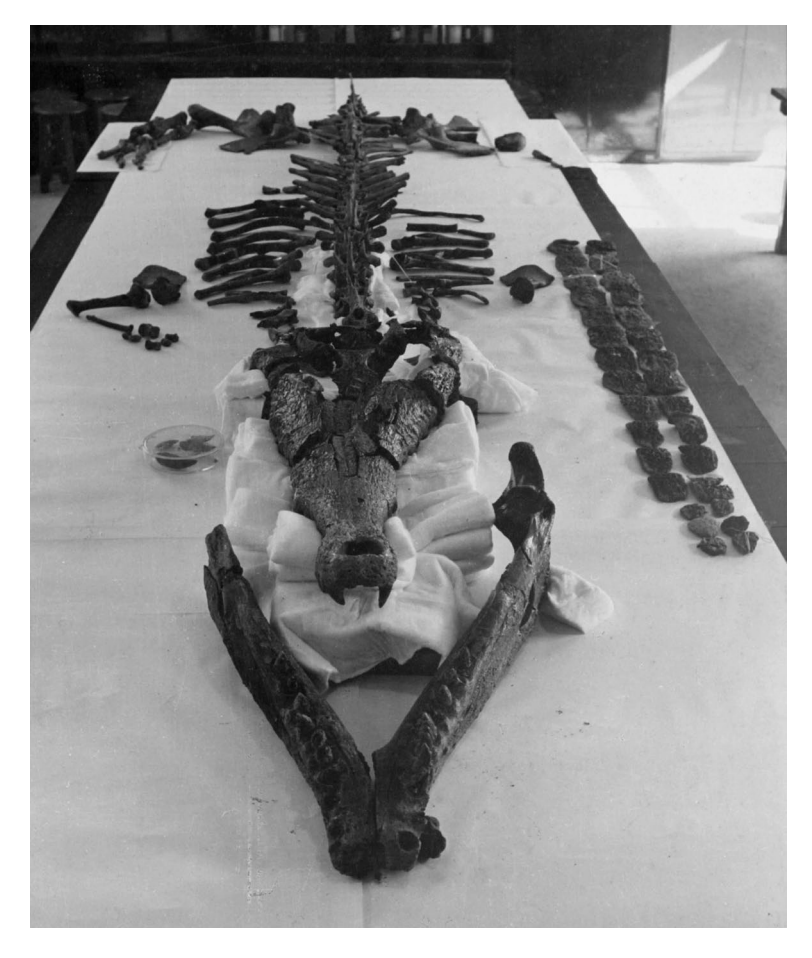


Fig. 3. Discovered skeleton of Toyotamaphimeia machikanensis.

Although three main previous studies on *Toyotamaphimeia machikanensis* (Kobatake et al., 1965; Kobatake and Kamei, 1966; Aoki, 1983) are remarkable, those studies focused on selected elements of the skull, lacking a thorough assessment of the specimen, especially postcranial elements. Also, phylogenetic relationships of Crocodylia have been recently proposed (e.g., Brochu, 1999, 2006; Delfino et al., 2005,), and the evolution of Crocodylia is better understood than before. The main goal of this paper is to provide the detailed description of the entire skeleton of *Toyotamaphimeia machikanensis* and to test the phylogenetic status of *Toyotamaphimeia machikanensis* on the basis of a new set of data matrix drawn from recent studies.

Institutional Abbreviations - MOU, Museum of Osaka University.



Fig. 4. Geographic distribution of crocodylians from the Pliocene and Pleistocene sediments of Japan (data are from Taruno, 1999).

GEOLOGY

Toyotamaphimeia machikanensis was discovered from the Ibaraki Formation of the Osaka Group. The Osaka Group and its equivalent formations (the Sinochou and Shoubudani formations and the Kobiwako and Tokai groups) is distributed in major plains along the coastlines of Pacific Ocean and Japan Sea, inland basins in northeastern Japan, and Setouchi Area in southwestern Japan (Itihara, 1993). The Osaka Group consists of lacustrine and fluvial sediments of the Pliocene-Pleistocene and outcrops in the Osaka Basin and its surrounding areas in the Kinki District, central part of Japan. This group contains twelve marine clay beds (termed Ma -1, Ma 0, Ma 1 and up to Ma 10, where Ma 10 is the youngest) with more than 150 volcanic ash layers, and its thickness is roughly 1,500 to 2,000 meters (Itihara and Inoue, 1993) (Fig. 5). In addition to the skeleton of *Toyotamaphimeia machikanensis* from the Osaka Group, many crocodilian remains such as teeth, bones and footprints have been found from the sediments of the Kobiwako Group. Stratigraphical correlation between the Osaka and Kobiwako groups shows that these fossils were found from different stratigraphic levels from the *Toyotamaphimeia* horizon (Hayashi and Kawabe, 1993; Yoshikawa, 1993).

The Osaka Group in the Senri Hill Area in the northern Osaka Basin is divided into the Ibaraki Formation, in which the skeleton of *Toyotamaphimeia machikanensis* was found, and the Senri Formation (Fig. 5). The stratigraphic boundary between these formations is at the lower limit of Ma 2, and the Ibaraki Formation is stratigraphically higher than the Senri Formation (Itihara and Inoue, 1993). The Ibaraki Formation is approximately 110 m in thickness and consists of eight marine clay beds (Ma 2 to Ma 9) and alternatives of claystone, siltstone, sandstone, and sandy conglomerates of lacustrine and fluvial sediments. The skeleton of *Toyotamaphimeia machikanensis* were recovered from the alternation of sand and silt sediments, associated with "Kasuri Tuff", and 1 meter below the Ma 8 marine clay bed (Fig. 5). "Kasuri Tuff" is radiometrically dated by fission track method as 0.38 Ma ± 0.03 m.y. for anthophylite granule (Nishimura and Sasajima, 1970) and 0.42 Ma ± 0.08 m.y. for apatite granule (Suzuki, 1988).

"Kasuri Tuff" has yielded molluscs (e.g., Cristaria plicata spatiosa, Lanceolaria oxyrhyncha, Lymnium biwae, Lymnium hirasei, Corbicula sandai, and Vivipalus longispira), plant fossils (e.g., Trapa macropoda, Trapa tetragona, and Nelumbo nucifera), and pollen (e.g., Alnus, Fagus, Pinus, and Criptomeria), indicating that its climate was moderate (Kamei, 1971). The Osaka Group and its equivalent sediments in Kinki District are divided into five zones based on mammalian fauna (Stegodon shinshuensis, Stegodon aurorae, Mammuthus shigensis, Stegodon orientalis, and Palaeoloxodon naumannni zones from lower to higher) (Taruno and Kamei, 1993). The Toyotamaphimeia bed is positioned as the Stegodon orientalis Zone because remains of Stegodon orientalis have been known from the horizons between Ma 6 and Ma 8. Ma 8 bed at Hotarugaike, near the Toyotamaphimeia excavation site, yielded an elephant tusk

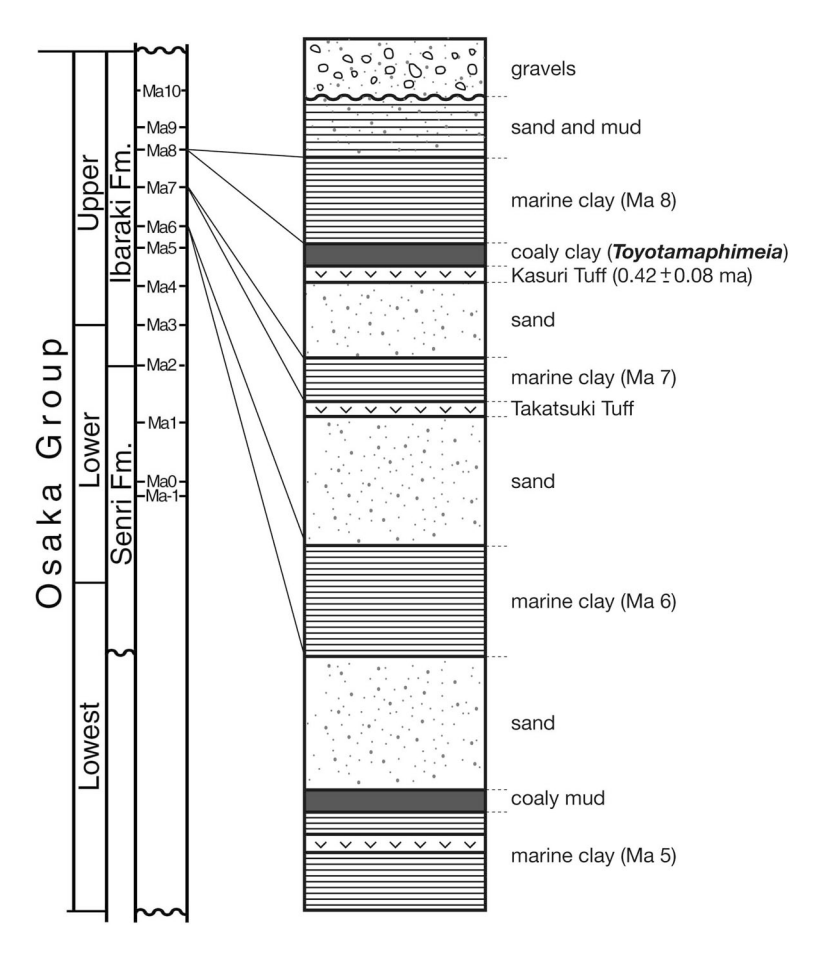


Fig. 5. Stratigraphic position of the Kasuri Tuff in the Ibaraki Formation of the Osaka Group (left). Stratigraphic section of the Ibaraki Formation in the Machikane-yama Area, showing the stratigraphic position of *Toyotamaphimeia machikanensis* horizon (right) (from Kobatake and Kamei, 1966).

referred to *Stegodon orientalis*. The *Stegodon orientalis* Zone also yields *Cervus kazusensis*, *Panthera youngi, Bubalus teihardi, Dicerorhinus nipponicus* and others, and this assemblage is similar to that of the mammalian fauna of central-northern part of China (Taruno and Kamei, 1993). This zone also corresponds to the mammalian zone QM 4 (middle Middle Pleistocene) of the Japanese Neogene biostratigraphy (Kamei et al., 1988), which is dominated by temperate forest mammalian type and contains a few immigrants of warm temperate forest elements from southern China (Kawamura, 1991). The flora of Ma 8 is characterized by the presence of abundant evergreen laurel forest trees, suggesting that it was warm and temperate and that evergreen forests, as seen in the present Pacific coast areas of Japan today, might have been distributed around the Osaka Bay during that time (Momohara, 1993).

The skeleton of *Toyotamaphimeia machikanensis* and the tree trunks of Rosaciae (*Prunis* and *Sorbes*) were recovered from an area of 5 m × 8 m (Kobatake et al., 1965; Kagemori, 1993). Despite of its disarticulated condition of the skeleton of *Toyotamaphimeia*

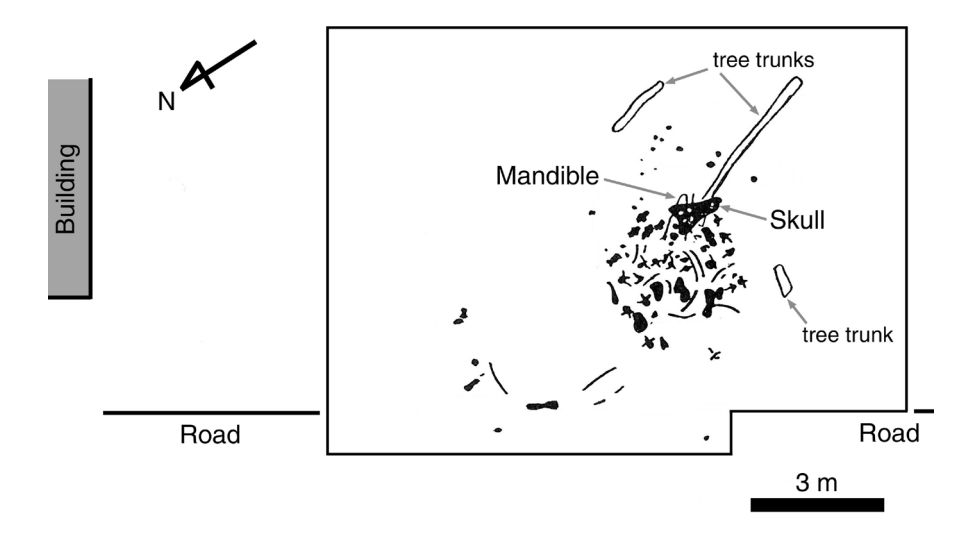


Fig. 6. Bone distribution map of Toyotamaphimeia machikanensis from Kobatake et al. (1965).

machikanensis, these skeletal elements were transported by only a short distance because of its general bone distribution and the preservation of three gastroltih pebbles and thirty-three osteoderms at the area of body (Fig. 6). The main axis of the skull was aligned along north-south direction, which is close to the direction of tree trunks. Most of postcranial elements were preserved north to the skull. Many plant remains and fresh water molluses had been unearthed in association closely with the skeleton and tree trunks (Kamei, 1971). Those fossils were autochthonous to be buried under the influence of slow water current.

SYSTEMATIC PALEONTOLOOGY

CROCODYLIA Gmelin, 1789 TOMISTOMINAE Kälin, 1955 *Toyotamaphimeia* Aoki, 1983

Type species Tomistoma machikanense Kamei et Matsumoto, 1965.

Diagnosis - As for Toyotamaphimeia machikanensis (Kamei et Matsumoto, 1965) given below.

Toyotamaphimeia machikanensis (Kamei et Matsumoto, 1965)

Tomistoma machikanense Kamei et Matsumoto, 1965:54 Toyotamaphimeia machikanensis (Kamei et Matsumoto, 1965) Aoki, 1983:90

Type MOUF00001, a nearly complete skeleton, missing anterior portion of mandibles, most of left dorsal ribs, right forelimb and left hindlimb elements, both pubes, and all caudal vertebrae posterior to fourth caudal vertebra.

Type locality and horizon The Kasuri Tuff, stratigraphically lower by a meter than the eighth marine clay bed (Ma 8) of the Osaka Group (approximately 0.4 million years ago) (Kobatake et al., 1965; Kobatake and Kamei, 1966; Itihara, 1993).

Definition - A stem-based group name including the type species (*Toyotamaphimeia machikanensis*) and all tomistomines more closely related to *Toyotamaphimeia machikanensis* than to *Tomistoma schlegelii*.

Emended diagnosis - Derived tomistomine crocodylian differing from other tomistomines in having the following characters: large seventh maxillary teeth, neural arch with a lateral process ("diapophysis"), axial hypapophysis toward the center of centrum, dorsal margin of atlantal rib with prominent process, prominent iliac anterior process, dorsal osteoderms without keel, four dorsal osteoderms per row, splenial with anterior perforation for mandibular ramus of cranial nerve V, all dentary teeth occlude lingual to maxillary teeth, ectpterygoid separated from maxillary toothrow, smooth posterior margin of otic aperture, lateral eustachian canal positioned lateral to medial eustachian canal, and internal choana not septate.

Note - Tomistoma machikanense was named in the original paper by Kamei and Matsumoto (1965). Aoki (1983) changed its specific name into Toyotamaphimeia machikanensis because its generic name is feminine (-ensis for masculine and feminine), whereas Tomistoma is neuter (-ense for neuter). Aoki (1983) noted that the generic name,

Toyotamaphimeia, was named after "Toyotamaphime", a Japanese goddess of crocodilian incarnate.

Description - Description of the holotype is in the nest chapter.

DESCRIPTION

Skull

The **cranial openings** are well described by Aoki (1983). The external narial opening is circular without a septum and opens dorsally (Fig. 7). The orbits are circular and open dorsally. The anterior edge of the orbits is more posteriorly positioned than the last maxillary tooth. The dorsal margins of orbits are slightly upturned relative to the skull surface. The ventral margin of the orbits are circular. The suborbital fenestrae are anterioly elongated (Fig. 8). The fenestra is bordered by the maxilla anteriorly, palatine medially, ectopterygoid laterally, and pterygoid posteriorly. The anterior end of the suborbital fenestra is located between thirteenth and fourteenth maxillary alveoli. The medial margin of the suborbital fenestra is nearly straight and lacks a posterior notch. The supratemporal fenestra is oval shaped with an anteroposteriorly oriented long axis (Fig. 7). The dorsal rim of the supratemporal fenestra is roughly same size as ventral rim of the fenestra and lacks an overhang rim. The supratemproral fenestra lacks fossa at its anteromedial corner. The infratemporal fenestra is triangular in shape in dorsolateral view and smaller than the supratemporal fenestra. It is bounded by the jugal ventrolaterally and quadratojugal and quadrate posteriorly. The choana is enclosed within the pterygoid and is a single opening without a septum (Fig. 8). The choana is circular and opens posteroventrally. The posterior rim of the choana is smooth and lacks a notch unlike in alligatorids (Brochu, 1997; Brochu, 1999). The external mandibular fenestra is located at a mid-point between the glenoid and the last dentary tooth (Figs. 11-12). The fenestra has a flat ventral border and a posterodorsal corner. The foramen intermandibularis caudalis is small, 42 mm long anteroposteriorly. The foramen intermandibularis medius is not preserved.

The **premaxillae** (Figs. 7, 8, 9, 15) are well described by Aoki (1983). The element is long anteroposteriorly, roughly same length as the nasal, and bears five premaxillary teeth on each side (Fig. 9). The premaxilla-maxilla suture in dorsal view originated from the rostral notch, which is the narrowest part of the rostrum. The notch is weak, and the transverse width of the premaxillae at the notch is 73% of the maximum width of the element (89 and 122 mm respectively) and is associated with an additional concavity on each side for the caniniform dentary tooth. The dorsal premaxillary process extends to the level between the sixth and seventh maxillary alveoli. The premaxillae articulate with each other along the sagittal plane up to the level of fourth maxillary tooth and separate the nasal from the external narial opening. The dorsal premaxillary processes diverge posteriorly, forming W-shaped suture with the nasals. At the posterior border of the external narial opening, the premaxillae form an anteriorly projecting small process (Figs. 7, 15A). The two premaxillae also form a posteriorly projecting small process at the anterior edge of the external narial opening, but the external narial opening is confluent. The dorsal surface of the premaxillae lateral to the external narial opening is smooth and



Fig. 7. Skull of *Toyotamaphimeia machikanensis* in dorsal view. Abbreviations: ect, ectopterygoid; f, frontal; j, jugal; l, lacrimal; m, maxilla; p, parietal; pf, prefrontal; pm, premaxilla; po, postorbital; pt, pterygoid; q, quadrate; qj, quadratojugal; sq, squamosal.

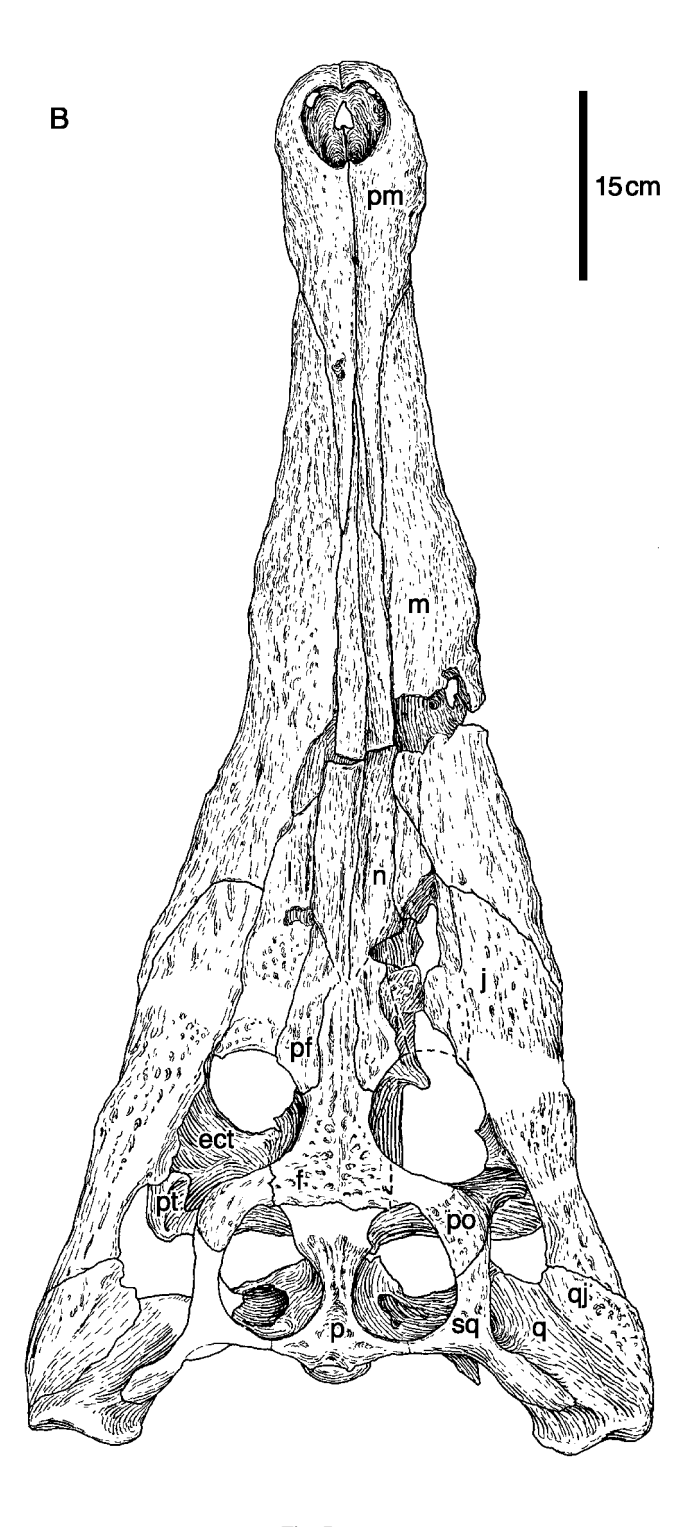


Fig. 7. cont.



Fig. 8. Skull of *Toyotamaphimeia machikanensis* in ventral view. Abbreviations: bo, basioccipital; ect, ectopterygoid; eo, exoccipital; j, jugal; m, maxilla; oc, occipital condyle; pal, palatine; pm, premaxilla; pt, pterygoid; q, quadrate; qj, quadratojugal.

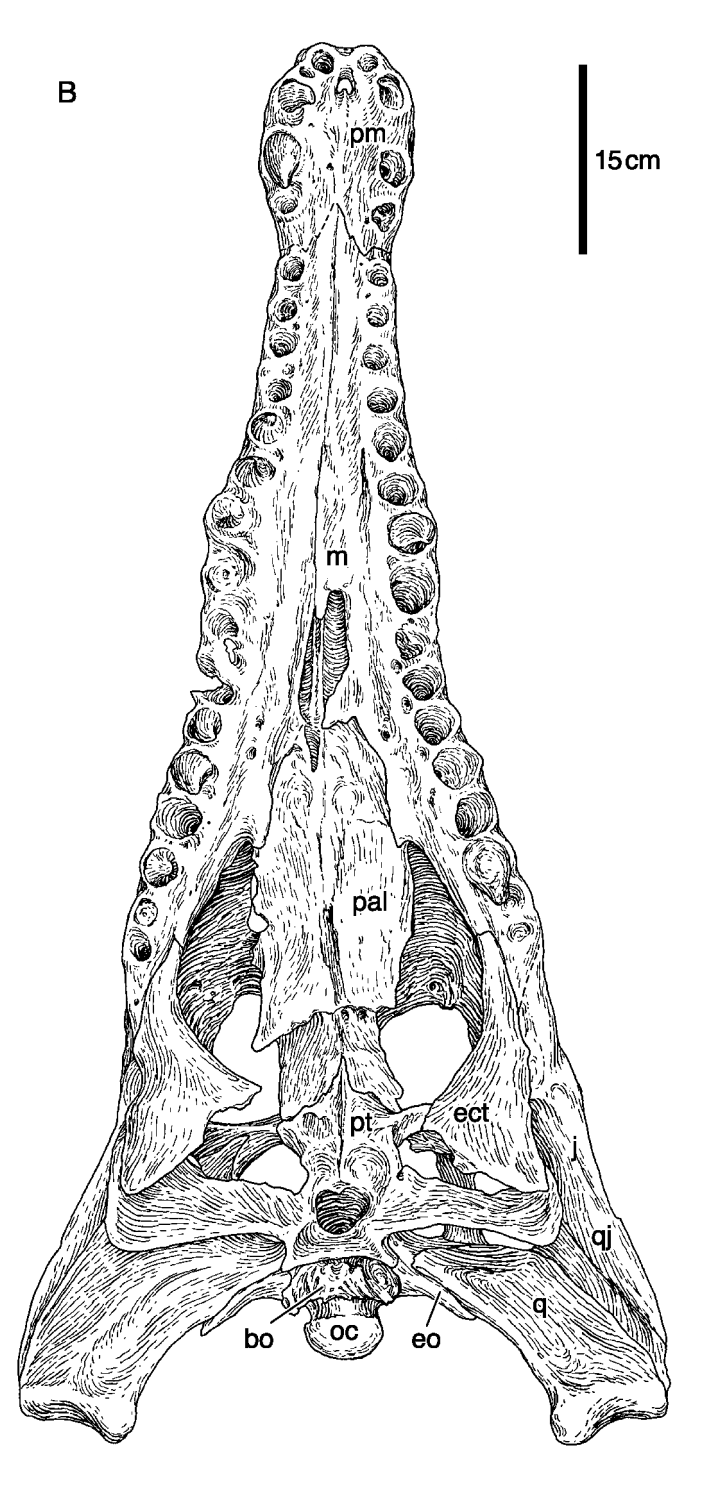


Fig. 8. cont.



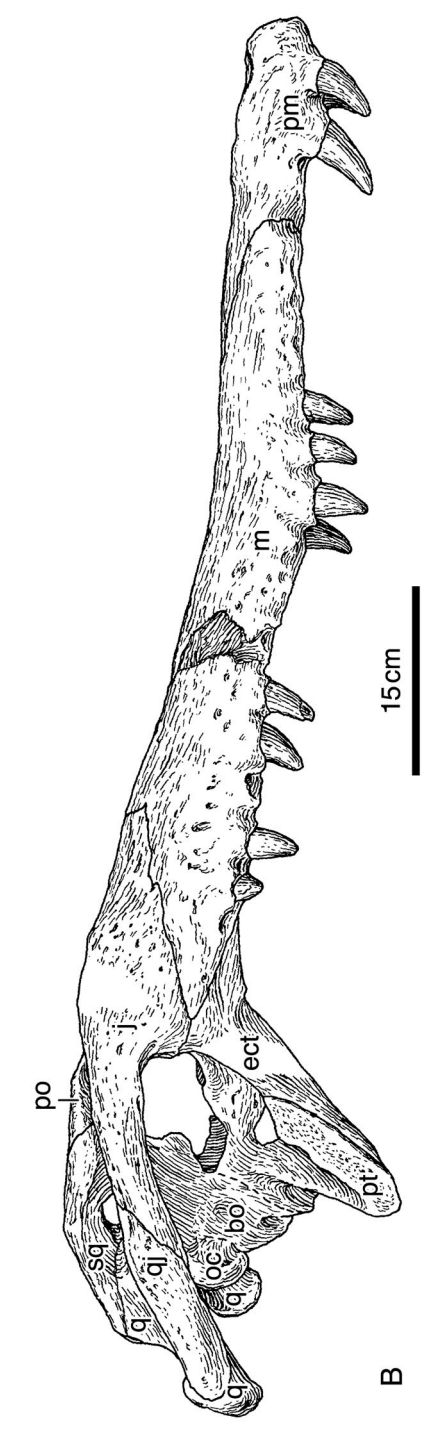


Fig. 9. Skull of *Toyotamaphimeia machikanensis* in right lateral view. Abbreviations: bo, basioccipital; ect, ectopterygoid; j, jugal; m, maxilla; oc, occipital condyle; pm, premaxilla; po, postorbital; pt, pterygoid; q, quadrate; qj, quadratojugal; sq, squamosal.

Table 1. Measurements in millimeters of the skull and mandible in the holotype of *Toyotamaphimeia machikanensis* in this study.

Measurement	mm
Skull length (premaxilla-parietal)	1025
Skull width (quadrate-quadrate)	496
External narial opening, length and width	62.2×70.2
Orbit, length and width	91.8×93.9
Supratemporal fenestra (left), length and width	102.6×78.8
Infratemporal fenestra (right), length and width	70.0×42.9
Suborbital fenstra (left), length and width	205.4×66.2
Choana, length and width	37.5×42.3
Foramen magnum, height and width	36.4×31.6
Preorbital length	770
Width between orbits	49.6
Skull table, length and width	127.8×210.1
Width between supratemporal fenestrae	21.7
Width between suborbital fenestrae	111.4
Occipital condyle, height and width	56.0×56.9
Mandibular fenestra (left), height and length	38.3×100.1
Hyoid length (left, incomplete)	159.7

lacks a groove seen in some *Alligator* (Brochu, 1997; Brochu, 1999) (Fig. 15A). The lateral and anterior sides of the premaxillae are more heavily ornamentated than the dorsal surface. The anterior surface is pitted, whereas the lateral surfaces have the mixture of pits and grooves. In ventral view, the incisive foramen is heart-shaped, with an anterior process at its posterior border (Fig. 15B). A weak sagittal ridge is present posterior to the anterior process. The foramen is positioned between the first and second premaxillary teeth, or close to the anterior border of the external narial opening in dorsal view, and the anterior end of the foramen is between the first premaxillary alveoli. The foramen is small, 22.1 mm long and 16.2 mm wide, which is much less than half the maximum width of the premaxilla. The wedge-shaped processes of the premaxillae and maxillae give the suture between the two bones in the form of a zigzag pattern. As described by Aoki (1983), one of the processes of the premaxillar reaches the level of the first maxillary tooth. A gap between the third and fourth premaxillary teeth is the largest distance between consecutive premaxillary teeth. Medial to the gap, one foramen is present on the right side and two on the left side. There is another foramen on the ventral surface of the right premaxilla.

The **maxilla** (Figs. 7, 8, 9, 16) is the longest cranial element and has sixteen teeth on each side. As suggested by Aoki (1983), one of the most interesting features of this taxon is the posterior position of the lateral expansion of the maxilla. This is related to the larege diameter of the seventh maxillary tooth. Posterior to the expansion or to seventh alveoli, the tooth raw curves medially (Fig. 8). The edge of each alveolus is surrounded by a ridge, which covers the base of tooth crown (Fig. 9). The height of the ridge is the largest at the seventh maxillary alveoli, indicating a strong support for the seventh maxillary teeth. Posterior to the eleventh maxillary alveolus, the lateral side of the element has a series of foramina at roughly 40 mm from the ventral edge of the maxilla, and each foramen is associated with a corresponding alveolus (Fig. 9). The ornamentation of the maxilla is a mixture of pits and anteroposteriorly running

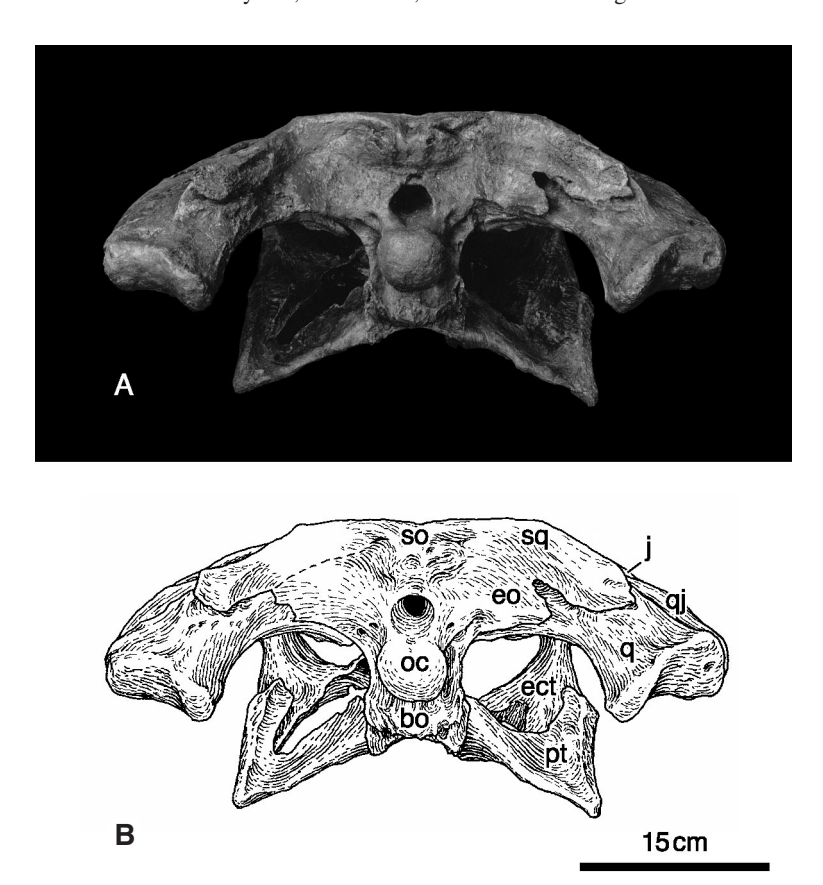


Fig. 10. Skull of *Toyotamaphimeia machikanensis* in occipital view. Abbreviations: bo, basioccipital; ect, ectopterygoid; eo, exoccipital; j, jugal; oc, occipital condyle; pt, pterygoid; q, quadrate; qj, quadratojugal; so, supraoccipital; sq, squamosal.

grooves, but the lateral surface, posterior to the eleventh maxillary alveolus, is less ornamented. In lateral view, the ventral border of the element is slightly concave ventrally and is more dorsally positioned than the level of the mandibular condyle of the quadrate. The anterior end of the maxilla in ventral view is wedged between the posterior processes of the premaxillae and reached the last premaxillary tooth (Fig. 15B), which disagrees with the interpretation on this region by Aoki (1983). The median region of the maxilla between eight and thirteenth maxillary teeth is damaged but preserves a part of the maxillar-palatine suture (Fig. 8). The anterior end of the suture is at the level of the eleventh maxillary tooth. The posterior end of the suture ends close to the anterior border of the palatal fenestra but is positioned more medially because of the presence of a short posteromedial process of the maxilla. Medial to the eleventh maxillaty tooth, there are two foramina for the palatine ramus of the trigeminal nerve (cranial nerve V) (Fig. 16A). These are much smaller than alveolus size. Cup-shaped depressions are present between adjacent teeth from the eighth to thirteenth maxillary teeth. These depressions are for dentary teeth when the lower jaw is occluded. The posterior process of the maxilla is pinched

out between the jugal and ectopterygoid (Figs. 8 and 17B). There is a gap between the posterior tip of the maxillae and the posterior-most maxillary alveolus, which is roughly 60 mm in length. The medial surface of the posterior process, forming the anterolateral border of the suborbital fenestra, has a large circular foramen (19.4 mm in diameter), which is as large as the diameter of the last maxillary alveolus (Fig. 16B).

Both **nasals** (Fig. 7) are nearly complete, but posterior parts are crushed dorsoventrally. The nasals are elongate and articulate each other with a straight suture. The nasal extends anteriorly between the dorsal processes of the premaxilla to the level of the third maxillary teeth. The posterior end of the nasal convergines for a short distance and meets the frontal at the level of the last maxillary alveoli. The ventral surface of the element between eighth to eleventh maxillary teeth is exposed because of the damage of the maxilla. The ventral surface of each nasal forms a shallow groove, and grooves on both sides are separated by a medial ridge.

A region just anterior to the orbits is damaged and it is difficult to observe some of sutures among the nasals, prefrontals, lacrimals, frontals, and jugals. Our reconstruction on the sutural relationships among these elements is close to the one proposed by Aoki (1983). The **lacrimal** is much longer than the **prefrontal** but shorter than the nasals (Fig. 7). It is longer than wide (three to four times as long as its width). The contact of the nasal with the lacrimal is longer than with the prefrontal. The anterior end of the lacrimal-maxilla suture ends at the lateral side of the nasal, roughly one-third of the nasal length from its posterior end. The lacrimal-maxilla suture is straight, lacking the posterior process of the maxilla (Fig. 7). Anteriorly, the lacrimal extends up to the level between the eleventh and twelfth maxillary teeth. The posterior edges of the lacrimal and prefrontal are concave for the anterior border of the orbit. The dorsal surface of the lacrimal is ornamented with pits, whose diameter reaches to 9 mm at maximum, as in the dorsal and lateral surfaces of the jugal. Most of the dorsal surface of the prefrontal is ornamented, similar to the lacrimal, but its medial part is smooth

No palpebral is preserved.

The dorsal portion of the **postorbital** (Fig. 7) forms the anterolateral area of the skull table. In dorsal view, the anterolateral border of the element is smoothly curved, but does not form a distinct corner. The postorbital-frontal suture is straight and anteroposteriorly directed from the anterior edge of the supratemporal fenestra. The postorbital-squamosal suture is originated from the lateral edge of the supratemporal fenestra to the base of the postorbital bar and is oriented at an angle to the sagittal plane, differing from a previous study (fig. 1; Aoki, 1983). The descending process that forms the dorsal part of the postorbital bar is preserved on the right side, but offset from the ascending process of the jugal by crushing (Fig. 17A). It is massive, slightly thicker than the width of the dorsal portion of the postorbital in dorsal view, and lacks prominence (Fig. 7). The proximal end of the descending process shows no offset from the anterolateral border of the skull table. Its ventral end is positioned medial to the ascending process of the jugal and inset from the lateral surface of the jugal (Fig. 17A). Ornamentation occurs only on the dorsal surface of the dorsal portion of the postorbital.

The **jugal** (Figs. 7, 8, 9, 17) is as long as the nasal. Anterior to the postorbital bar it is massive and is much wider than the posterior part. The anterior part of the element articulates with the maxilla laterally and lacrimal medially, and forms the anterolateral part of the orbit. The ascending process is positioned on the lateral side of the main body of the jugal and is triangular in cross-section. Anterior to the postorbital bar, the right jugal is damaged, but there is no

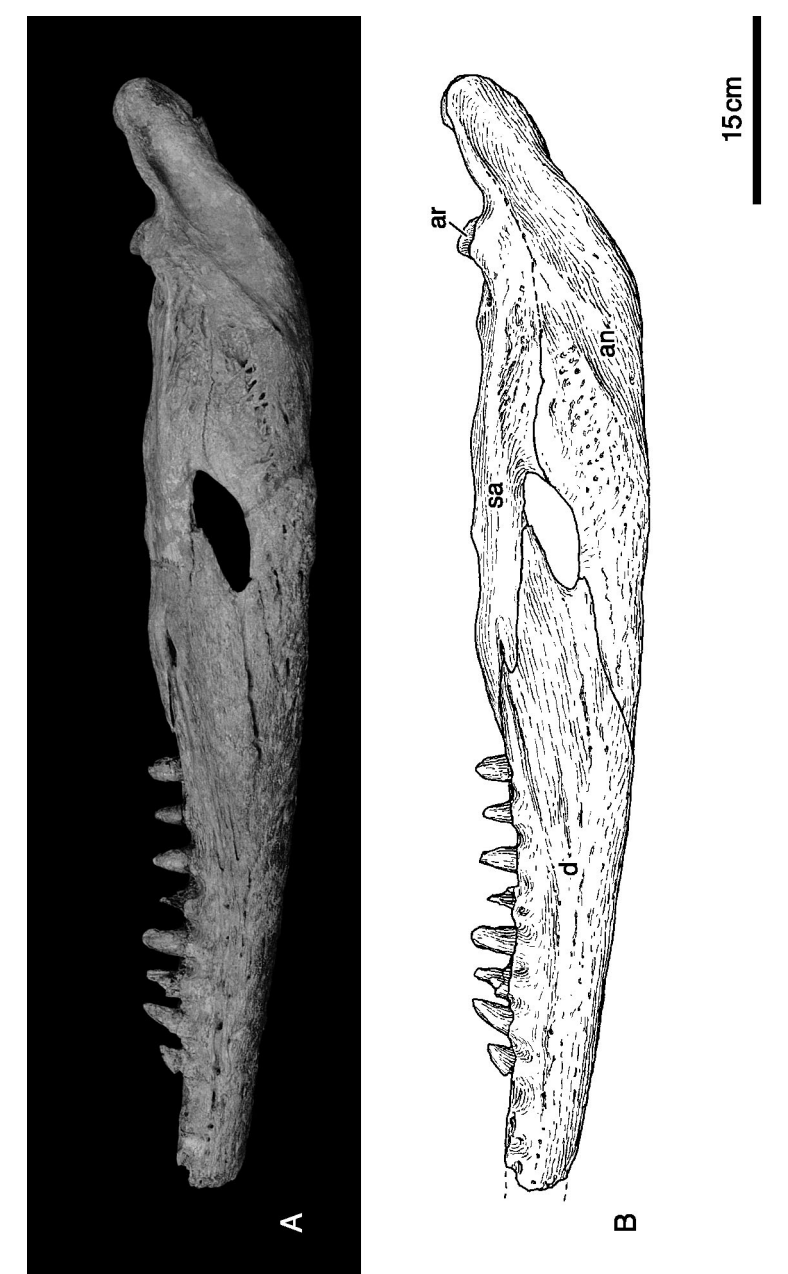
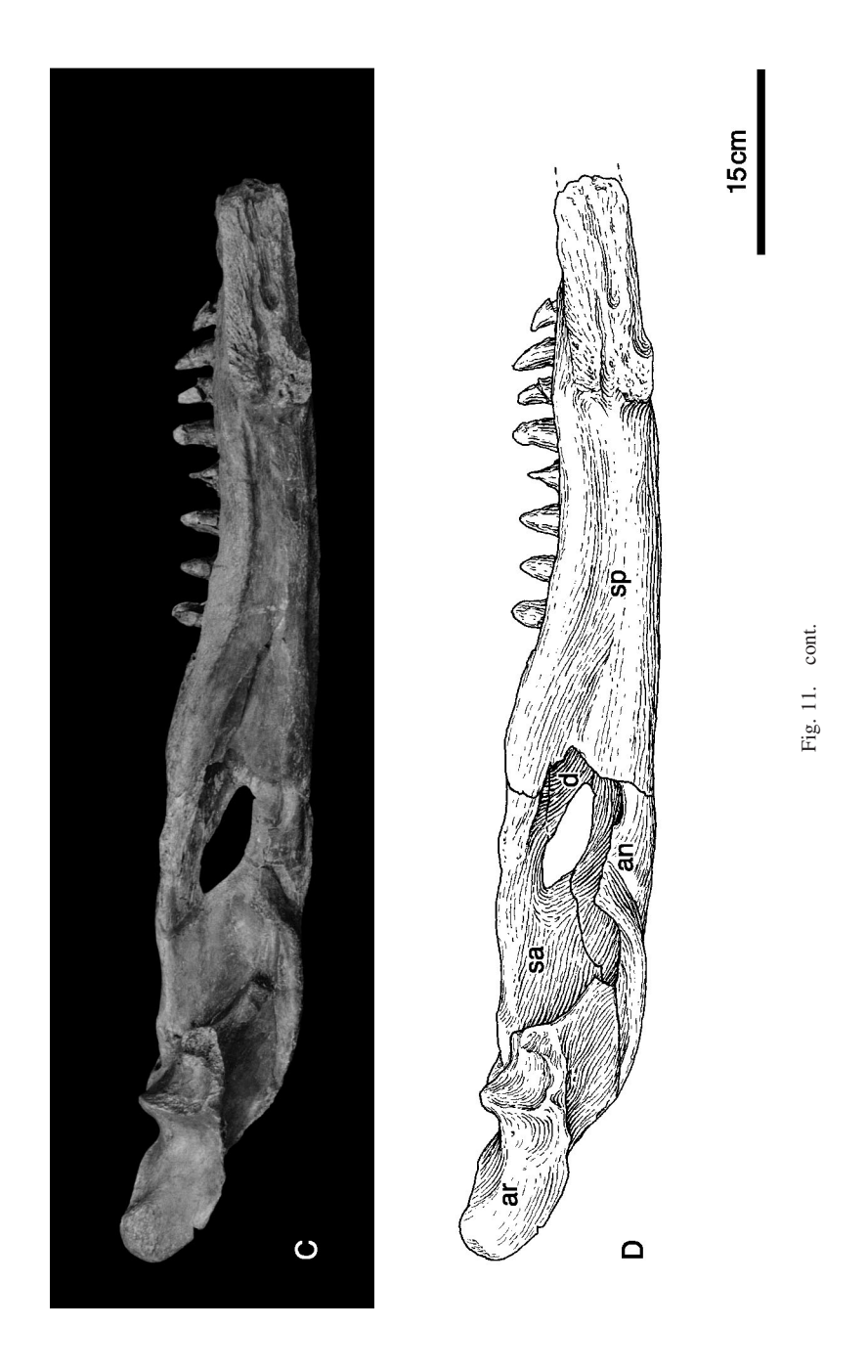


Fig. 11. Left mandibular ramus in lateral (A and B) and medial (C and D) views. Abbreviations: an, angular; ar, articular; d, dentary; sa, surangular; sp, splenial.



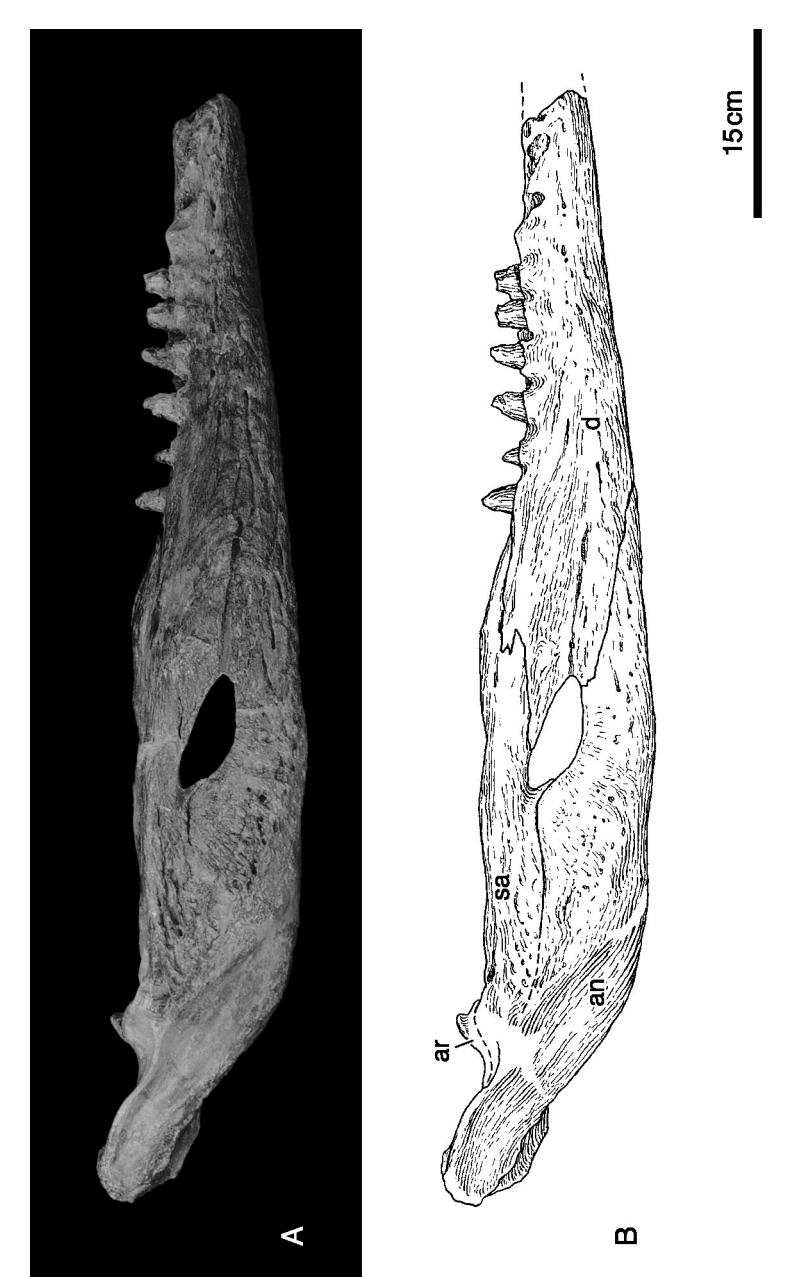


Fig. 12. Right mandibular ramus in lateral (A and B) and medial (C and D) views. Abbreviations: an, angular; ar, articular; d, dentary; sa, surangular; sp, splenial.

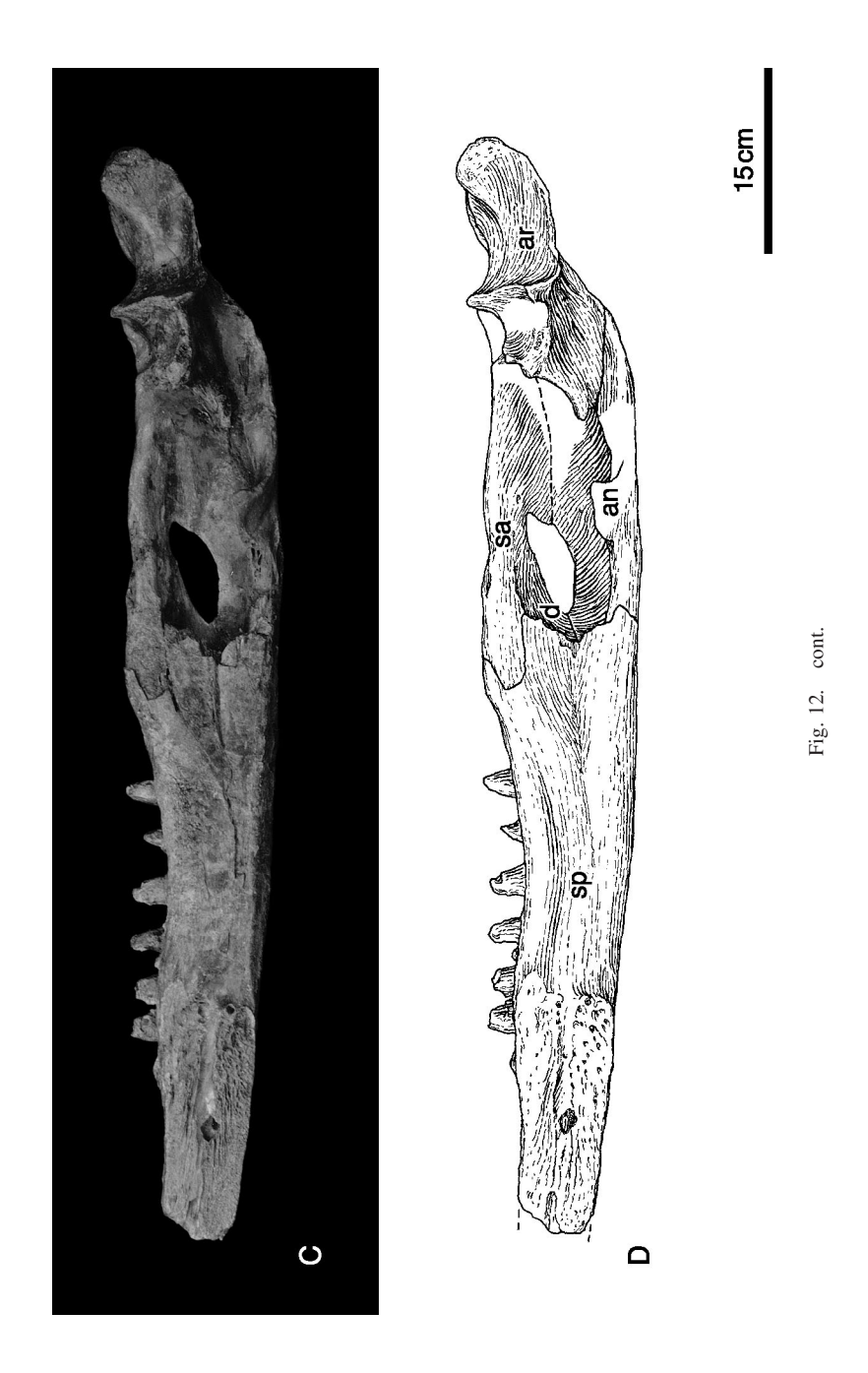




Fig. 13. Mandibules in dorsal view. Abbreviations: an, angular; ar, articular; d, dentary; sa, surangular; sp, splenial.

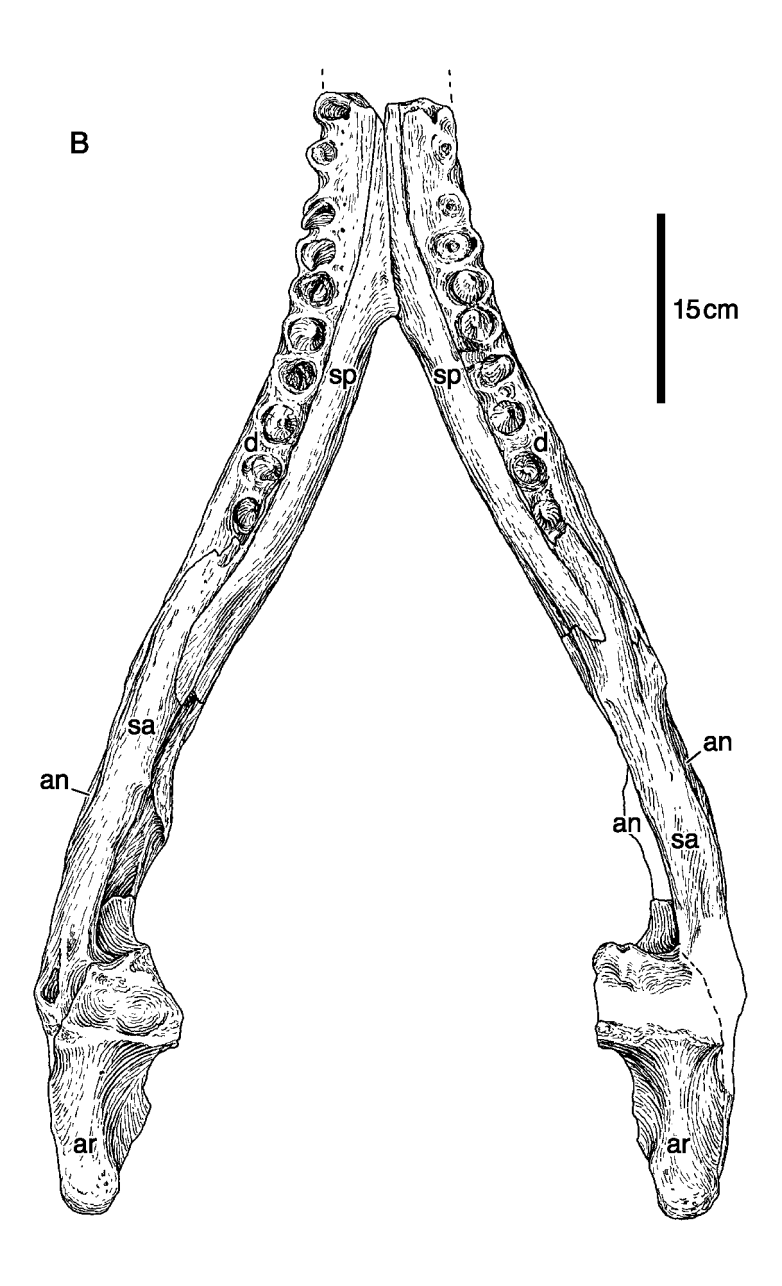


Fig. 13. cont.



Fig. 14. Mandibules in ventral view. Abbreviations: an, angular; ar, articular; d, dentary; sp, splenial.

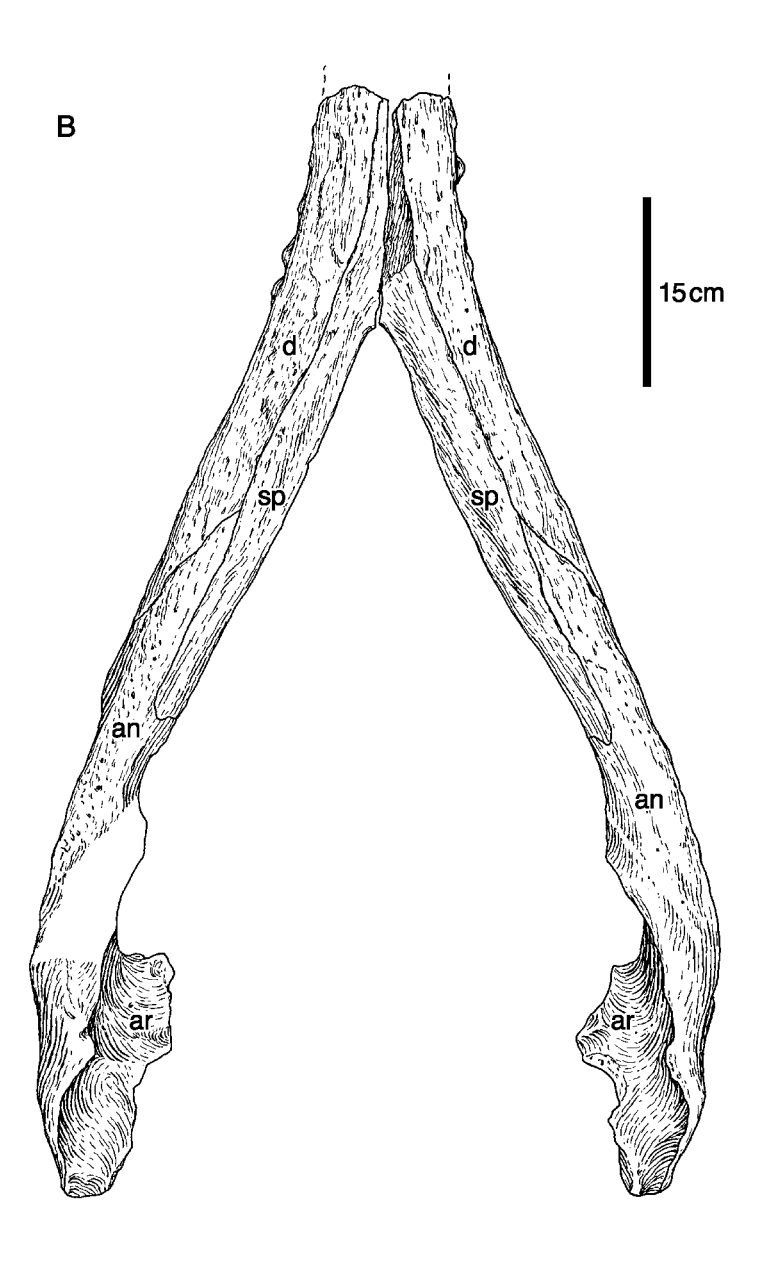


Fig. 14. cont.

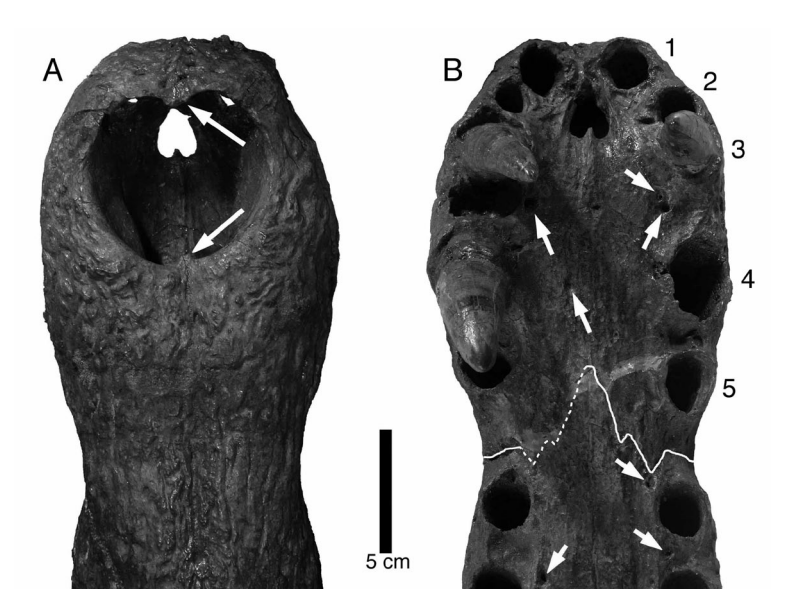


Fig. 15. Anterior region of the upper jaw in dorsal (A) and ventral (B) views. Large arrows in A show small processes at the anterior and posterior edges of the external narial opening. Small arrows in B indicate the positions of foramina. Numbers are alveolus position in the left premaxilla.

indication of a large jugal foramen. Posterior to the base of the ascending process, a large foramen is present and is roughly 14 mm in diameter, and its canal for the passage of blood vessel or nerve is directed anteroposteriorly (Fig.17A). In lateral view, the dorsal edge of the element is curved dorsally, and its highest point at the orbital border is close to the level of the skull table. Posterior to the postorbital bar, the jugal is thin, less than a half of the maximum width of the jugal, which may be exaggerated by the crushing of the skull table. Although the jugal-quadratojugal suture is described as originating from the posterior end of the infratemporal fenestra by Aoki (1983), it is interpreted in this study to originate from the ventral edge of the fenestra (Fig. 18A). The jugal and quadratojugal are firmly sutured in ventral view. The ventral surface of the jugal near the jugal-maxilla-ectopterygoid sutures has an oval-shaped depression (Fig. 17B). A single foramen is present at the anterior end of the depression. The ornamentation of the jugal is comprised of oval-shaped pits, which are deepest and largest in the skull.

The right **quadratojugal** (Figs. 7, 8, 9, 18, 20) is the better preserved. Although the anterior one-third of the quadrate-quadratojugal suture is not clear, it seems that the quadrate-quadoratojugal suture extends posteroventrally to the level of the posterior end of the infratemporal fenestra (Fig. 18A). The suture is visible posteriorly and is medially concaved (Fig. 7). The quadratojugal lacks an anterior process along the lower temporal bar. The medial end of the jugal-quadratojugal suture is positioned along the lateral border of the infratemporal fenestra, and the quadratojugal forms the posterior angle of the infratemporal fenestra. The posterior border of the right infratemporal fenestra is straight and the edge is smooth and does not show any trace of breakage, but the border of the left infratemporal fenestra may preserve the base of the quadratojugal spine near the posterior angle of the infratemporal fenestra (Fig. 18B).

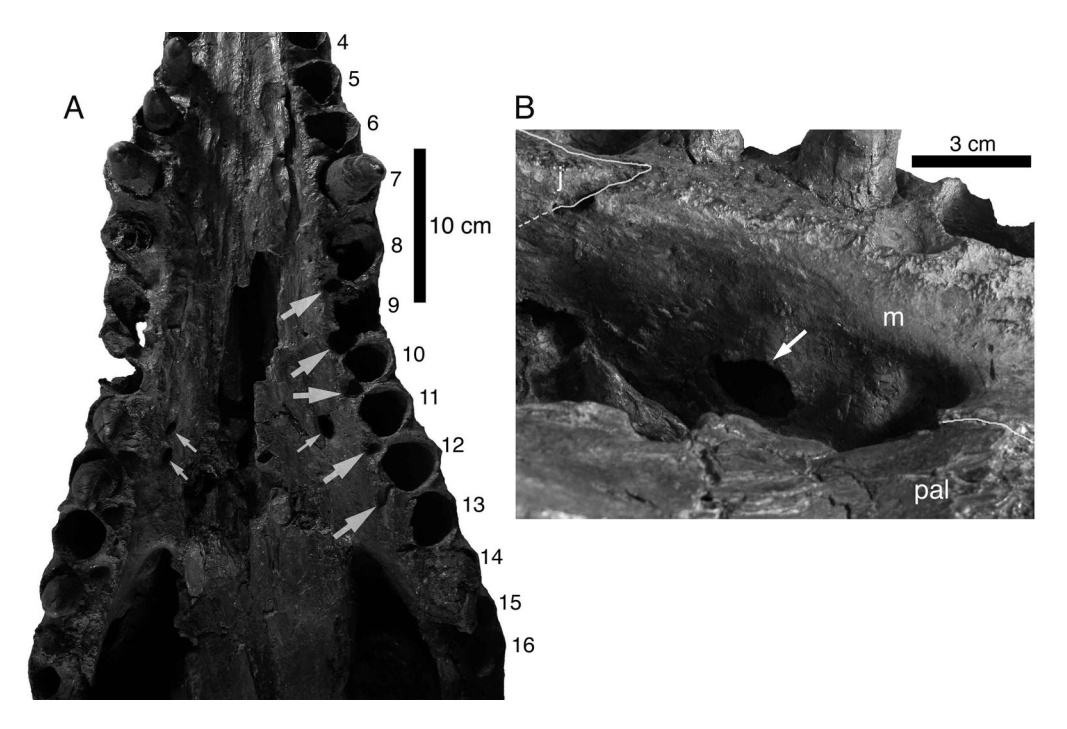
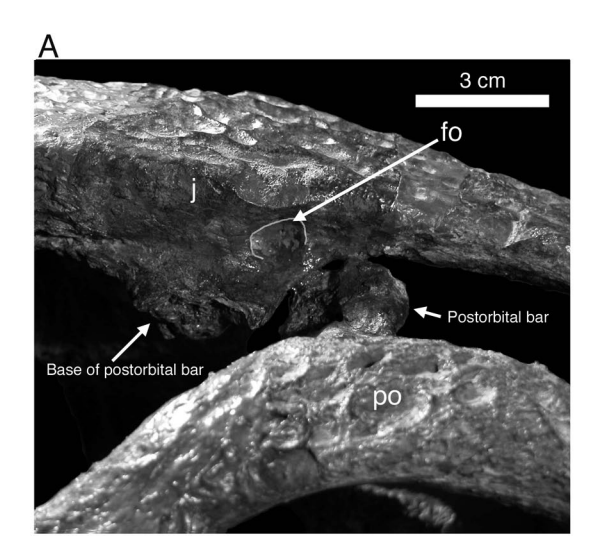


Fig. 16. Middle region of the *Toyotamaphimeia* palate (A) and an opening in the maxilla (B). Large arrows in A show cup-shaped depressions, and small arrows in A are foramina for palatine ramus of the trigeminal nerve. An arrow in B points a large foramen on the medial surface of the posterior process of the maxilla. Numbers are alveolus positions in the left maxilla. Abbreviations: j, jugal; m, maxilla; pal, palatine.

Either side may be obscured by its preservational artifact, making it impossible to know whether the bone joined the formation of the posterior border of the infratemporal fenestra. The lateral half of the dorsal surface of the quadratojugal is heavily ornamented, but the medial half is smooth.

The **frontal** is single (Fig. 7). It is triangular in shape in dorsal view and is slightly shorter than the anteroposterior length of the skull table (Table 1). The lateral sides of the middle portion of the element form the medial borders of the orbits. The interorbital width of the frontal is 50.4 mm, much wider than the interfenestral distance. The frontal-parietal suture on the skull table is straight, perpendicular to the sagittal plane, and is positioned at the level of the anterior end of the supratemporal fenestrae. The suture is entirely on the skull table, indicating that the frontal does not enter the supratemporal fossa (Fig. 7). The frontal-postorbital suture is straight and directed anteroposteriorly. The dorsal surface of the frontals is slightly concave and heavily pitted. Between the orbits, the frontal bears a weak sagittal ridge (Fig. 7).

The single **parietal** (Fig. 7) is damaged anteriorly. It forms the well-defined medial border of the supratemporal fossa. The dorsal surface of the parietal has a median ridge between the supratemporal fenestrae. The parietal-squamosal suture in dorsal view is originated from the posterior border of the supratemporal fenestra. The postsupratemporal bar is narrow. The ventral portion of the parietal is damaged so that the relationships with the squamosal and quadrate



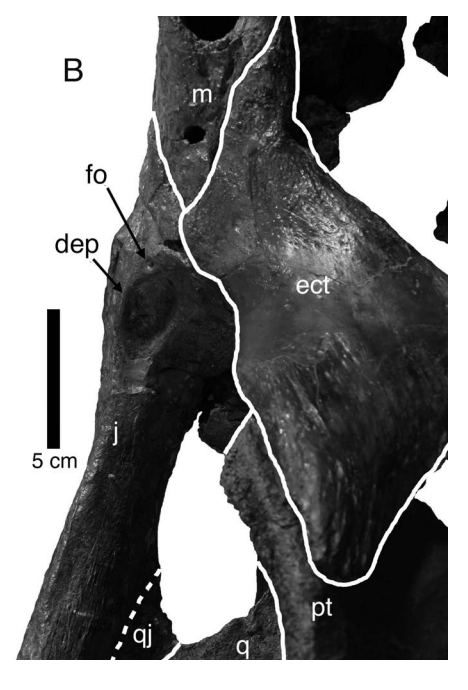


Fig. 17. A foramen at the base of the postorbital bar (A) and contact relationships of the maxilla, ectopterygoid, and jugal in ventral view (B). Abbreviations: dep, depression; ect, ectopterygoid; fo, foramen; j, jugal; m, maxilla; po, postorbital; pt, pterygoid; q, quadrate; qj, quadratojugal.

in this region are not clear.

The right **squamosal** (Figs. 7, 9, 10, 18) is well preserved. The anterior process of the squamosal is long and is wedged in lateral view. Its anterior end is terminated near the posterior side of the postorbital bar. The suture with the quadrate, anterior to the auditory maetus, leads to the dorsal border of the maetus. The squamosal-quadrate suture, posterior the maetus, is not clearly defined but is positioned more dorsolaterally than the posteovental corner of the maetus. At the base of the anterior process, the squamosal forms an overhang for the otic recess. The posterolateral corner of the skull table has an elongate process. This posterolateral process extends along the dorsal edge of the paroccipital process of the exoccipital. The tip of the process is dorsal to the paroccipital process in lateral view (Fig. 18A). The dorsal edge of the squamosals is nearly horizontal in occipital view (Fig. 10).

The **quadrates** (Figs. 7–8) participate in the posterior border of the infratemporal fenestrae. Their mandibular condyles are separated by a faint and vertical sulcus, with the main axis close to horizontal (Fig. 19). In caudal view, the main axis of the lateral condyle is nearly vertical, but that of the medial condyle is obliquely inclined laterally (Fig. 19). The medial condyle is larger, extended more caudally in dorsal view (Figs. 7–8), and dorsoventrally taller in caudal view than the lateral condyle. The transverse width of the main body of the quadrate in ventral view is consistent from the mandibular condyle to the level of the infratemporal fenestra. The anterior portion of the quadrate has an anterodorsal process and ventromedially positioned pterygoid ramus. The anterodorsal process extends from the ventral surface of the

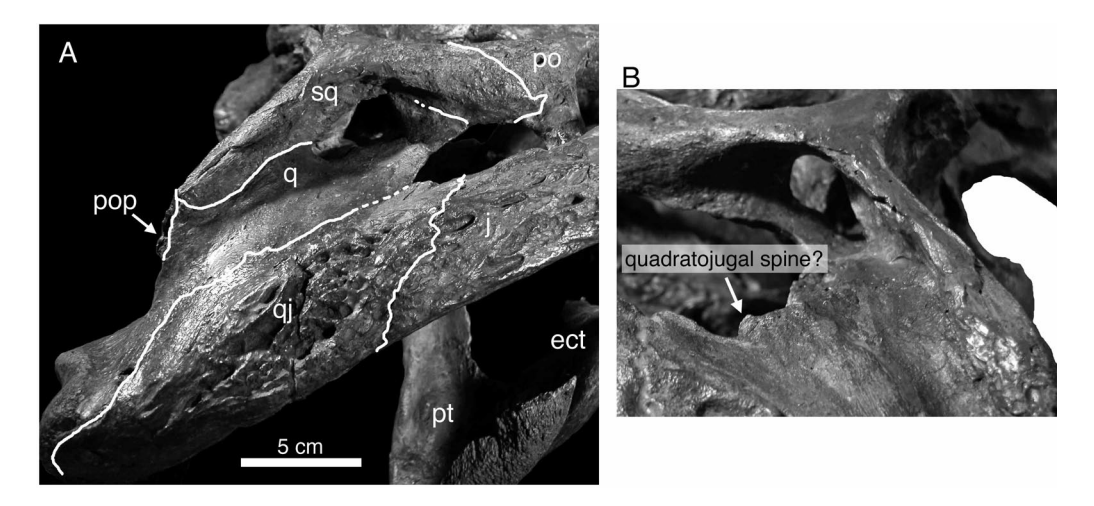


Fig. 18. Temporal region of the left (A) and right (B) sides. Abbreviations: ect, ectopterygoid; j, jugal; po, postorbital; pop, paroccipital process; pt, pterygoid; q, quadrate; qj, quadratojugal; sq, squamosal.

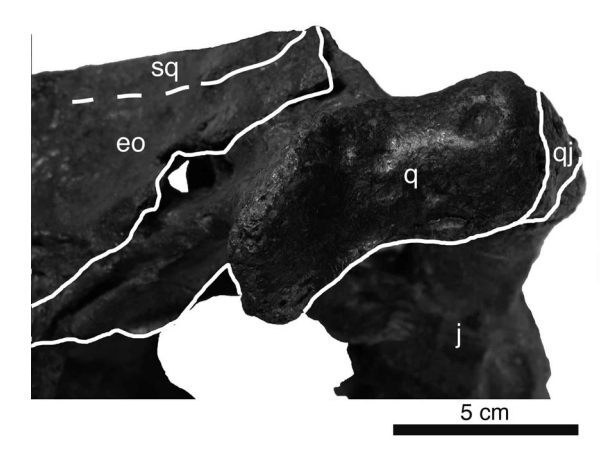


Fig. 19. Right mandibular condyle in posterior view. Abbreviations: eo, exoccipital; j, jugal; q, quadrate; qj, quadratojugal; sq, squamosal.

upper temporal bar up to the level of the anterior end of the supratemporal fenestra but does not reach the orbit. Because the tip of the pterygoid ramus is damaged, the sutural arrangements with the basicranial and braincase elements are obscured. A fragment of the pterygoid ramus is preserved and borders a portion of the lateral exit of the cranial nerve V. The quadrate lacks a foramen aerum on the dorsal surface, unlike other crocodylians (Fig. 13). The cranio-quadrate canal is large (Fig. 10). The ventral surface of the quadrate has weak crests (Fig. 20B). The crests of the right quadrate are stronger than the ones in the left quadrate, and it has four ridges. Among these crests, the most robust one is positioned cranial to the mandibular condyle and is rounded in its cross-section. The pterygoid ramus bears another crest, which is the shortest but

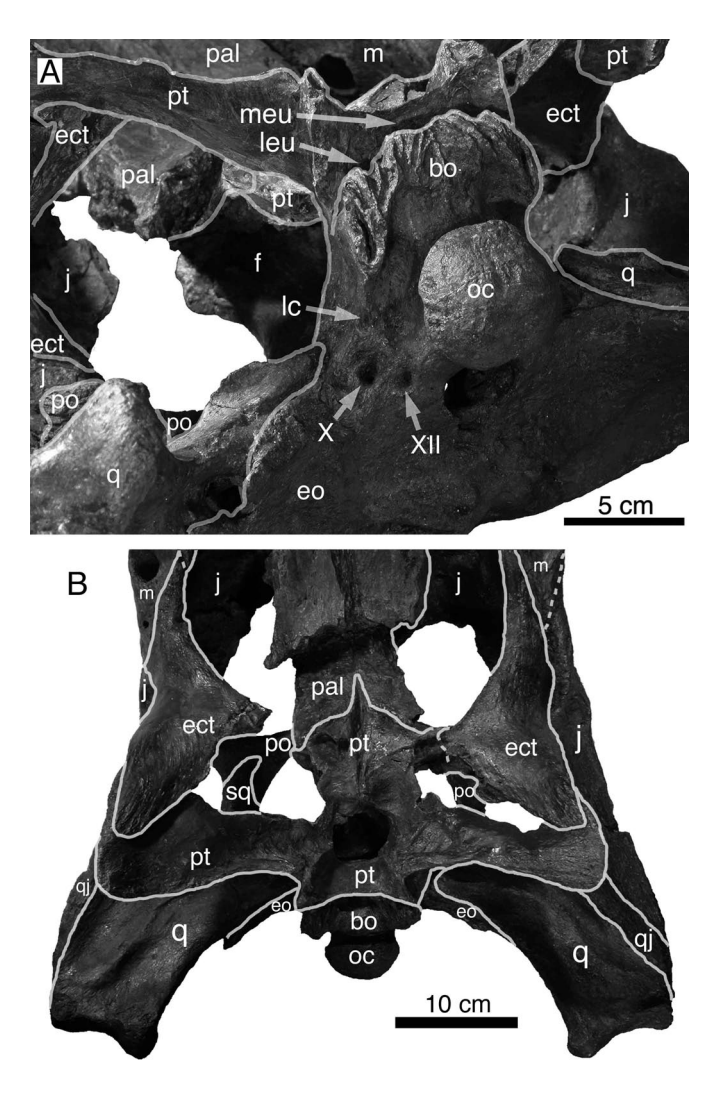


Fig. 20. Occipital region in oblique ventral view (A) and posterior portion of the skull in ventral view (B). Abbreviations: X, exit for the cranial nerve X; XII, exit for the cranial nerve XII; bo, basioccipital; ect, ectopterygoid; eo, exoccipital; f, frontal; j, jugal; lc, lateral carotid foramen; leu, lateral eustachian opening; m, maxilla; meu, median eustachian opening; oc, occipital condyle; pal, palatine; po, postorbital; pt, pterygoid; q, quadrate; qj, quadratojugal; sq, squamosal.

highest and sharpest crest. Two other crests are very weak and are located caudal to the infratemporal fenestrae.

The sutures of **supraoccipital** (Fig. 10) with its surrounding elements are not well preserved. Its transverse width is twice as long as its height. In occipital view, the supraoccipital has an inverted W-shaped dorsal edge. The dorsolateral edge of the supraoccipital borders the posttemporal fenestra. Medioventral to the posttemporal fenestra, the supraoccipital has a pair of prominences associated with accessory foramina. The suture with the exoccipital is nearly

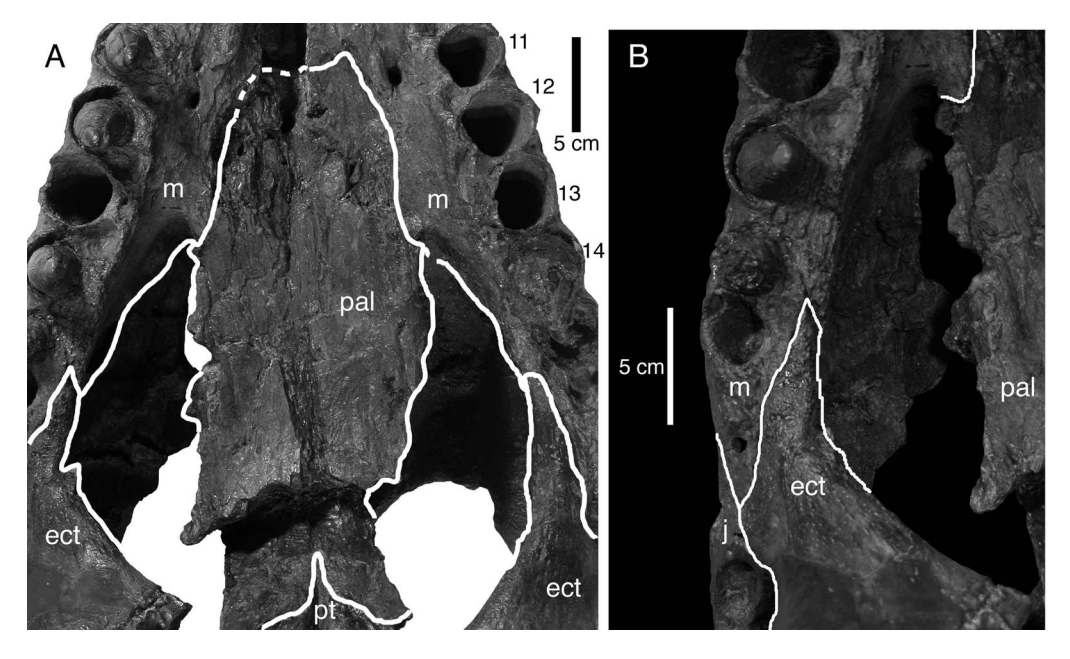


Fig. 21. Palatine and surrounding elements in ventral view (A) and maxilla-ectopterygoid contact (B). Abbreviations: ect, ectopterygoid; j, jugal; m, maxilla; pal, palatine; pt, pterygoid.

straight but is gently concave ventrally.

The paroccipital process of the **exoccipital** is smooth and lacks a boss (Figs. 10, 19). The paroccipital process diverges into two processes laterally. The dorsal process reaches to the level of the medial condyle of the quadrate and extends more ventrally than the process of the squamosal in lateral view (Fig. 18A). The ventral process is much shorter than the dorsal one. The cranio-quadrate canal is positioned at the bases of the dorsal and ventral processes. The ventral rami of the exoccipital form most of the foramen magnum. The foramen magnum is circular in shape (35 mm wide) and is much smaller than the occipital condyle (Fig. 10). At the base of the ventral rami and lateroventral to the foramen magnum, a minute nerve opening for the cranial nerve XII is present, and a much larger opening for the cranial nerves X is present lateral to the opening of the cranial nerve XII (Fig. 20). Ventral to the opening for the cranial nerve X, there is the lateral carotid foramen, but the relative position with the basisphenoid is not clear because the sutures of the basisphenoid are not well exposed.

The occipital condyle of the **basioccipital** is spherical in shape with a constricted neck and lacks a vertical shallow sulcus (Figs. 10, 20). The main axis of the occipital condyle is close to but is slightly angled relative to the main axis of the skull. The suture between the exoccipital and basioccipital is not clear. The anteroventral portion of the basioccipital has a roguse ventral surface with grooves, forming the basioccipital tubera, but lacks a midline sagittal crest (Fig. 20). The tubera is well developed as is seen in some longirostrine taxa (Bruchu, 1997; Brochu, 1999). Each lateral side of the anterior portion of the basioccipital has a ridge. In occipital view, the basioccipital extends ventrally at the same level as the pterygoid. The small median eustachian opening opens at the same level as the pterygoid and anterior to the basioccipital, but

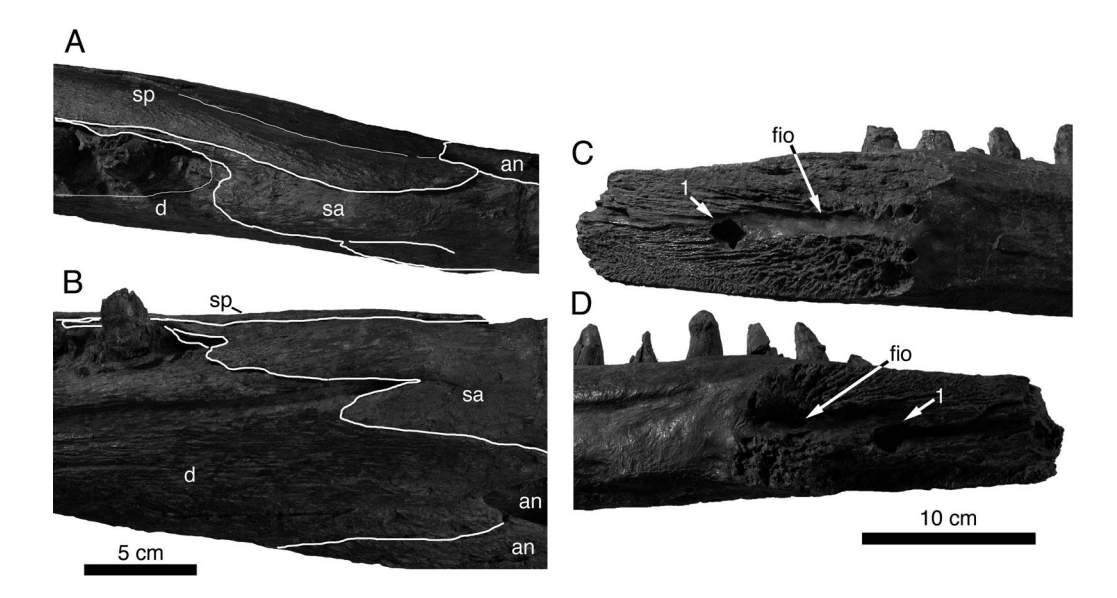


Fig. 22. Middle portion of the left dentary in dorsal (A) and lateral (B) views and anterior portion of the left (C) and right (D) mandibles. Abbreviations: an, angular; d, dentary; fio, foramen intermandibularis oralis; sa, surangular; sp, splenial; 1, a large circle hole by the breakage of the area.

sutures with the basisphenoid are not clearly defined. The lateral eustachian openings are not well preserved, but the left one is positioned lateral to the median opening (Fig. 20). However, a space between the basioccipital and pterygoid indicates that the exposure of the **basisphenoid** is small. The lateral exposure of the basisphenoid is not clear. A portion of the **laterosphenoid** and **prootic** are probably preserved because the foramen ovale is preserved, but their sutures between them and with other related elements are not clear.

The anterior portion of the palatines are damaged, as in the posterior portion of the maxillae, but the sutures with the maxillae are preserved (Figs. 8, 20, 21). These are broken between the suborbital fenestrae and the posterior portion has shifted dorsally from its original position. The anterior process of the palatines extend up to the level of the eleventh maxillary alveolus, which is more anteriorly positioned than the anterior limit of the suborbital fenestrae (Figs. 8, 21). The anterior ends of the palatines are poorly preserved, but the left palatine preserves a portion of the maxilla-palatine suture and shows that the suture lacks an acute anterior tip unlike other longistrine crocodylians (Brochu, 1997; Brochu, 1999) and is U-shaped in ventral view, which may produce a heart-shaped outline. The lateral borders of the palatines do not flare posteriorly, but rather parallel each other towards the posterior end of the maxilla-palatine suture at the anterior end of the suborbital fenestrae. Aoki (1983) recostructed the lateral borders of the suborbital fenestrae as being convex laterally, but these are nearly straight and parallel to each other. The width of the palatines between the suborbital fenestrae is greater than the transverse width of the suborbital fenestra (Table 1). The palatine-pterygoid suture runs more anterior than the posterior end of the suborbital fenestrae. An anterior process of the pterygoid result in the suture being V-shaped. The lateral end of the suture is positioned anterior to the

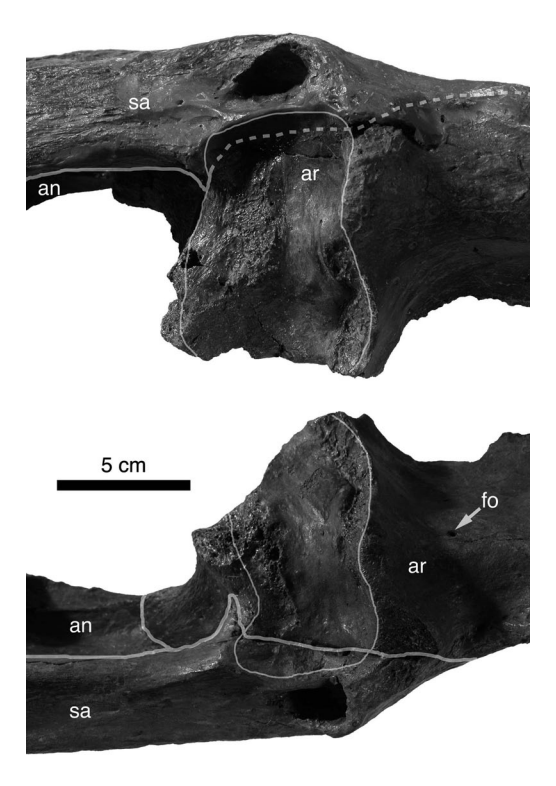


Fig. 23. Glenoids of right (top) and left (bottom) mandibles in dorsal view. Abbreviations: an, angular; ar, articular; fo, foramen; sa, surangular.

posterior corner of the suborbital fenestra, and the palatine does not contact the ectopterygoid, being separated by the involvement of the pterygoid into the posterior boundary of the suborbital fenestra.

The **pterygoid** is damaged at the anterior part of the pterygoid-ectopterygoid suture and its quadrate ramus is missing (Figs. 8, 20B). The ventrally exposed pterygoid is short anteroposteriorly. In ventral view, the pterygoids have a palatal process with an acute tip between the palatines. The process extends more anterior than the posterior end of the suborbital fenestrae but is more posterior than the posteriormost maxillary alveolus. The ventral surface of the process has a groove, which runs along the suture between the pterygoids. The pterygoids enclose the choana and have a pair of bowl-shaped depressions, divided by a low median ridge, anterolateral to choana. The pterygoids form a vertical plate that forms the posterior border of the choana. The plate is more posteriorly positioned than the posterior border of the pterygoid flanges in ventral view. The ventral border of the pterygoid, posterior to the choana, is slightly ventral to the basioccipital tubera (Fig. 10A). The posterior processes of the pterygoid are short and project posteroventrally. The pterygoid flanges have straight posterior border, vertical to the sagittal plane (Figs. 8, 20B). The flanges are thin medially but thicken laterally and have rugose lateral surfaces that may have been covered by cartilaginous material (Fig. 9). In lateral view, the pterygoid flanges are tilted posteriorly and its angle with respect to an imaginary horizontal plane is more than 45 degrees. The articulation of the pterygoid with the ectopterygoid shows

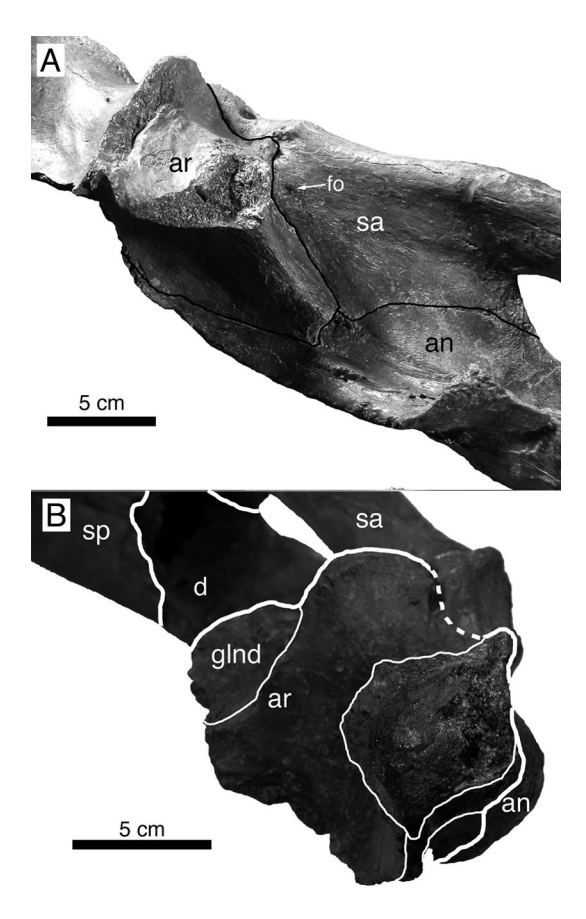


Fig. 24. Medial surface of the left mandible, anterior to the glenoid, (A) and retroarticular process of the right mandible ramus in posterior view (B). Abbreviations: an, angular; ar, articular; d, dentary; fo, foramen; glnd, glenoid; sa, surangular; sp, splenial.

a firm articulation, but it pattern is not clear (Fig. 20B). Posteriorly the flange of the pterygoid overlaps the ectopterygoid. The sutures with the braincase elements are not preserved.

The **ectopterygoids** are well preserved (Figs. 8, 9, 10, 17B, 20B). Anteriorly, the ectopterygoid has a process that pinches out on the ventral surface of the maxilla (Figs. 8, 21). The anterior process is short and extends up to the level between the fifteenth and sixteenth (posterior most maxillary alveolus) alveoli. The process does not join the formation of tooth alveoli. The base of the dorsal process of the ectopterygoid is preserved on the medial surface of the postorbital bar. The descending process of the ectopterygoid becomes wider posteriorly. The lateral edge of the process extends along the lateral edge of the process is thick medially for a suture with the pterygoid and is thin laterally.

The **vomer** is not visible at the premaxilla-maxilla suture, but the exposure of the vomer near the maxilla-palatine suture can not be confirmed because of the damage of the specimen (Fig. 8).

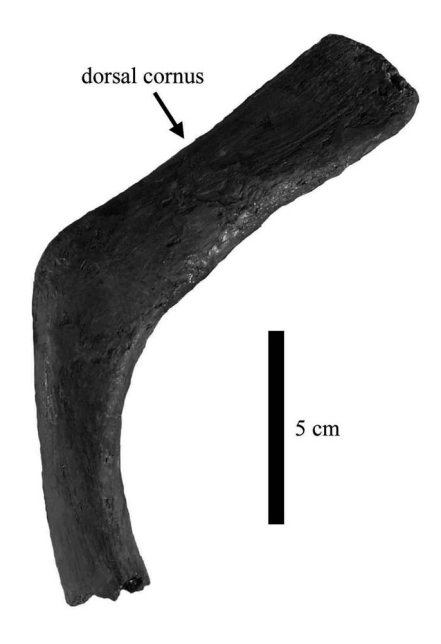


Fig. 25. Hyoid in dorsal (left) and ventral (right) views.

Mandible

The anterior portion of the mandible is missing (Figs. 11–14), which has been considered as a pathological feature (Katsura, 2004). The symphysis extends posteriorly up to the level between the ninth and tenth maxillary teeth. Both rami of the mandible diverge with an angle of roughly 30 degrees (Figs. 13–14). Anterior to the posterior end of the symphysis, the mandible is wider than high, but each ramus becomes higher posteriorly, reaching its maximum close to the mandibular fenestra (Figs. 11–12). The retroarticular process curves upward, and its tip is more dorsal to the glenoid in lateral view. The **coronoids** are not preserved.

The **dentary** is the longest element in the mandible (Figs. 11–14). Each dentary, with its anterior tip missing, preserves ten alveoli (labeled A-J in Fig. 28). The lateral surface of the dentary has a series of foramina below the tooth row, which are associated with shallow grooves (Figs. 11–12). The dorsal surface of the dentaries up to the posterior end of the symphysis is straight. In lateral view, the dentary has three processes. The dorsal one articulates with the anterior processes of the surangular, and the middle and ventral processes form the anterior border of the mandibular fenestra. The dorsal process is short and its lateral surface has a long and horizontally extending groove, starting from the level of the second most posterior dentary tooth. The middle process is longer than the ventral process and extends more posteriorly than the mid-length of the mandibular fenestra. The ventral process terminates more anteriorly than the mid-length of the mandibular fenestra and articulates with the angular ventrally.

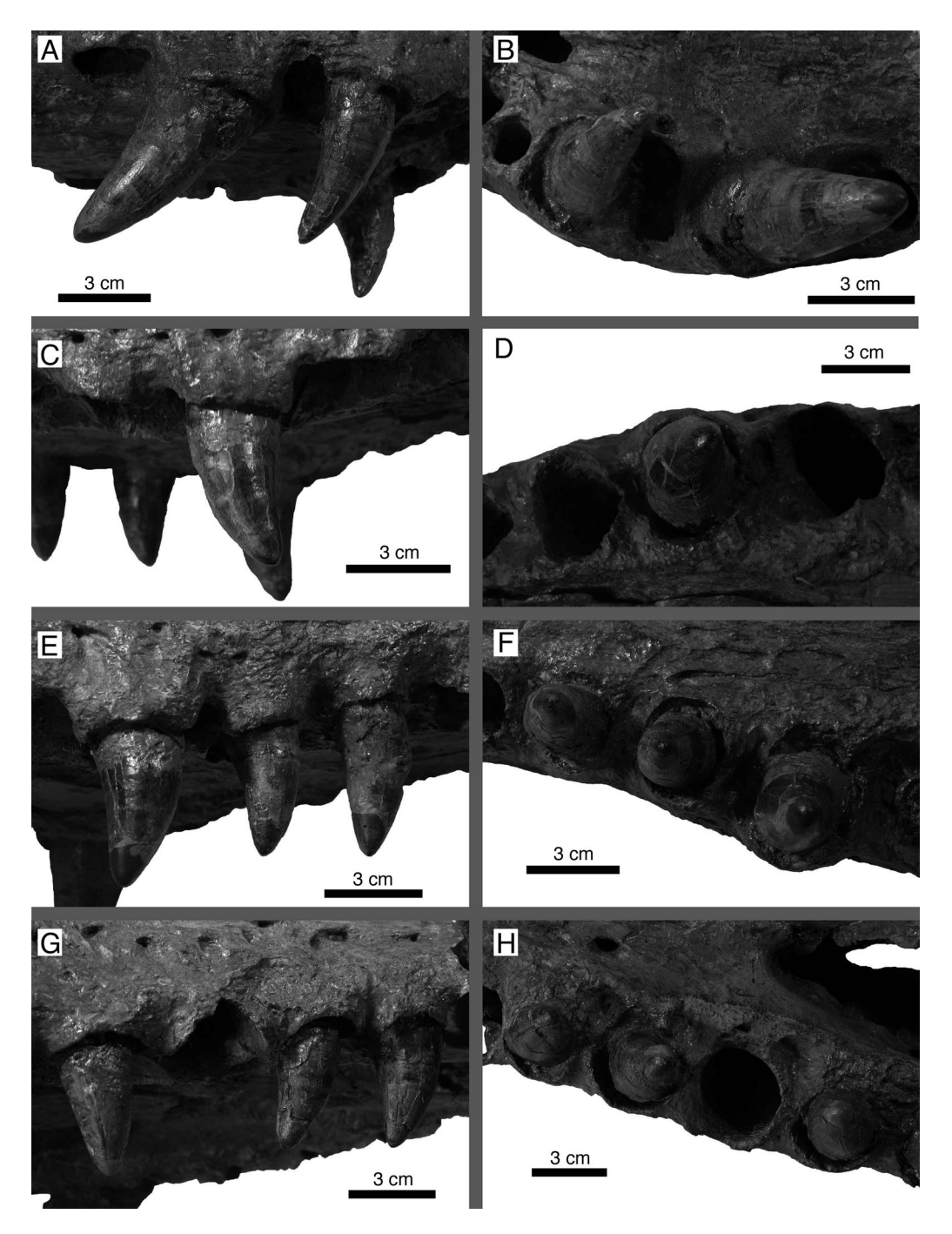


Fig. 26. Premaxillary teeth in right lateral (A) and occlusal (B) views and maxillary teeth in lateral (C, E, and G) and occlusal (D, F, and H) views.

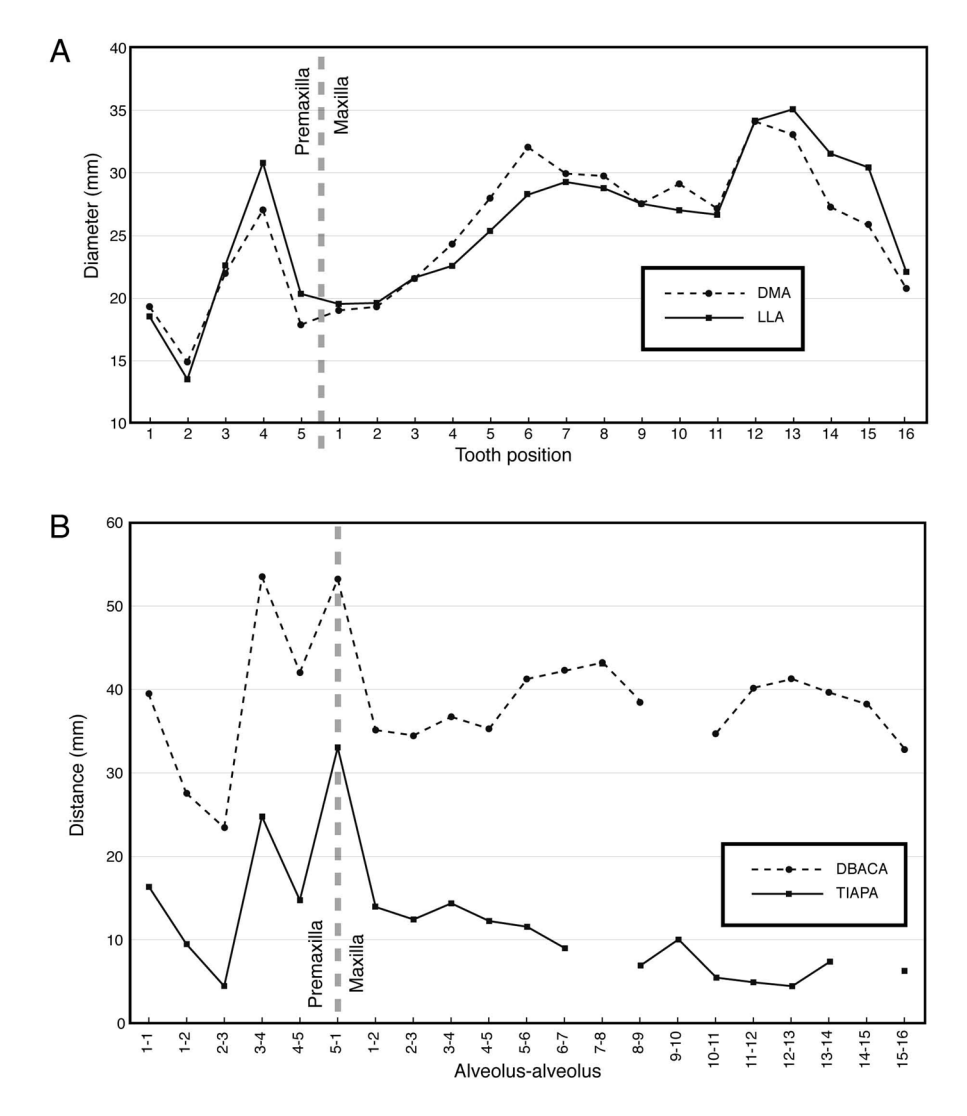


Fig. 27. Changes in alveolus diameters in the upper jaw (A) and changes in the distance between the centers of consecutive alveoli in the upper jaw (B). Abbreviations: DMA, diameter of alveolus in distal-mesial direction (average of left and right sides); LLA, diameter of alveolus in labial-lingual direction (average of left and right sides); DBACA, distance between alveoli's centers (average of left and right sides); TIAPA, thickness of inter-alveolus plate (average of left and right sides).

The anterior tips of the **splenials** are missing (Figs. 11–14). The splenials participate in the posterior portion of the symphysis for roughly the length of five alveoli (Fig. 13). In dorsal view, the articulated splenials become thinner anteriorly, forming a constricted V-shape. In medial view, the lingual surface of the splenial has a large circle hole, which is a result of breakage of the area (Figs. 11, 12, 22). Near the posterior end of the symphysis and posterior to the broken hole, the splenial has a single exit for the ramus of intermandibularis oralis of cranial nerve

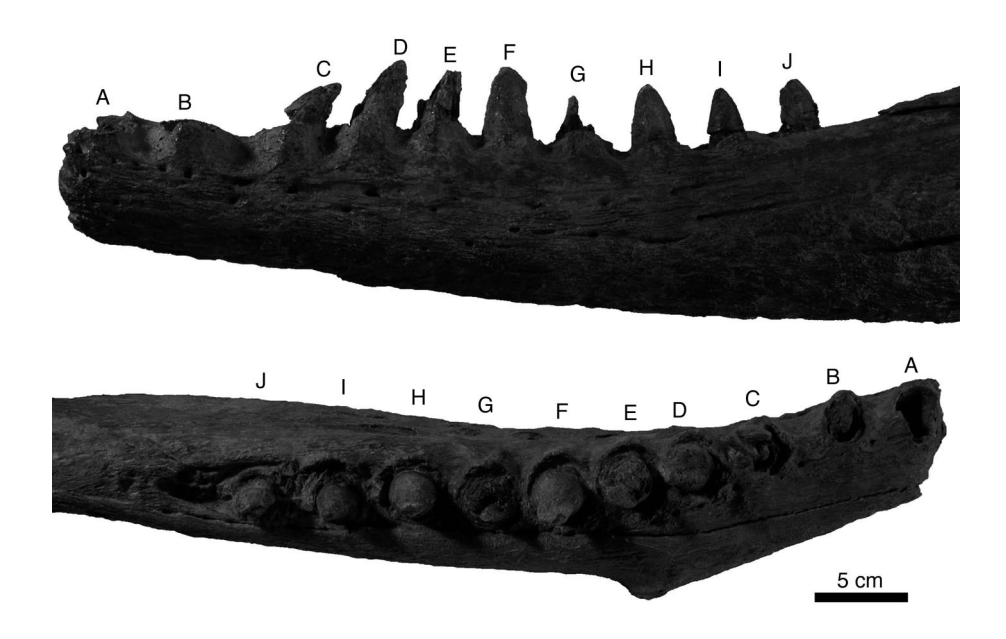


Fig. 28. Dentary teeth in left dentary in lateral (top) and occlusal (bottom) views.

V, and there is no other opening posteriorly, as in *Gavialis* (Brochu, 1997; Brochu, 1999). The splenial extends posteriorly to the level anterior to the mandibular fenestra (Figs. 11–12).

The lateral surface of the **surangular**, posterior to the mandibular fenestra, is heavily ornamented (Figs. 11-12). The dorsal surface of the element posterior to the fenestra is nearly flat and its medial marging is smooth. There is a large and deep depression lateral to the glenoid fossa (Fig. 23). The depression is oval-shaped, 32 mm long anteroposteriorly and 13 mm wide transversely. The surangular has two anterior processes interfingering with the posterior processes of the dentary (Fig. 22A). The dorsal process is long, reaching the tooth alveoli and articulating with the splenial medially. The process has another accessory thin process extending more anteriorly medial to the tooth alveoli up to the level of the second last dentary tooth. The ventral process is much shorter than the dorsal process and ends slightly anterior to the external mandibular fenestra. The ventral border of the ventral process forms a suture with the dentary. In lateral view, the surangular-angular suture extends posteriorly from the posterior angle of the mandibular fenestra but its posterior end is poorly preserved (Figs. 11-12). In medial view, the surangular-angular suture is more ventrally located than the suture in lateral view and posteriorlyends close to the tip of the anterior process of the articular. A minute foramen for the articular artery and alveolar nerve is present very close to the surangular-articular suture, anterior to the gleonid (Fig. 24A). In lateral view the anterior end of the surangular-angular suture terminates at the posteroventral border of the external mandibular fenestra (Figs. 11-12). The medial surface of the surangular has three formanina dorsal to the external mandibular fenestra.

The angular is the second longest element in the mandible with a long anterior process

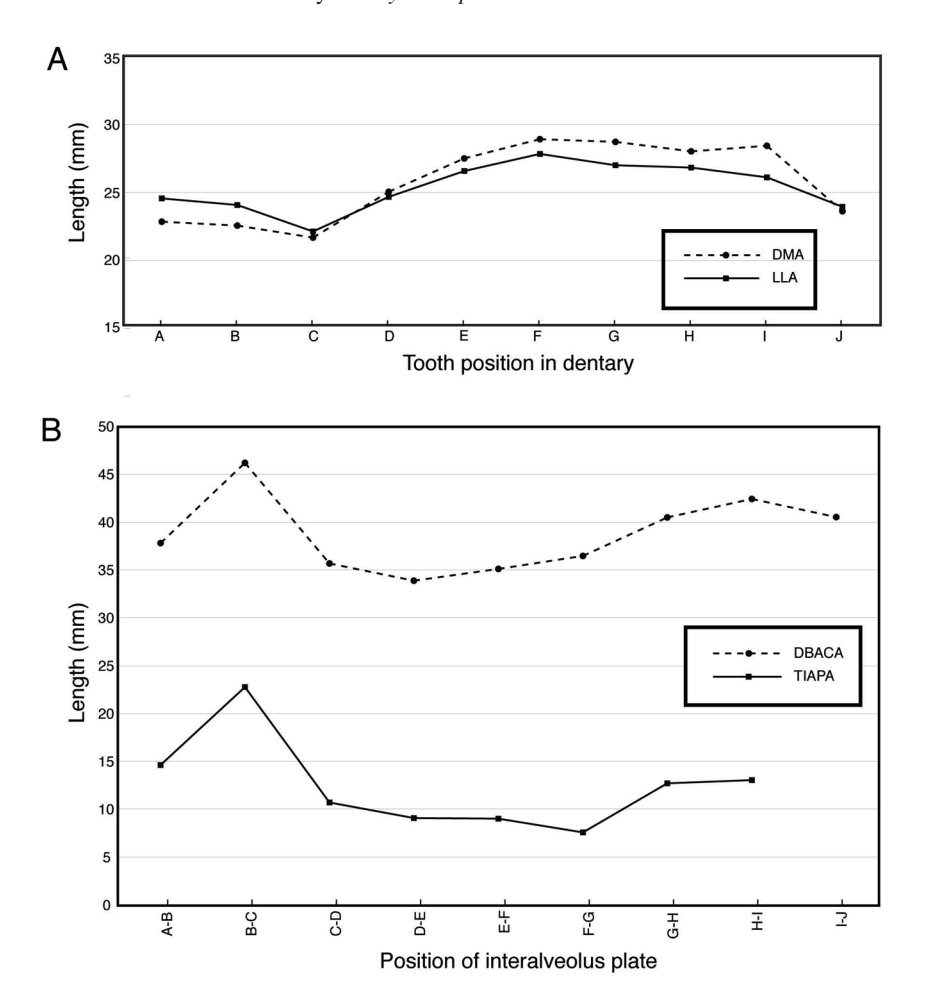


Fig. 29. Changes in alveolus diameters in the lower jaw (A) and changes in the distance between the centers of consecutive alveoli in the lower jaw (B). Letters (A-J) of the X-axis (Tooth position in dentary and Position of interalveolus plate) corresponds to ones in Fig. 28. Abbreviations: DMA, diameter of alveolus in distal-mesial direction (average of left and right sides); LLA, diameter of alveolus in labial-lingual direction (average of left and right sides); DBACA, distance between alveoli's centers (average of left and right sides); TIAPA, thickness of inter-alveolus plate (average of left and right sides).

(Figs. 11–12). In ventral view, the process extends anteriorly to the level of the second last dentary tooth and is wedged between the dentary and splenial (Fig. 14). The anterior process forms the ventral floor of the Meckelian canal and the ventral edge of the foramen intermandibularis caudalis in medial view. The dorsal process of the element, which forms the posterodorsal edge of the foramen, has broken off. The position of the foramen is more ventrally positioned than the ventral border of the external mandibular fenestra, suggesting that the foramen intermandibularis caudalis is no visible through the external mandibular fenestra in lateral view. The suture with the dentary in lateral view ends close to the anterior edge of the mandibular fenestra (Figs 11–12). The lateral surface of the main body of the angular has pits

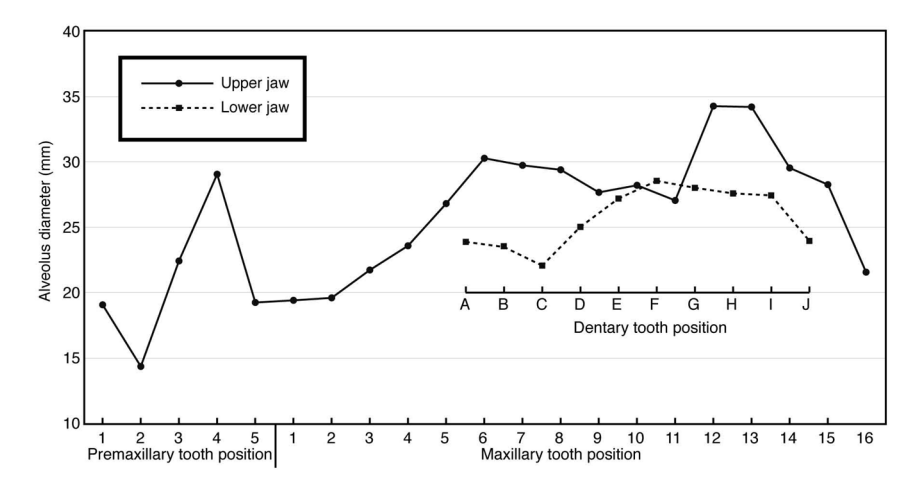


Fig. 30. Alveolus diameters in both upper and lower jaws.

and grooves, but the lateral surface of the posterior process is smooth, suggesting an area for an attachment of the *M. pterygoideus posterior*.

The **articular** forms the fossa-like glenoid (Figs. 11, 12, 13, 23, 24). The glenoid is divided into two depressions by a low ridge. The glenoid is bordered posteriorly by a ridge that runs perpendicular to the sagittal plane. The extreme medial end of the glenoid does not preserve a foramen aerum. The articular has an anteroventrally extending process and its lateral border forms a suture with the surangular (Fig. 24A). On its medial surface the surangular-articular suture is simple and straight. The suture lacks a "crocodyline process" (Aoki, 1992) although the presence of the process is mentioned by Taruno (1999). The anterior surface of the process is flat, lacking a sulcus like that seen in some longirostrine crocodylians, and is nearly perpendicular to the medial surface of the surangular. The retroarticular process of the articular was described as "distorted ventromedially" by Aoki (1983). The dorsal surface of the retroarticular process is divided into two areas by a low ridge running anteroposteriorly from the posterior tip of the retroarticular process (Fig. 24B). The lateral area is nearly horizontal and the medial one is facing mediodorsally.

The ossified **hyoid** (Fig. 25) elements (cornu branchiale I) are nearly complete. The cornu branchiale I is bent at its mid-length. The dorsal projection of the hyoid cornu is flat and has parallel side. The medial portion is rounded in cross section.

Dentition

Toyotamaphimeia has five **premaxillary** and sixteen **maxillary alveoli** on each side (Figs. 8, 15, 26). As described earlier, the preserved portion of each dentary bears ten posterior alveoli. All alveoli are circular in outline and are separated from each other. No groove or confluence of alveoli is present, suggesting a mature status of the specimen. Three premaxillary, nine maxillary, and eighteen dentary alveoli have partial or complete teeth in place. The tooth crown of all teeth is genrally similar in shape although the crown size and the position of the crwon

Table 2. Diameters of alveoli in premaxillae, maxillae, and dentaries in millimeters. Abbreviations: A-P length, anteroposterior lengths of alveoli; PM, premaxillary alveolus; M, maxillary alveolus; D, dentary alveolus.

Alveolus position —	A-P length				Transverse width			
	Left	Right	Ave	Left	Right	Ave		
PM-1	18.0	19.2	18.6	19.9	18.9	19.4		
PM-2	15.6	11.6	13.6	17.5	12.5	15.0		
PM-3	22.9	22.5	22.7	21.0	23.1	22.0		
PM-4	34.2	27.6	30.9	26.6	27.6	27.1		
PM-5	23.7	17.1	20.4	17.8	18.1	17.9		
M-1	20.0	19.2	19.6	19.9	18.3	19.1		
M-2	20.3	19.1	19.7	20.0	18.7	19.4		
M-3	23.3	20.2	21.7	23.1	20.2	21.6		
M-4	23.2	22.1	22.7	23.8	25.0	24.4		
M-5	28.7	22.2	25.4	27.1	29.0	28.1		
M-6	29.2	27.5	28.3	32.7	31.5	32.1		
M-7	31.0	27.7	29.4	38.2	21.8	30.0		
M-8	30.0	27.8	28.9	32.8	26.9	29.8		
M-9	27.6	_	_	_	27.6	_		
M-10	26.1	28.1	27.1	29.2	_	_		
M-11	31.0	22.5	26.7	31.5	23.0	27.2		
M-12	33.5	35.0	34.3	32.4	36.0	34.2		
M-13	35.9	34.4	35.2	31.1	35.2	33.2		
M-14	33.3	29.9	31.6	_	27.4	_		
M-15	30.5	_	_	25.9	_	_		
M-16	20.7	23.7	22.2	21.4	20.3	20.8		
D-A	22.8	_	22.8	24.5	_	24.5		
D-B	22.2	22.9	22.5	23.0	25.1	24.0		
D-C	21.5	21.7	21.6	23.6	20.6	22.1		
D-D	24.2	25.8	25.0	25.0	24.3	24.6		
D-E	27.0	27.9	27.5	25.7	27.4	26.5		
D-F	28.1	29.6	28.9	26.4	29.2	27.8		
D-G	29.0	28.4	28.7	26.1	27.9	27.0		
D-H	29.2	26.7	28.0	26.9	26.7	26.8		
D-I	29.2	27.5	28.4	25.9	26.3	26.1		
D-J	23.6	23.5	23.6	24.0	23.8	23.9		

carinae changes through the tooth series. The tooth crown is conical and its main axis is curved mesially in anterior teeth (up to seventh maxillary teeth) and lingually in more posterior teeth. The crown has two carinae. The carinae in posterior teeth are placed distally and mesially, but those in more anterior teeth are more lingually (distal carina) and labially (mesial carina) placed than the posterior teeth. In occlusal view, the direction of the distal and mesial carinae of the third premaxillary tooth is angled more than 45 degrees with respect to the sagittal plane. The crown has a series of faint striations.

The largest maxillary tooth was considered to be the seventh tooth (Aoki, 1983). However, our measurements of diameters of alveoli indicate that alveoli 12 and 13 are larger than the seventh alveolus. The tooth series in the upper jaw of *Toyotamaphimeia* has three enlargements in diameter, which are at the fourth premaxillary and seventh and twelfth maxillary alveoli (Fig. 27A). The increase in diameter of the fourth premaxillary alveolus from the third or fifth alveolus is enormous compared to seventh and twelfth maxillary alveoli, which are more gradual.

The distance between the centers of two consecutive alveoli corresponds with the thickness of the inter-alveolus plate. Both have two peaks at third-fourth premaxillary alveoli and the boundary between premaxillary and maxillary teeth (Fig. 27). The thickness of inter-alveolus plates in the maxilla shows a gradual decrease leading to a close spacing of the posterior maxillary teeth.

Although the anterior end of the dentary is not preserved, a pair of notches at the premaxilla-maxilla suture indicates that a large dentary tooth, presumably the fourth, occludes lateral to the premaxilla and maxilla. As described by Aoki (1983), occlusal pits are present along the lateral edge of the secondary palate medial to the tooth row and between consecutive maxillary teeth (Fig. 16A), suggesting that all teeth (except the fourth (?) dentary tooth and posterior most three teeth) in the lower jaw occlude medial to the tooth row of the upper jaw. Because the exact number of dentary teeth is unclear, in this paper the ten preserved dentary teeth are labelled from "A" to "J", where "J" is the last dentary tooth, (Fig. 28). Among preserved ten dentary alveoli with teeth in situ, tooth "C" is the smallest and the teeth become larger posteriorly. The distance between teeth "B" and "C" is large and is probably positioned at the level of the seventh maxillary tooth (Fig. 29). More posterior dentary teeth are relativley closer to one another as in posterior maxillary teeth. The lack of occlusal pits from thirteenth to sixteenth maxillary teeth indicates that the posterior most three dentary teeth meet with corresponding maxillary teeth in occlusion. This suggests that the large but more widely spaced fourth premaxillary teeth (and anterior maxillary teeth as well) are useful for grabing and piercing preys (Fig. 30). Closely placed, but laterally placed, in occlusion, the large seventh maxillary tooth may have been used for grabing and piercing with stronger force for fatal bites. The large posterior maxillary (thirteenth to sixteenth) and dentary teeth (posterior most three or H to J in Fig. 28) may be adapted for crushing.

Axial Skeleton

All cervical (9), dorsal (15), and sacral (2) vertebrae and three caudal vertebrae are preserved. The neurocentral sutures of all of preserved vertebrae are fused, indicating that specimen MOUF00001 is from an adult individual (Brochu, 1996).

Cervical Vertebrae

The **proatlas** (Fig. 31) is thin and plate-like, with its ventral surface and posterior margin very concave. It has a dorsomedian ridge along the midline. The ridge is low and becomes the tallest at its anterior end (roughly 4 mm high). The anterior edge of the element is wide and straight as in *Crocodylus americanus* (Mook, 1921) for a contact with the occipital region of the skull but lacks an anterior process, in contrast to the condidition in gavialoids (Bruchu, 1997; Brochu, 1999). The outline of the proatlas is boomerang-shaped in dorsal view, differing from massive and block shaped proatlas of some tomistomines (*Gavialosuchus americanus* and *Tomistoma schlegelii*). The posterolateral process is wide and has rounded posterior edge, and the transverse width of the proatlas becomes larger posteriorly in dorsal view. In lateral view, the ventral tubercle measured anteroposteriorly is less than half of the anteroposterior length of the proaltas measured along its medial ridge. The ventral surface of the posterolateral process has a depression bordered by scars.

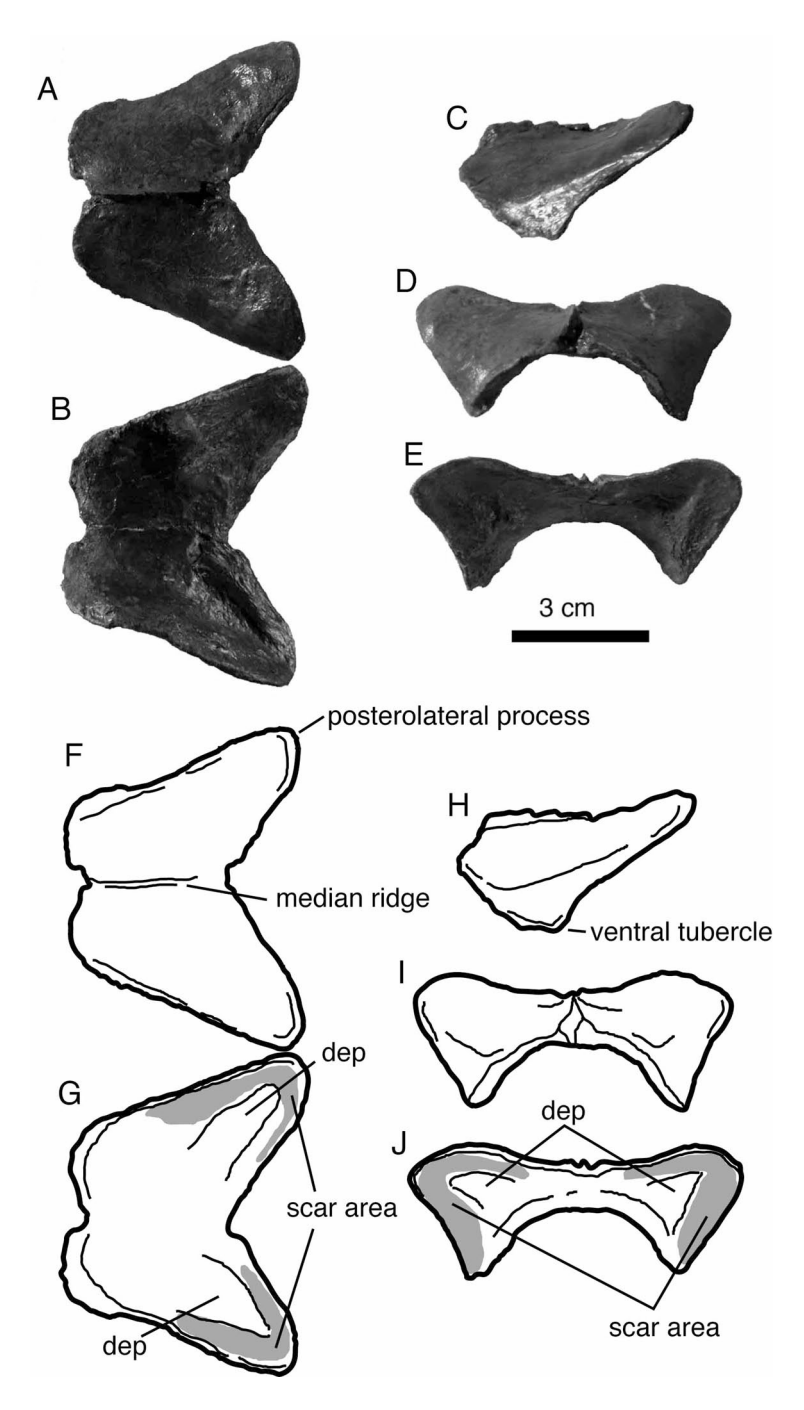


Fig. 31. Proatlas in dorsal (A and F), ventral (B and G), left lateral (C and H), anterior (D and I), and posterior (E and J) views. Abbreviation: dep, depression.

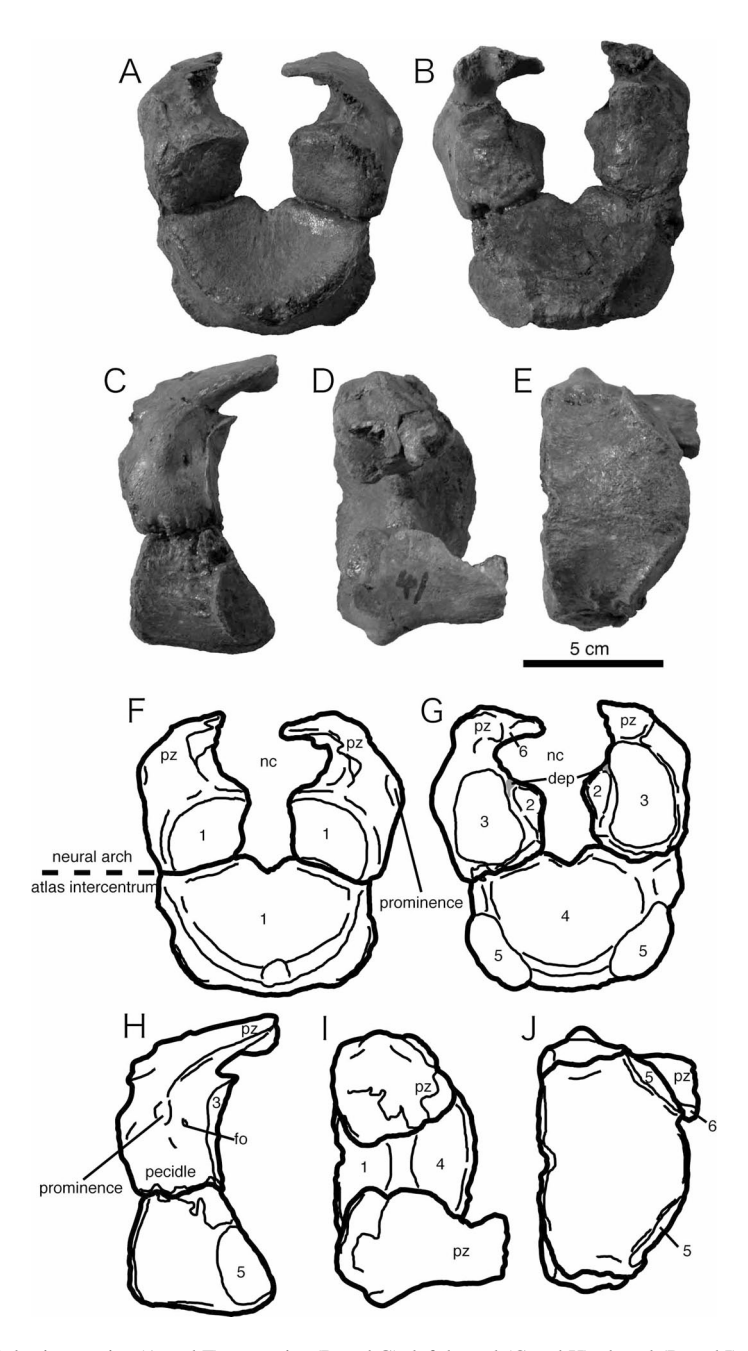


Fig. 32. Atlas in anterior (A and F), posterior (B and G), left lateral (C and H), dorsal (D and I), and ventral (E and J) views. Abbreviations: dep, depression; fo, foramen; pz, postzygapophysis; nc, neural canal; 1, articular surface with occipital condyle; 2, articular surface with odontiod process; 3, accessory articular surface for axial centrum; 4, articular surface with axial centrum; 5, articular surface with atlantal rib; 6, articular surface of postzygapophysis.

The right neural arch of the **atlas** (Fig. 32) is damaged. The paired neural arches do not contact each other but are well-sutured with the intercentrum. The transverse width of the atlas is much greater than that of the proatlas (Table 3). The neural arch has a thin and medially extending plate-like process but does not contact the other neural arch. The postzygapophysis extends posteriorly and has a small articular surface for the axis on its medial surface. The pedicels are massive. Anteriorly, the pedicel has slightly concave articular surface, facing anteroventrally, for the occipital condyle. Posteriorly, it is concave for an accessory articular surface of the axial centrum. The medial surfaces of the pedicels meet the odontoid process of the axis and have triangular shaped depressions posterior to the contact surface with the odontoid process. A prominence is present on the lateral surface of the pedicel. There is a single foramen posterior to the prominence. The neural canal is twice as wide as high. The atlas intercentrum is wedge-shaped in lateral view, unlike alligatorids. The posterolateral side of the intercentrum has an oval-shaped articular surface for the atlantal ribs.

The **axial** neural spine is low but longitudinally broad (Fig. 33). The dorsal edge of the spine is straight and slopes anteriorly at an angle of roughly 30 degrees from the neural canal and is without a crest, which is unlike tomistomines except *Dollosuchus dixoni* (Brochu, 2006). In lateral view, the neural spine is acute as in longirostrine taxa (Brochu, 1997; Brochu, 1999), and the posterior edge of the neural spine is straight and slightly tilted posteriorly. The posterior extremity of the spine ends posterior to the posterior limit of the neural arch pedicel but more anteriorly than the posterior end of the centrum and is low and acute as in longiostrine taxa. There is a shallow sulcus on the posterior edge of the spine.

The prezygopophysis on the right side is more complete than that on the other side and is small and short with a rugose articular surface. The postzygapophysis is thick and its dorsal border in posterior view is continuous from the neural spine. A pit is present at the anterior end of the articular surface. The pit is not perforated but is deep. The lateral sides of the neural arch are smooth and continuous from the dorsal edge of the neural spine. A week prominence tenatitively identified as a diaphophysis is presence close to the anterior end of the base of the neural arch. This is similar position and size to the one in *Gavialis gangeticus* (Brochu, 1997; Brochu, 1999). The neural canal is higher than wide in anterior/posterior view and is much smaller than the neural canal of the atlas.

The odontoid is fused with the axial centrum. The cone-shaped odontoid process is located on the dorsal half of the odontoid-axis complex. The dorsal surface of the odontoid process grades into the bottom of the neural canal. Lateral to the odontoid process are convex articular surfaces (19 mm wide and 31 mm high) for the atlantal neural arch. A depression is present on the lateral surface of the axial centrum ventral to the articular surfaces and a parapophysis is located ventral to the depression. The axial centrum has smooth and concave lateral surfaces. The height of the centrum is greater anteriorly. The cross-section of the ventral half of the centrum is box-shaped with vertical lateral surfaces. In lateral view, the anterior and posterior rims of the centrum are not parallel each other. The anterior rim is close to the vertical line with respect to the direction of the neural canal, but the posterior one is tilted anteriorly. The anterior portion of the ventral surface is smooth and may lack a hypapophysis, which may be due to its preservation. Even if this is due to preservation, the hypapophysis would probably have been small. The anterior portion of the ventral surface has a pair of ridges. A shallow depression is present lateral to the prominence. The posterior portion of the ventral surface bears a weak ridge. The

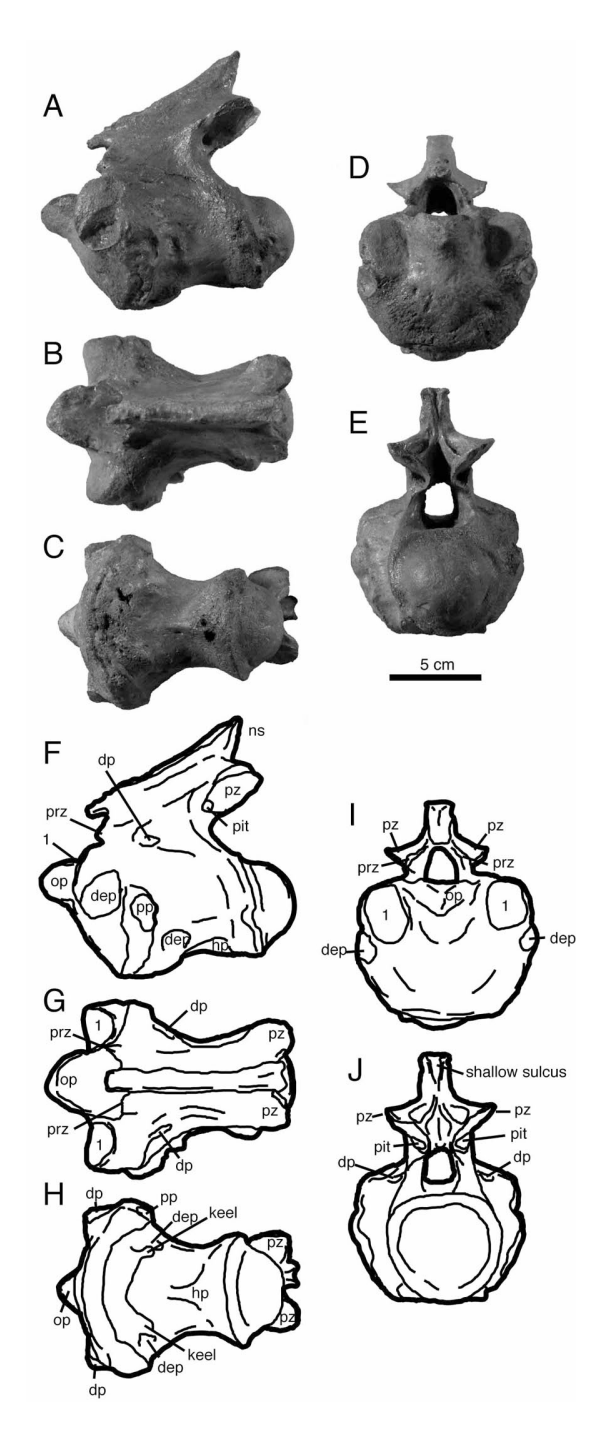


Fig. 33. Axis in left lateral (A and F), dorsal (B and G), ventral (C and H), anterior (D and I), and posterior (E and J) views. Abbreviations: dep, depression; dp, diapophysis; hp, hypapophysis; ns, neural spine; op, odontoid process; pp, parapophysis; prz, prezygapophysis; pz, postzygapophysis; 1, articular surface with atlantal neural arch.

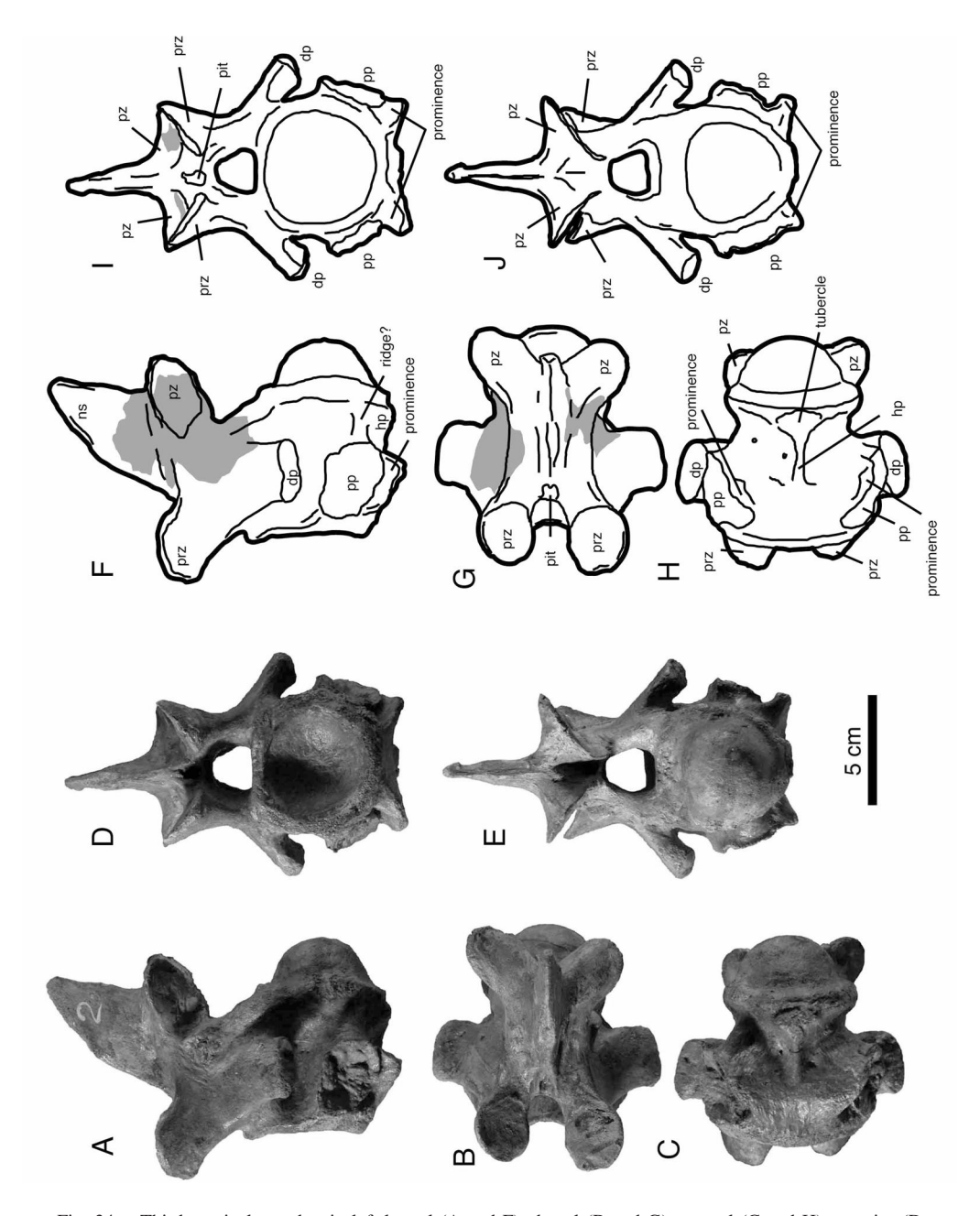


Fig. 34. Third cervical vertebra in left lateral (A and F), dorsal (B and G), ventral (C and H), anterior (D and I), and posterior (E and J) views. Abbreviations: dp, diapophysis; hp, hypapophysis; ns, neural spine; pp, parapophysis; prz, prezygapophysis; pz, postzygapophysis. Gray areas are missing parts, filled with plaster.

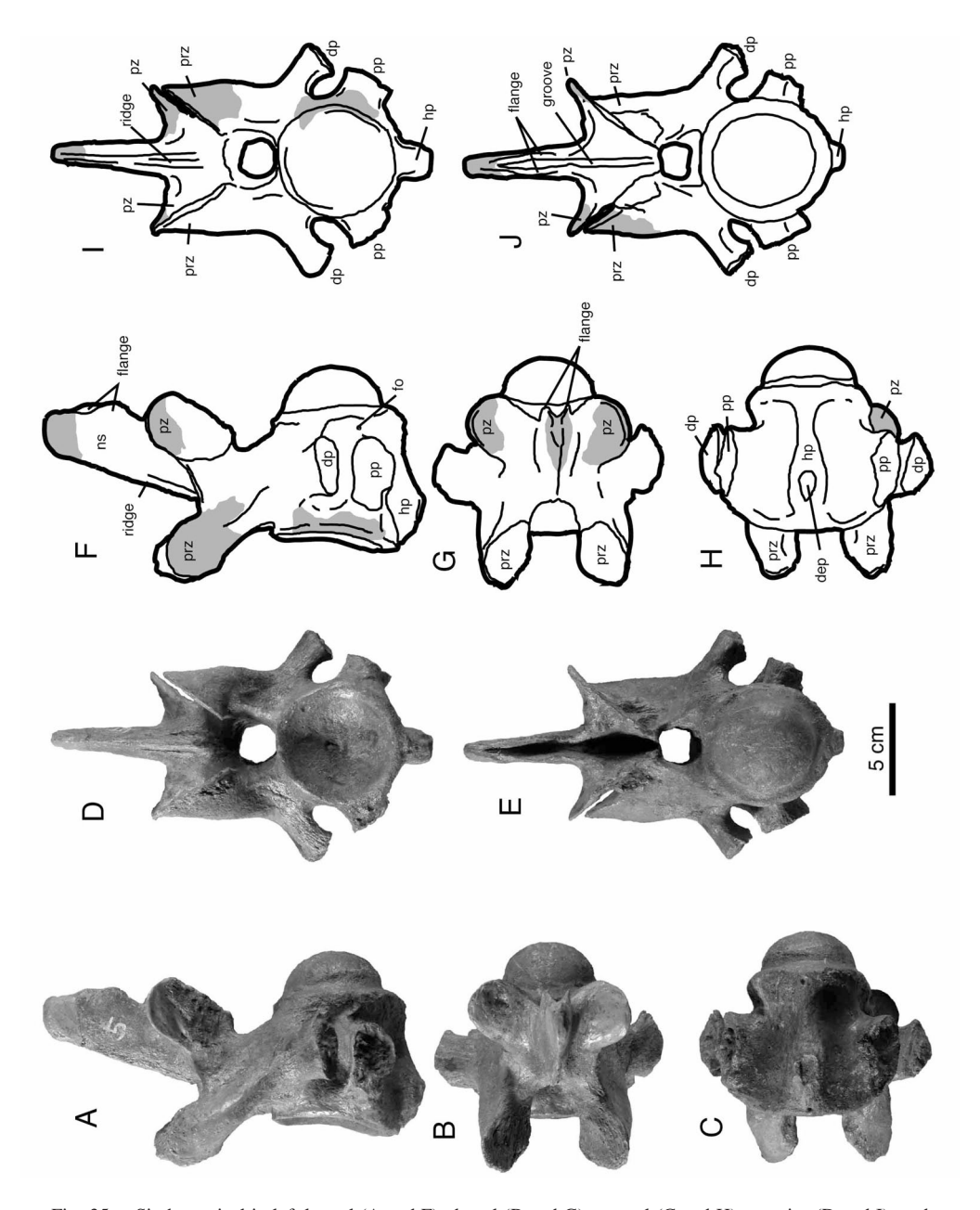


Fig. 35. Sixth cervical in left lateral (A and F), dorsal (B and G), ventral (C and H), anterior (D and I), and posterior (E and I) views. Abbreviations: dep, depression; dp, diapophysis; fo, foramen; hp, hypapophysis; ns, neural spine; pp, parapophysis; prz, prezygapophysis; pz, postzygapophysis. Gray areas are missing parts, filled with plaster.

Table 3. Measurements of vertebrae in the holotype of *Toyotamaphimeia machikanensis*. Abbreviations: CL, centrum length; CW, centrum width; CH, centrum height; AIVAS, anteroposterior depth of concave anterior intervertebral articular surface; PIVAS, anteroposterior height of convex posterior intervertebral articular surface; CoH, dorsoventral height of the condyle of the posterior intervertebral articular surface in posterior view; CoW, transverse width of the condyle of the posterior intervertebral articular surface in posterior view.

	Length	Width	Height				
Proatlas	53.6	68.6	29.0				
Atlas	47.0	92.0	95.5				
Axis	133.6	90.4	124.1				
	CL	CW	СН	AIVAS	PIVAS	СоН	CoW
Cervical 3	89.8	57.9	58.2	13.5	19.7	44.1	44.0
Cervical 4	92.7	62.1	60.5	14.0	23.0	50.5	46.1
Cervical 5	98.8	64.8	64.6	13.3	20.7	50.8	46.8
Cervical 6	98.0	64.1	71.0	14.7	28.6	53.8	51.0
Cervical 7	95.6	66.3	66.8	15.2	25.6	56.9	54.6
Cervical 8	96.1	68.8	67.8	17.1	26.4	59.0	59.3
Cervical 9	93.3	72.8	65.6	18.7	26.3	57.6	60.3
Dorsal 1	102.8	71.7	67.8	20.2	30.2	59.3	59.2
Dorsal 2	103.0	65.0	69.8	20.2	31.2	63.5	56.0
Dorsal 3	108.5	61.7	70.4	19.8	31.8	63.3	56.2
Dorsal 4	111.2	58.5	73.1	19.1	29.9	66.5	56.1
Dorsal 5	110.3	62.1	71.3	19.1	31.3	64.0	58.2
Dorsal 6	113.7	65.9	73.3	20.9	31.2	66.7	62.9
Dorsal 7	113.3	64.4	73.4	16.8	28.7	66.8	61.7
Dorsal 8	116.1	62.4	69.9	18.7	28.7	64.9	61.8
Dorsal 9	115.5	68.2	70.1	16.9	28.8	61.7	61.5
Dorsal 10	121.7	68.6	69.0	18.3	26.7	60.0	_
Dorsal 11	118.1	73.1	68.3	18.9	25.6	57.7	61.0
Dorsal 12	117.5	66.1	66.1	16.8	29.2	57.2	60.5
Dorsal 13	113.9	74.1	66.5	18.5	30.1	57.0	63.0
Dorsal 14	108.8	82.7	66.9	18.5	26.4	54.4	63.3
Dorsal 15	101.2	92.4	60.7	17.1	26.9	49.3	79.9
Sacral 1	86.9	74.4	51.7				
Sacral 2	84.0	87.6	58.6				
Caudal 1	105.3	72.3	65.5				
Caudal 2	84.9	77.2	62.2				
Caudal 3	80.8	68.0	62.8				

ridge is higher posteriorly and fades away anteriorly. The sphere-shaped posterior intervertebral articulation is large.

Post-axial cervical vertebrae (Figs. 34–36) are different from the axis in having a high neural spine, short processes for the parapophyses and diapophyses, and spherically concave anterior intervertebral articular surface.

The third cervical vertebra is distinguishable from the other post-axial cervical vertebrae based on the structures of the neural spine, hypapophysis, and paired ridges ventral to the diapophyses (Figs. 34, 36). The dorsal half of the neural spine is triangular in lateral view. The anterior edge of the neural spine is not ridged or the posterior edge is not grooved as in other post-axial cervical vertebrae. Unlike other vertebrae a pit is present at the base of the neural spine on the anterior edge between prezygapophyses. The hypapophysis is located at the

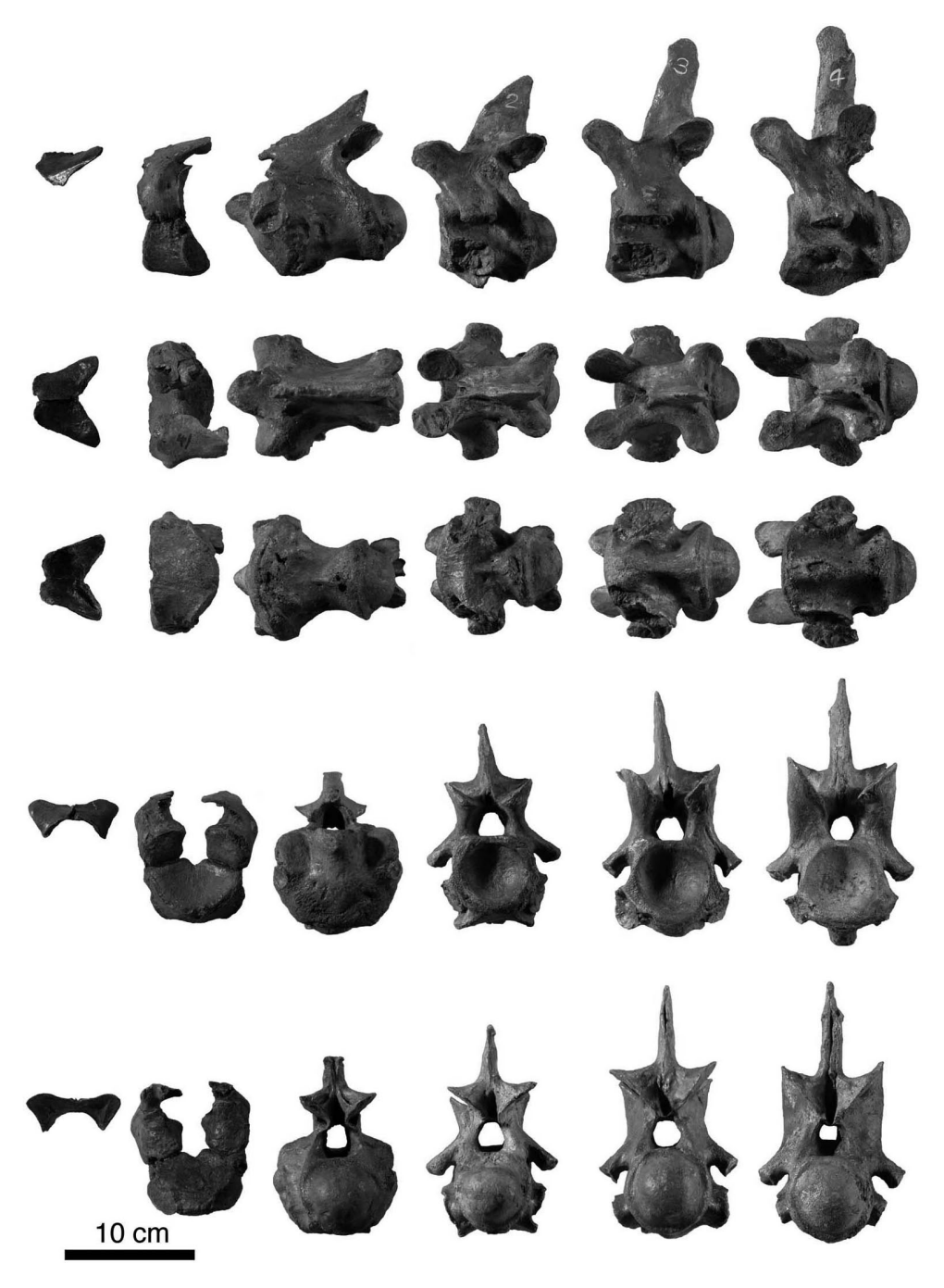


Fig. 36. All cervical vertebrae in left lateral, dorsal, ventral, anterior and posterior views. Parts filled by plaster are: cervical 4, whole neural spine, right portion of neural arch, and part of left postzygapophysis; cervical 5, base and tip of left prezygapophyses; cervical 7: neural spine and tip of left postzygapophysis; cervical 8, left postzygapophysis, tip of right postzygapophysis, and left posterior portion of the centrum; cervical 9, base of right prezygapophysis and right anterior portion of the centrum.

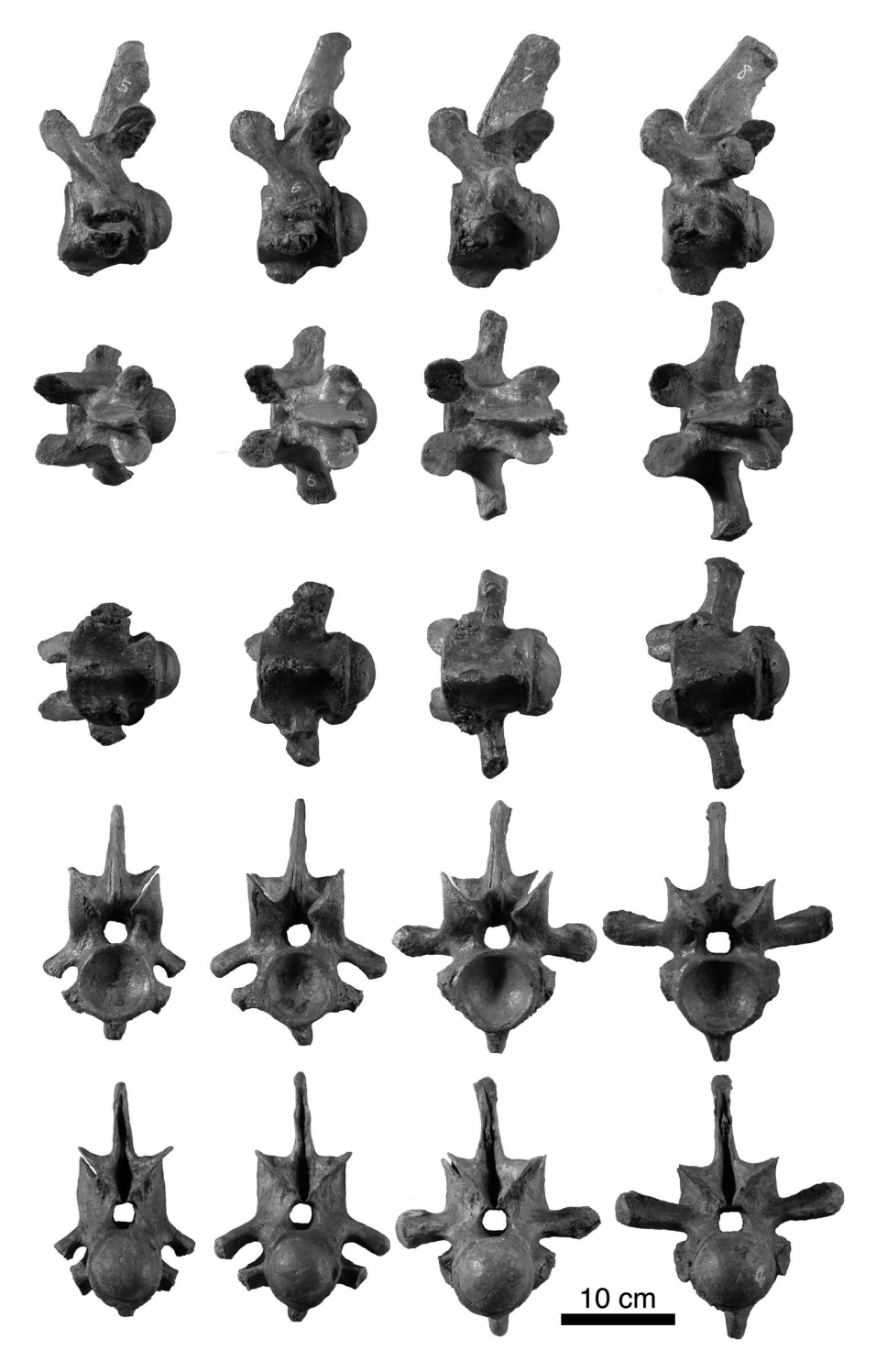


Fig. 36. cont.

posterior half of the ventral surface of the centrum as in the axis. It is weak but stronger than the one in the axis. The hypapophysis forms a tubercle posteriorly for the attachement of some fibers of the M. longus capiti (Cong et al., 1998). Paired ridges on the ventral surface are ventrolaterally projecting and anteromedial-posterolaterally oriented in ventral view and are similar to the prominences on the ventral surface of the axis in their arrangment. The ridge becomes higher posteriorly and ends at the same level of the posterior border of the parapophysis. The prezygapophyses and postzygapophyses are similar in shape among the post-axial cervical vertebrae (Fig. 36). The pre- and postzygapophyses are short in the third cervical vertebra and becomes longer posteriorly. The prezygapophyseal articular surfaces of the third cervical vertebra are circular in shape and are angled by approximately 45 degrees from an imaginary horizontal line. The postzygapophyses are tilted by 45 degrees in lateral view and these articular surfaces are oval-shaped. The diapophysis is originated from the base of the neural arch, dorsal to the fused neurocentral suture, and oriented lateroventrally. It is slightly longer than the parapophysis. Its anteroposterior length is twice as long as the thickness of the diapophysis. The distal end is slightly expanded and is placed close to the sutural surface of the parapophysis. The articular surface of the diapophysis with the cervical rib is convex and relatively smooth to the rib articular surface of the parapophysis. The anterior edge of the diapophysis is smoothly continuous to the anteroventral border of the prezygapophysis. The parapophysis on the lateral side of the centrum is ventral to the fused neurocentral suture and lateroventrally directed. It is short and occupies the anterior half of the lateral surface of the centrum. The sutural surface with the cervical rib is convex and rugose and is semicircle-shaped in lateral view. The anteroposterior length of the sutural surface is as long as half of the centrum length. Posterior to the sutural surface, a ridge leading to the posterior edge of the centrum divides the lateral surface of the centrum into dorsal and ventral concave surfaces. The dorsal concave surface is larger than the ventral one. The ridge is rounded in its cross-section.

The centra of all vertebrae expect the sacral vertebrae are procoelous. The size (central height, width, and length) of the cervical centra gradually becomes larger in more posterior cervical vertebrae (Table 3). The anterior and posterior intervertebral articular surfaces, having ball-and-socket articulation, are deeper and higher, respectively, posteriorly. The diameter of the sphere-shaped posterior intervertebral articular surface in posterior view is between 75 and 85% of the dorsoventral depth of the centrum in the third to sixth cervical vertebrae but is more than 85% in more posterior cervical vertebrae. These indicate that the anterior (third to sixth) cervical vertebrae have better degree of freedom in intervertebral movement and the posterior cervical vertebrae are adapted for the stability of intervertebral articulations.

The cervical vertebrae, posterior to the third cervical vertebra, are morphologically similar to each other except for the shape of ridges on the central ventral surfaces, diapophyses, and parapophyses (Fig. 36). The fourth cervical vertebra is distinguishable from the other post-axial cervical vertebrae in having diminished paired ridges with anteriorly positioned hypapophysis on the ventral surface. The paired ridges are absent in all vertebrae posterior to the fourth cervical vertebra. In the fourth to seventh cervical vertebrae, the diapophyses and parapophyses are positioned close to each other in lateral view as in the third cervical vertebra (Fig. 35). The diapophyses are slightly longer than the parapophyses. The articular surfaces of the parapophyses are oval-shaped with an anteroposteriorly oriented long axis. In the eighth and ninth cervical vertebrae, the diapophyses are much longer than the parapophyses and

horizontally oriented as transverse processes (Fig. 37). The parapophyses are small and their articular surfaces are circular. The parapophysis is more dorsally positioned in more posterior cervical vertebrae, but still ventral to the fused neurocentral suture in the last cervical vertebra.

The posteriorly tilted neural spine becomes higher and anteroposteriorly longer posteriorly. The dorsal ends of the neural spines are squared-off. The dorsal tip of the fifth cervical vertebra is thin but the neural spines of the eighth and more posterior cervicals are transversely wider at their dorsal tip. The anterior edge of the neural spine is ridged and the posterior edge is grooved for the supraspineous ligaments. The ridge along the anterior edge is stronger ventrally. The posterior groove is deepest between the postzygapophyses and becomes deeper in more posterior cervical vertebrae. Posteriorly extending flanges are present on the posterior edge. In anterior and posterior views, the angles of the prezygapophyseal and postzygapophyseal articular surfaces are steeper in the more posterior vertebrae and the long axes of the oval shaped articular surfaces are nearly vertical to the sagittal plane, indicating that this neck region was better functioned for dorsoventral movement. The centra have a foramen posterior to the parapophysis on each side. The hypapophysis extends along the ventral edge of the centrum and is strongest at the anterior end. The ventral surface of the hypapophysis has a cup-shaped depression.

Dorsal Vertebrae (Figs. 37–42)

The dorsal vertebrae can be separated into three segments, anterior (first and second dorsals), middle (third to tenth dorsals) and posterior (eleventh to fifteenth dorsals). The anterior dorsal vertebrae are similar to the eighth and ninth cervical vertebrae in having the parapophyses on the centra and the hypapophysis, which are stronger than the ones in the cervical vertebrae (Fig. 37). The middle dorsal vertebrae have parapophyses on the transverse processes (Fig. 38), whereas the posterior dorsal vertebrae (also termed "lumber" vertebrae by some) lack the parapophyses (Fig. 39).

In lateral view, the neural spines of the first seven dorsal vertebrae are posteriorly tilted, that of the eighth dorsal vertebra is perpendicular to the horizontal plane, and those of the ninth to fifteenth dorsal are anteriorly tilted (Figs. 40–42). The dorsal edges of all dorsal neural spines are horizontal. The anterior length of the neural spine is consistent in all of middle dorsal vertebrae and smaller in anterior and greater in posterior vertebrae. The dorsal edge is transversely expanded. The anterior edge of the neural spine has a keel, which fits into a groove along the posterior edge of the neural spine (hyposphene-hypantrum articulation). The anterior keel is the most pronounced at the ventral half of the neural spine. Corresponding with this, the posterior groove is deepest on the ventral half of the neural spine and between the postzygapophyses. A pit is present ventral to the anterior keel at the base of the neural spine.

The prezygapophyses are shorter than those in the cervical vertebrae, and the postzygapophyses become gradually smaller in more posterior dorsal vertebrae (Figs. 40–42). The articular surfaces are oval-shaped with a transversely oritented long axis. In anterior and posterior views, the prezygaposphyseal and postzygapophyseal articular surfaces of the second, third, and posterior dorsal vertebrae are angled less than 45 degrees with respect to the horizontal plane. The angles of the postzygopophyseal surfaces of the first and fourth to tenth dorsal vertebrae are roughly 45 degrees. The medial sides of the postzygapophyses have shallow depressions.

The transverse processes of the anterior dorsal vertebrae are short. They increase in length

posteriorly and are longest in the middle dorsal vertebrae, and become shorter on the posterior dorsal vertebrae (Figs. 40–42). The processes are rounded in cross section in the anterior dorsal vertebrae and are dorsoventrally flat in the other dorsal vertebrae. The ventral surfaces of the transverse processes of the third to tenth dorsal vertebrae have the parapophyses. The parapophyses of the third dorsal vertebra are positioned more proximal than the mid-length of the transverse processes, whereas these of the fourth to tenth dorsal vertebrae are more distally located. In dorsal view, the anterior and middle dorsal vertebrae have squared-off distal ends of the transverse processes because of the presence of the diapophyses. The transverse processes of the posterior dorsal vertebrae become narrower distally.

The centra of dorsal vertebrae are longer anteroposteriorly than the cervical vertebrae (more than 100 mm in length). The length of the centra increases towards the tenth dorsal vertebra and the decreases in the posterior dorsal vertebrae (Figs. 40-42) (Table 3). The central heights are nearly consistent up to the eleventh dorsal vertebra (roughly 70 mm in height) but are smaller in the more posterior dorsal vertebrae. The centra of the anterior and middle dorsal vertebrae are higher than wide. Those of the posterior dorsal vertebrae are wider than high, and the last dorsal vertebra (fifteenth) reaches to the maximum relative width (152%). The diameters of the sphere-shaped condyle of the posterior intervertebral articular surfaces are roughly 90% of the diameter of the centra in the anterior and middle dorsal vertebrae. The diameters in the posterior dorsal vertebrae are less and are similar to the cervical vertebrae. This differences may be a result of a reduced amount of freedom of movement between the anterior and middle dorsal vertebrae than the posterior dorsal vertebrae or the cervical vertebrae because the anterior and middle dorsal vertebrae have articulations with the dorsal ribs. The condyles of the posterior intervertebral articular surfaces are spherical in anterior and middle ones but those of the posterior dorsal vertebrae are not because of a concave dorsal edge in posterior view. The lateral surfaces of the dorsal centra are smooth, except for the anterior dorsal vertebrae, which have parapophyses, and have a single foramen on each side (Fig. 37). In lateral view, the anterior and posterior intervertebral articular surfaces of the anterior and middle dorsal vertebrae are nearly vertical relative to the horizontal plane, but on the posterior dorsal vertebrae these surfaces are slightly tilted anteriorly (Figs. 40-42). The hypapophyses are present at the anterior end of the ventral surface up to the third dorsal vertebra (Fig. 37), but that of the third dorsal vertebra is weak. The ventral surfaces of the fourth to seventh dorsal vertebrae are smooth (Fig. 38), whereas the eighth and ninth dorsal vertebrae have a weak median ridge on the ventral surface. The ventral surfaces of the tenth to fifteenth dorsal vertebrae are flat in cross section and have a shallow and wide sulcus (Fig. 39).

Sacral Vertebrae (Figs. 43–44)

The two **sacral vertebrae** are fused with the sacral ribs. The neural spine, missing in the first, of the second sacral vertebra is similar to that of the posterior dorsal vertebrae (Fig. 44). The spine is tilted slightly anteriorly and has a horizontal dorsal border in lateral view. Its distal end is transversely expanded. Both the anterior and posterior edges of the neural spine of the second sacral vertebra have a keel. At the base between the postzygapophyses the neural spine has a depression. The prezygapophyses of the first sacral vertebra are as large as the last dorsal vertebra (Fig. 43). The prezygapophyses of the second sacral vertebra and the postzygapophyses of the both sacral vertebrae are smaller than those of the dorsal vertebrae. The width of

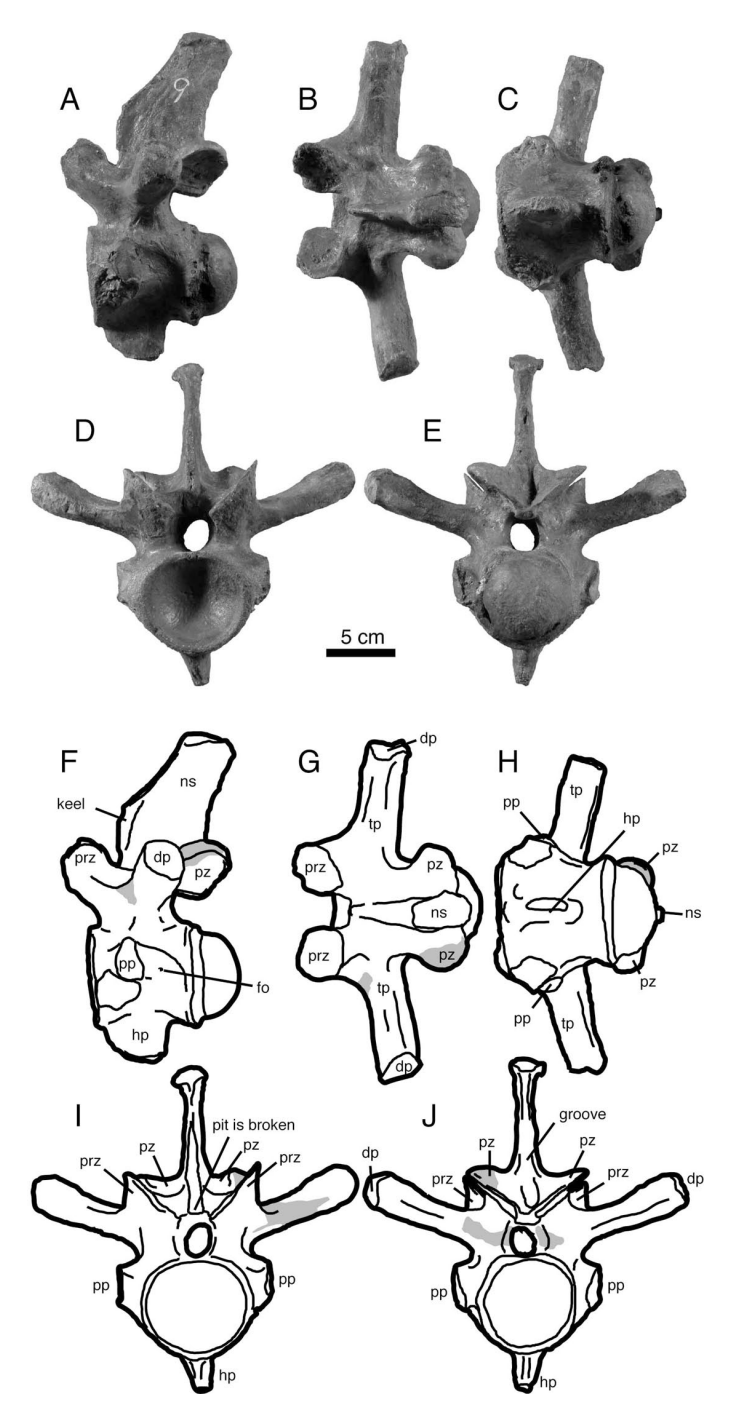


Fig. 37. Anterior (first) dorsal vertebra in left lateral (A and F), dorsal (B and G), ventral (C and H), anterior (D and I), and posterior (E and J) views. Abbreviations: dp, diapophysis; fo, foramen; hp, hypapophysis; ns, neural spine; pp, parapophysis; prz, prezygapophysis; pz, postzygapophysis; tp, transverse process. Gray areas are missing parts, filled with plaster.

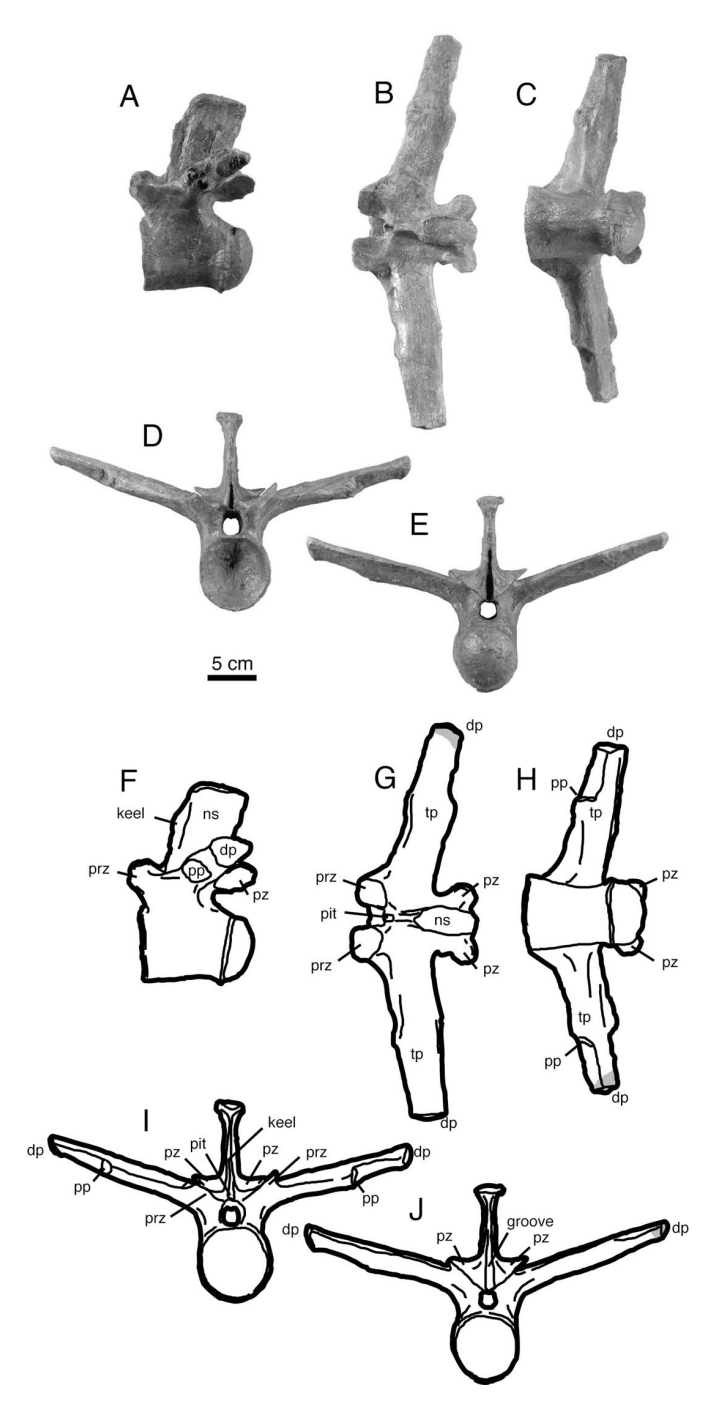


Fig. 38. Middle (fifth) dorsal vertebra in left lateral (A and F), dorsal (B and G), ventral (C and H), anterior (D and I), and posterior (E and J) views. Abbreviations: dp, diapophysis; ns, neural spine; pp, parapophysis; prz, prezygapophysis; pz, postzygapophysis; tp, transverse process. Gray areas are missing parts, filled with plaster.

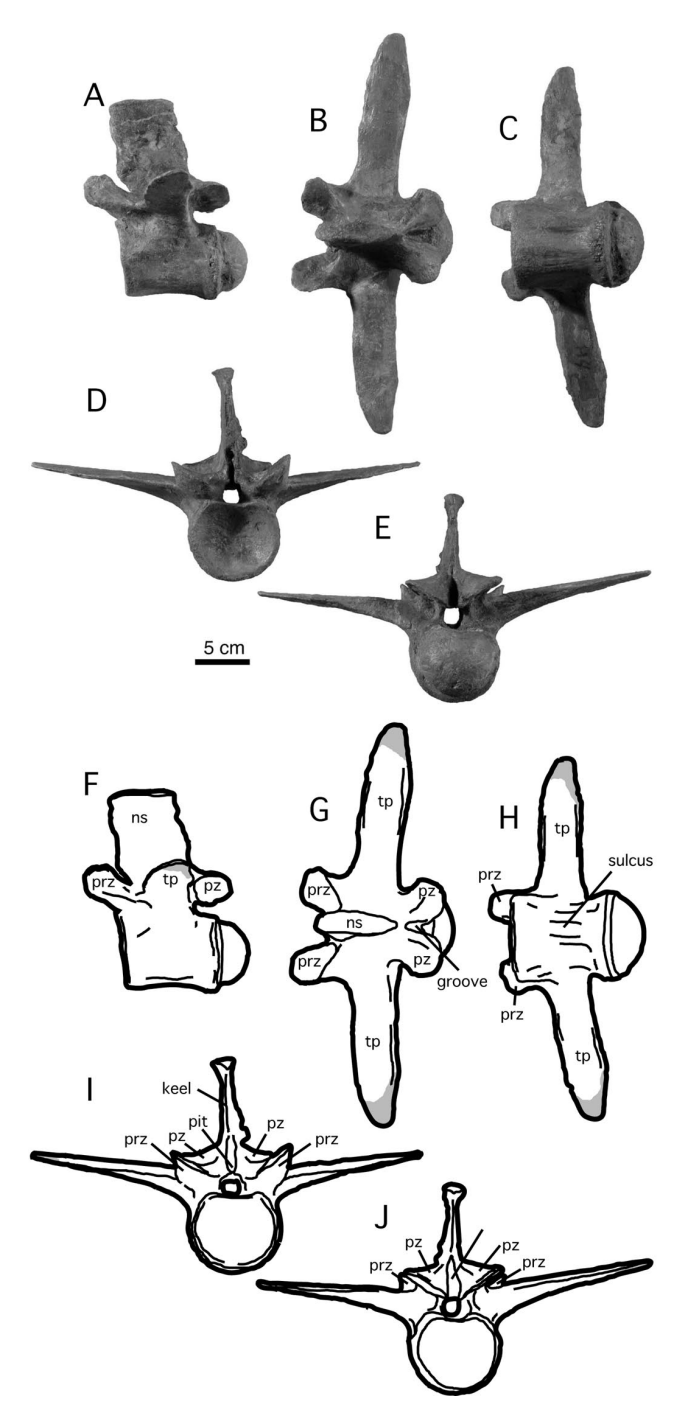


Fig. 39. Posterior (thirteenth) dorsal vertebra in left lateral (A and F), dorsal (B and G), ventral (C and H), anterior (D and I), and posterior (E and J) views. Abbreviations: ns, neural spine; prz, prezygapophysis; pz, postzygapophysis; tp, transverse process. Gray areas are missing parts, filled with plaster.

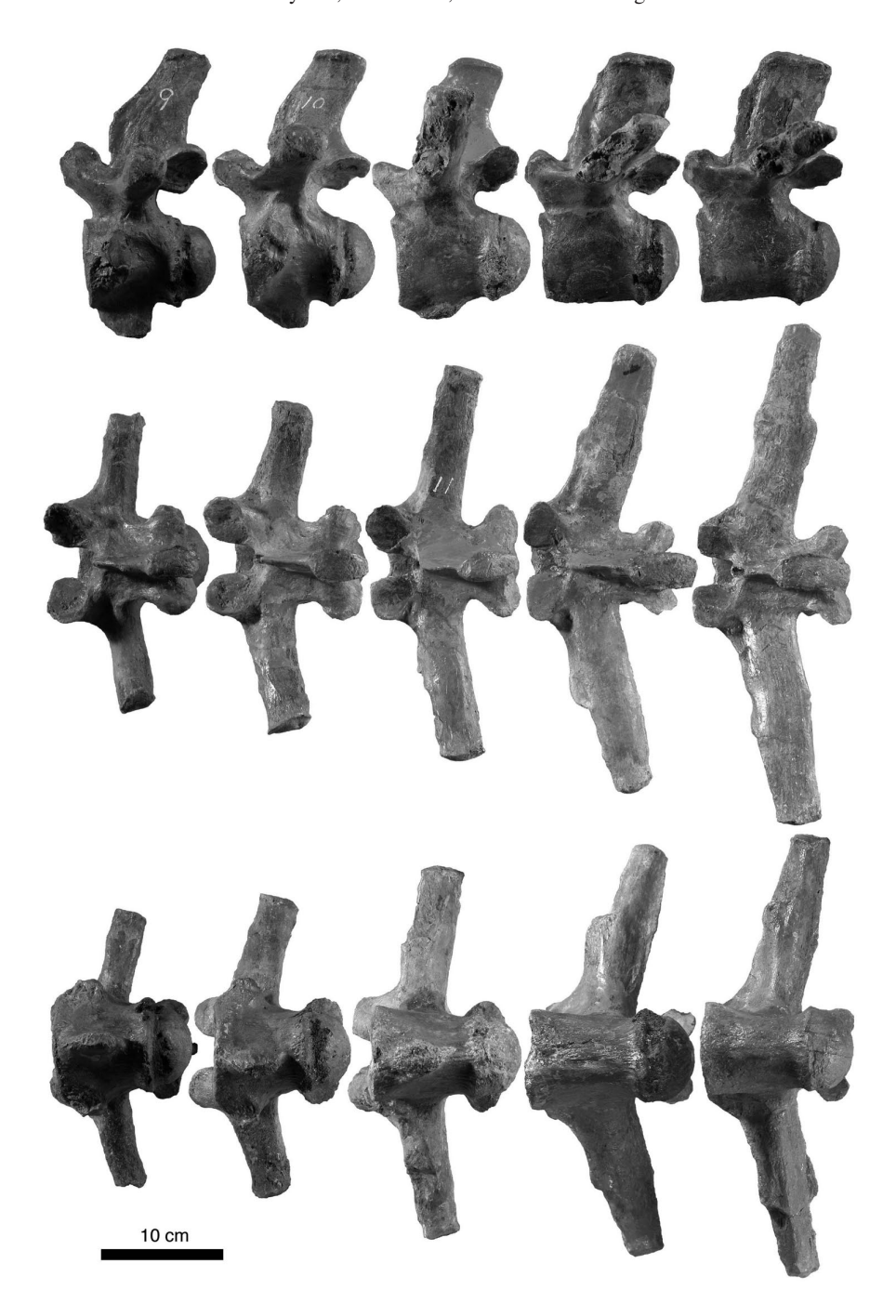


Fig. 40. First to fifth dorsal vertebrae in left lateral, dorsal, ventral, anterior and posterior views. Parts filled by plaster are: dorsal 6, tip of left transverse process; dorsal 7, dorsal tip of neural spine, tip of left transverse process, and tips of both prezygapophyses; dorsal 8, base of neural arch and right postzygapophysis; dorsal 9, tip of left transverse process, right prezygapophysis, left postzygapophysis, and base of neural spine; dorsal 10, left posterior part of centrum.

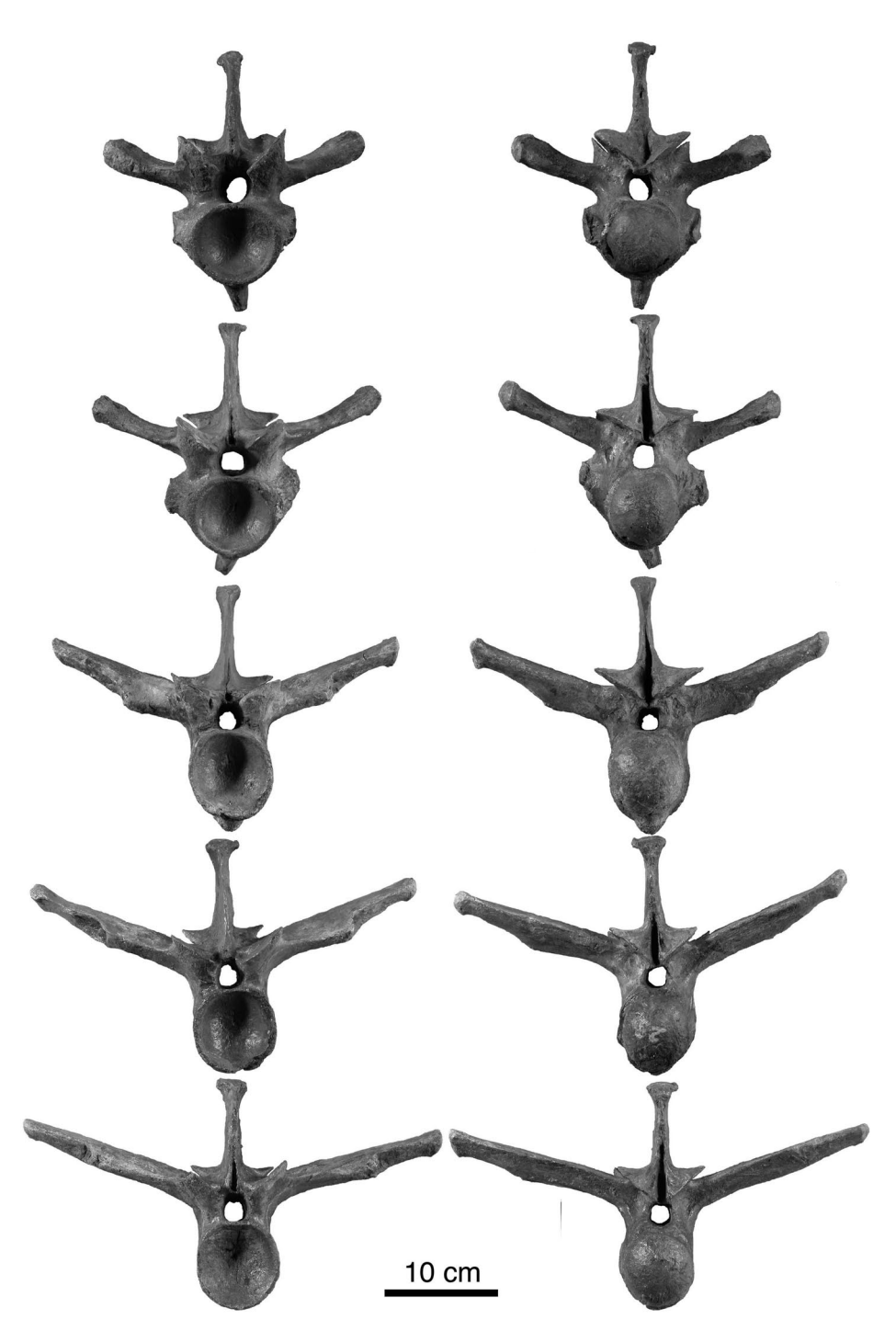


Fig. 40. cont.

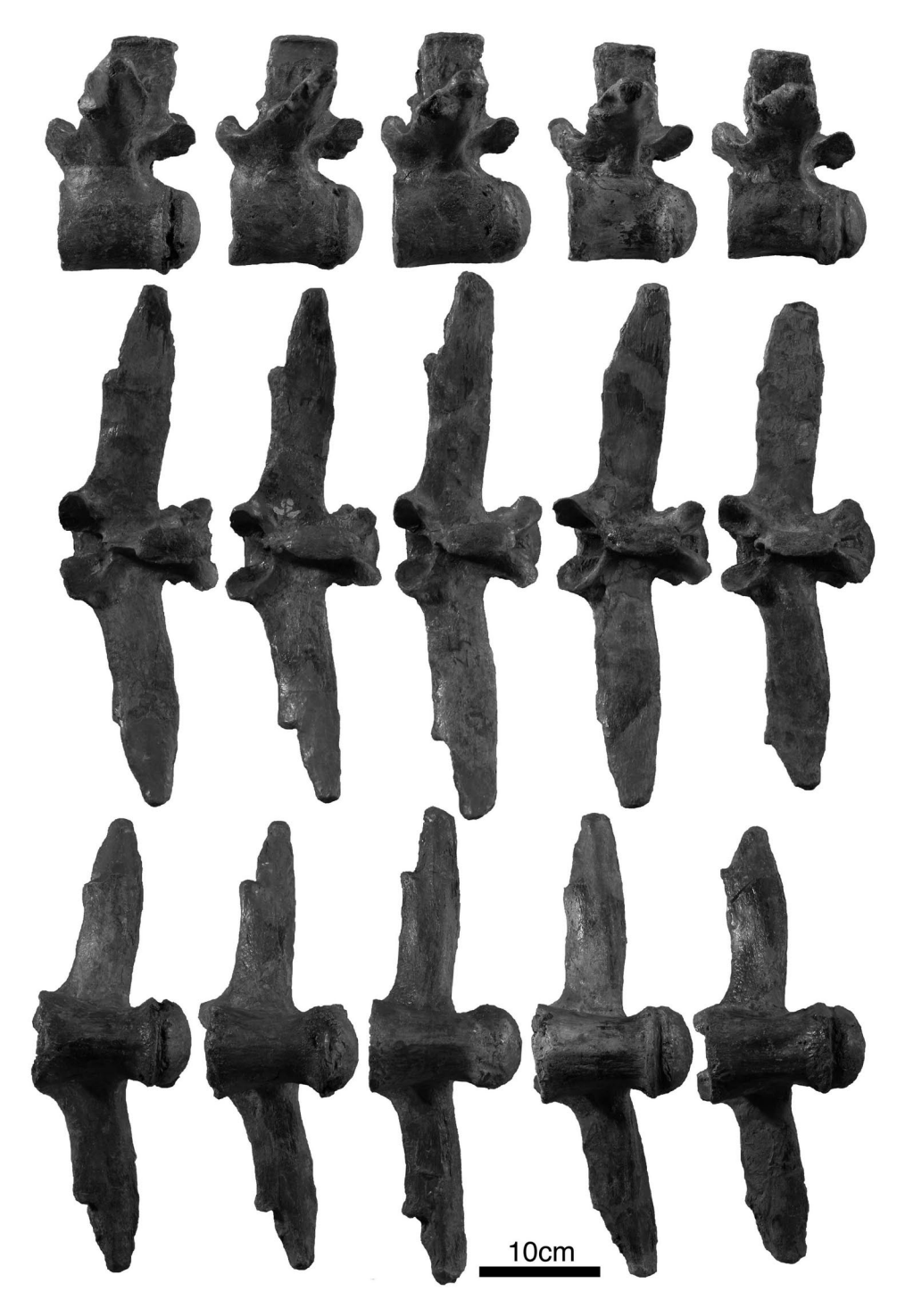


Fig. 41. Sixth to tenth dorsal vertebrae in left lateral, dorsal, ventral, anterior and posterior views.

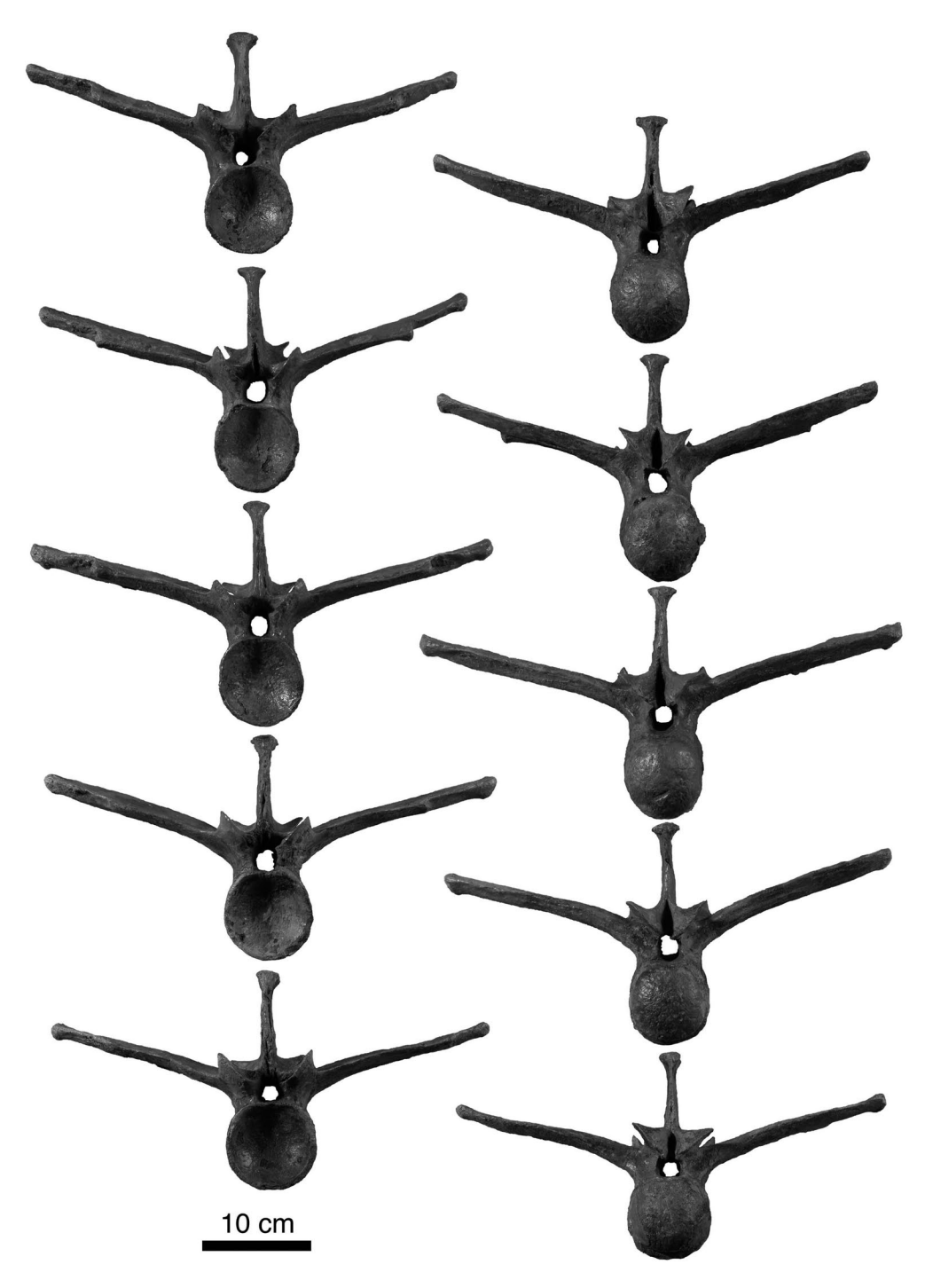


Fig. 41. cont.

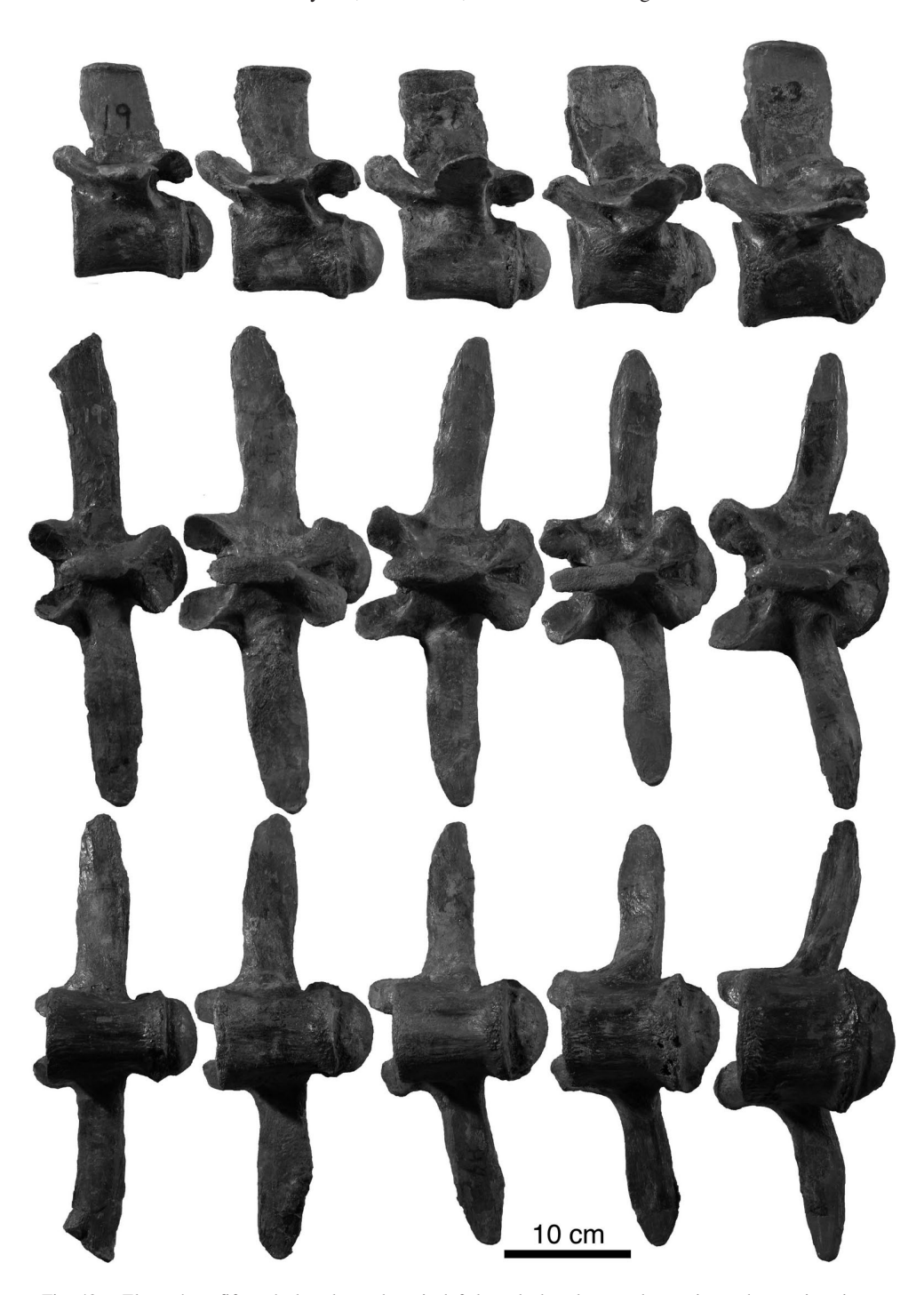


Fig. 42. Eleventh to fifteenth dorsal vertebrae in left lateral, dorsal, ventral, anterior and posterior views. Parts filled by plaster are: dorsal 11, 19: neural spine; dorsal 12, tip of left transverse process; dorsal 14, tip of right transverse process; dorsal 15, dorsal end of neural spine and tip of right transverse process.



Fig. 42. cont.

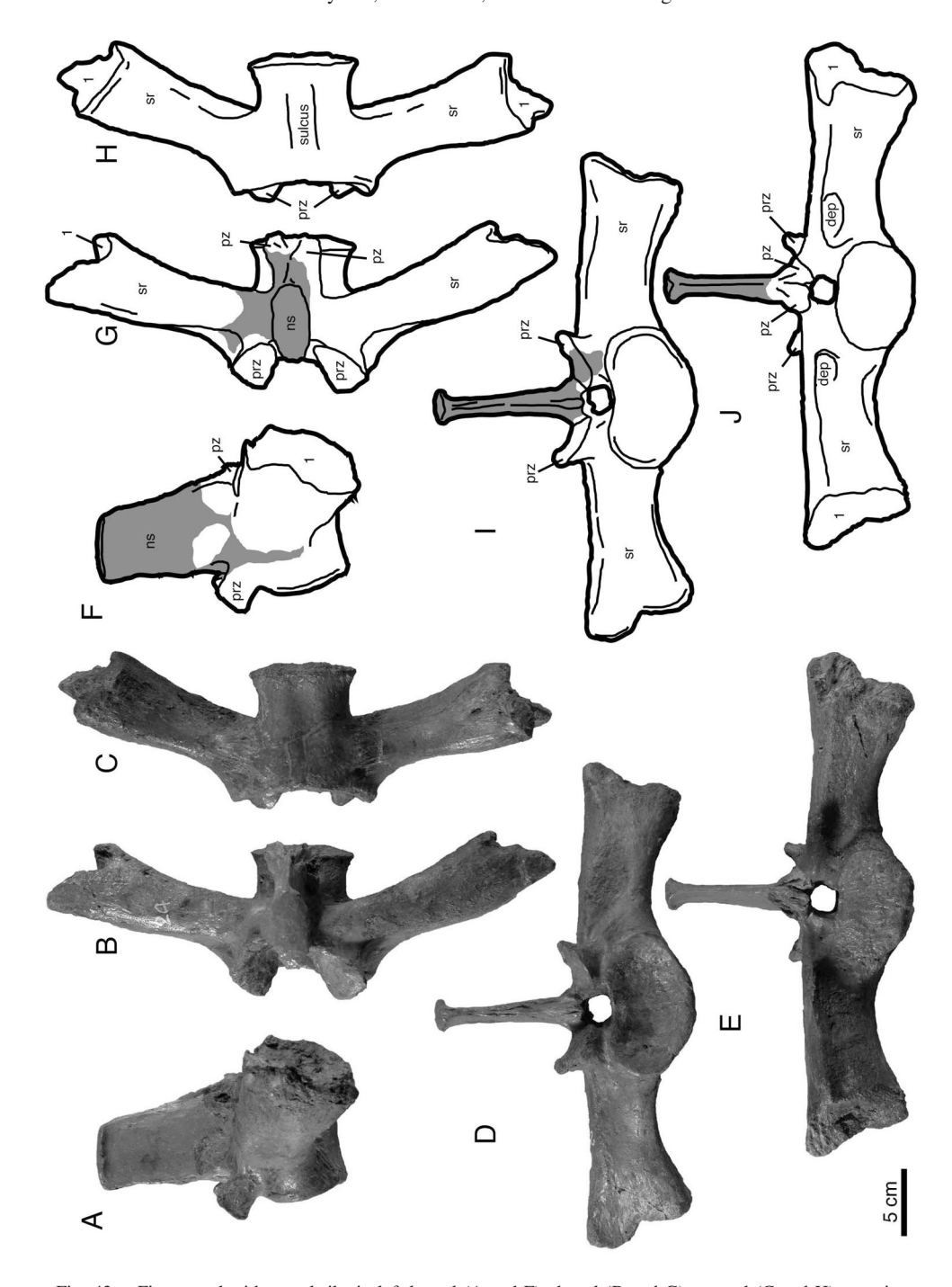


Fig. 43. First sacral with sacral ribs in left lateral (A and F), dorsal (B and G), ventral (C and H), anterior (D and I), and posterior (E and J) views. Abbreviations: ns, neural spine; prz, prezygapophysis; pz, postzygapophysis; sr, sacral rib; 1, sutural surface with ilium. Gray areas are missing parts, filled with plaster.

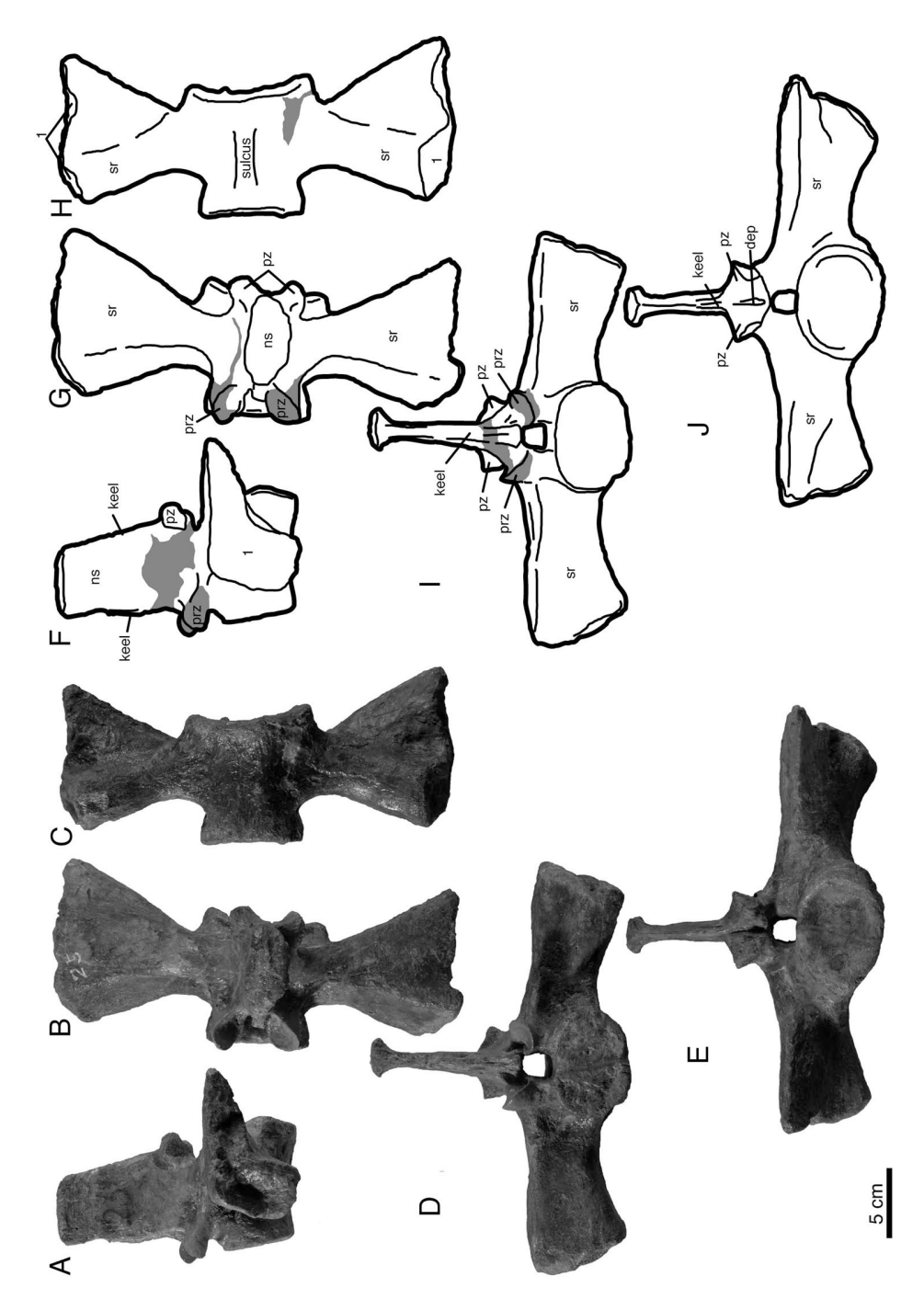


Fig. 44. Second sacral with sacral ribs in left lateral (A and F), dorsal (B and G), ventral (C and H), anterior (D and I), and posterior (E and J) views. Abbreviations: ns, neural spine; prz, prezygapophysis; pz, postzygapophysis; sr, sacral rib; 1, sutural surface with ilium. Gray areas are missing parts, filled with plaster.

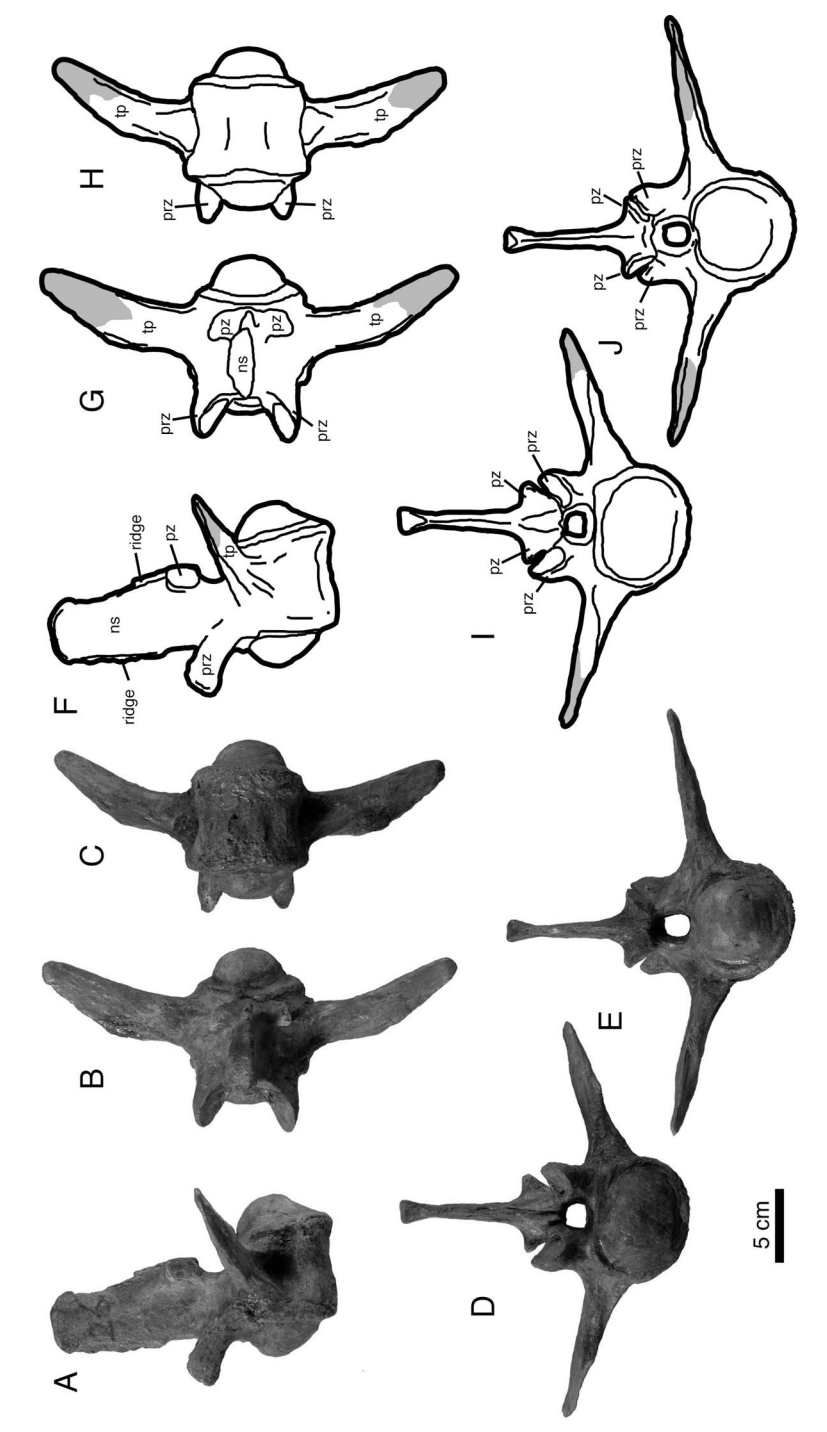


Fig. 45. First caudal vertebra in left lateral (A and F), dorsal (B and G), ventral (C and H), anterior (D and I), and posterior (E and J) views. Abbreviations: ns, neural spine; prz, prezygapophysis; pz, postzygapophysis; tp, transverse process. Gray areas are missing parts, filled with plaster.

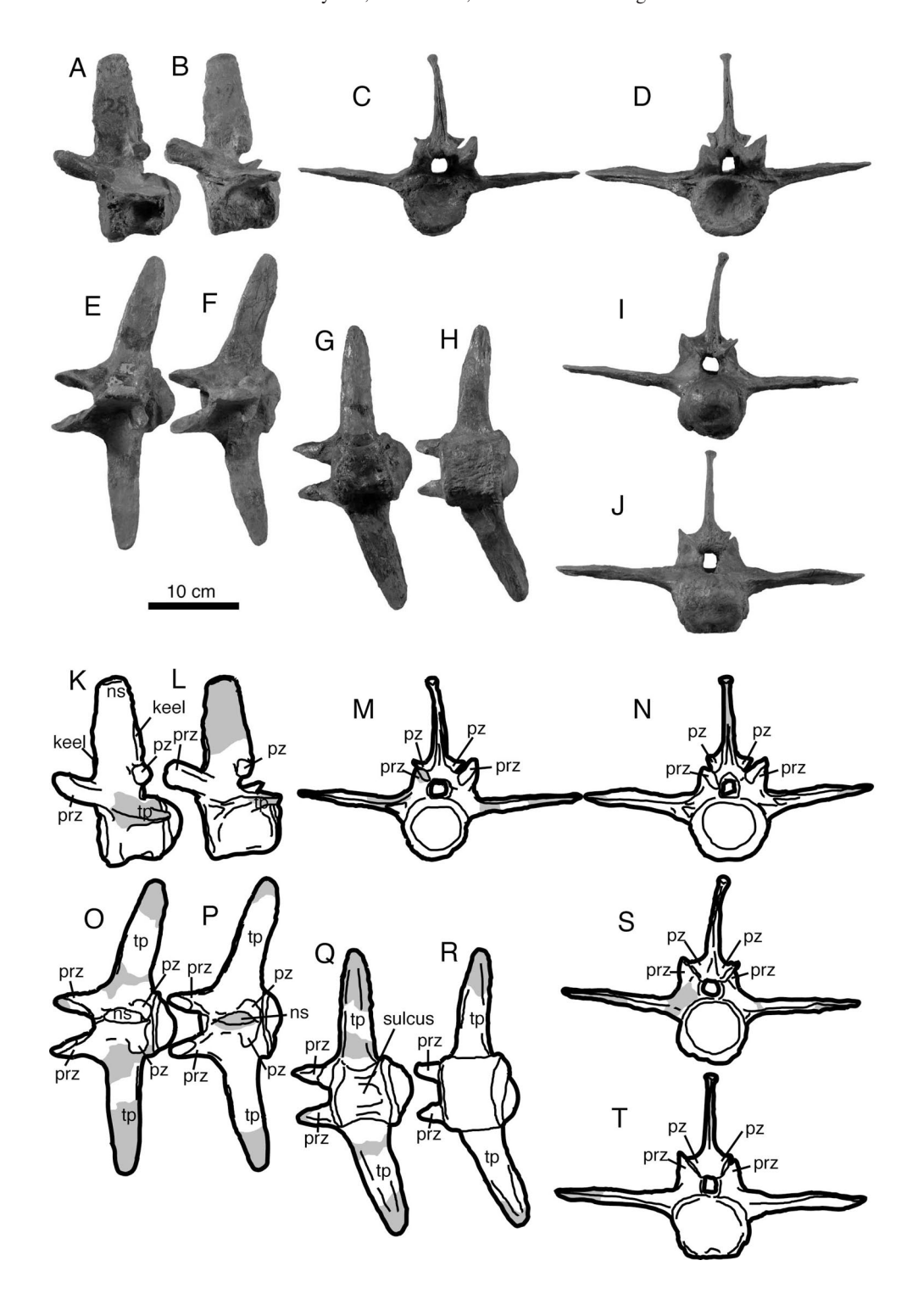
the anterior intervertebral articular surface of the first sacral vertebra is the largest of all of the vertebrae and twice as wide as high (Table 3). The posterior intervertebral articular surface of the first sacral vertebra is transversely narrow, being as wide as the intervertebral articular surfaces of the second sacral. The intervertebral articular surfaces between the first and second sacral vertebrae are flat and rugose. The posterior intervertebral articular surface of the second is concave for the biconvex first caudal vertebra. In lateral view, the anterior intervertebral articular surface of the first sacral vertebra is nearly perpendicular to the horizontal plane, whereas the posterior intervertebral articular surface of the second sacral vertebra is anteriorly tilted. The ventral surfaces of both sacral vertebrae have shallow sulci.

Caudal Vertebrae (Figs. 45–46)

The preserved three **caudal vertebrae** are the first three ones. The main axis of the neural spine of the first caudal vertebra is nearly vertical, and the spines of the other two are posteriorly tilted in lateral view. The neural spines are distally expanded but are less so than the dorsal vertebrae. The anteroposterior length is nearly consistent from the base to tip of the spine in the first caudal vertebra but narrows distally in the second and third caudal vertebrae. The neural spines have ridges along the anterior and posterior edges of the spines for supraspineous ligaments. Unlike the dorsal vertebrae, the posterior edge of the neural spine lacks a groove or depression at the base of the spine. The prezygapophyses and postzygapophyses are much smaller than the ones of cervical and dorsal vertebrae. The prezygapophyses of the second and third caudal vertebrae are longer than the first caudal and extend far anterior to the anterior intervertebral articular surface. The prezygapophyseal articular surfaces are oval shaped, and their long axes are oriented anteroposteriolry. In anterior and posterior views, the prezygapophyseal and postzygapophyseal articular surfaces are steeper than 45 degrees from the horizontal plane. The postzygapophyses are much smaller than the prezygapophyses and those of the third caudal vertebra are more anteriorly positioned than the first caudal vertebra. The transverse processes are positioned at the fused neurocentral suture. They are tilted posteriorly and narrow towards the distal ends in dorsal view. The transverse processes of the first caudal vertebra differ from those of the more posterior caudals in being bent posteriorly midway along the process. The first caudal vertebra has a biconvex centrum. The other two caudal vertebrae are procoelous. In the first caudal, the anterior extension of the condyle of the anterior intervertebral articular surface is much less than that of the posterior surface. The ventral surface of the second caudal vertebra has a deep sulcus, and that of the third is flat. The contact surfaces for the chevrons are not well preserved.

Ribs

Both **altantal ribs** are preserved (Fig. 47). These are elongated and their length is more than five times as long as the dorsoventral height of the proximal end $(203.11 \times 37.70 \text{ mm})$. The lateral surface is convex and the medial surface is concave. The articular surface for the atlas is bean-shaped in proximal view. The ventral side of the proximal end is rugose for the atlantodental ligament, connecting the atlantal ribs each other (Frey, 1988), but lacks a medial process. The shaft has a dorsal process at about two-thirds of the length from the proximal end as in alligatorids, as is also the case in *Alligator mississippiensis* (Brochu, 1997). Distal to the expansion, the medial surface has scars. The distal tip has a rounded condyle.



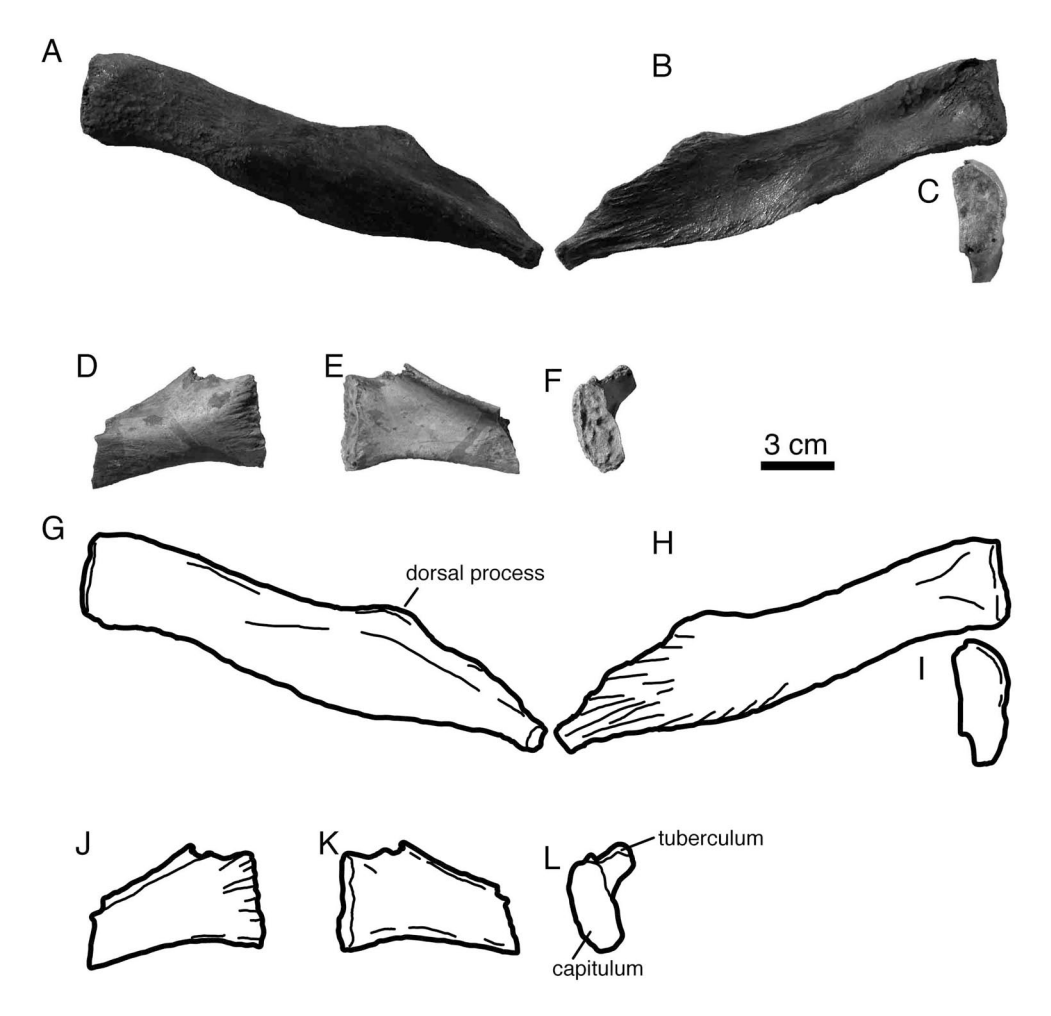


Fig. 47. Atlantal rib in lateral (A and G), medial (B and H), and proximal (C and I) views. Axial rib in lateral (D and J), medial (E and K), and proximal (F and L) views.

The proximal ends of the **axial ribs** are preserved (Fig. 47). The capitulum is much larger and more massive than the tuberculum. The articular surface of the capitulum is rounded, similar in shape to the atlantal articular surface of the atlantal rib. The lateral surface of the capitulum is striated. The tuberculum has the form of a crest that projects dorsomedially from the shaft.

The **cervical ribs** of the third to seventh cervical vertebrae are similar in shape (Fig. 48). In lateral view, these are T-shaped with a horizontal ventral edge of the shaft. The capitulum

Fig. 46.Second caudal vertebra in left lateral (A and K), anterior (C and M), dorsal (E and O), ventral (G and Q), and posterior (I and S) views and third caudal vertebra in left lateral (B and L), anterior (D and N), dorsal (F and P), ventral (H and R), and posterior (J and T) views. Abbreviations: ns, neural spine; prz, prezygapophysis; pz, postzygapophysis; tp, transverse process. Gray areas are missing parts, filled with plaster.

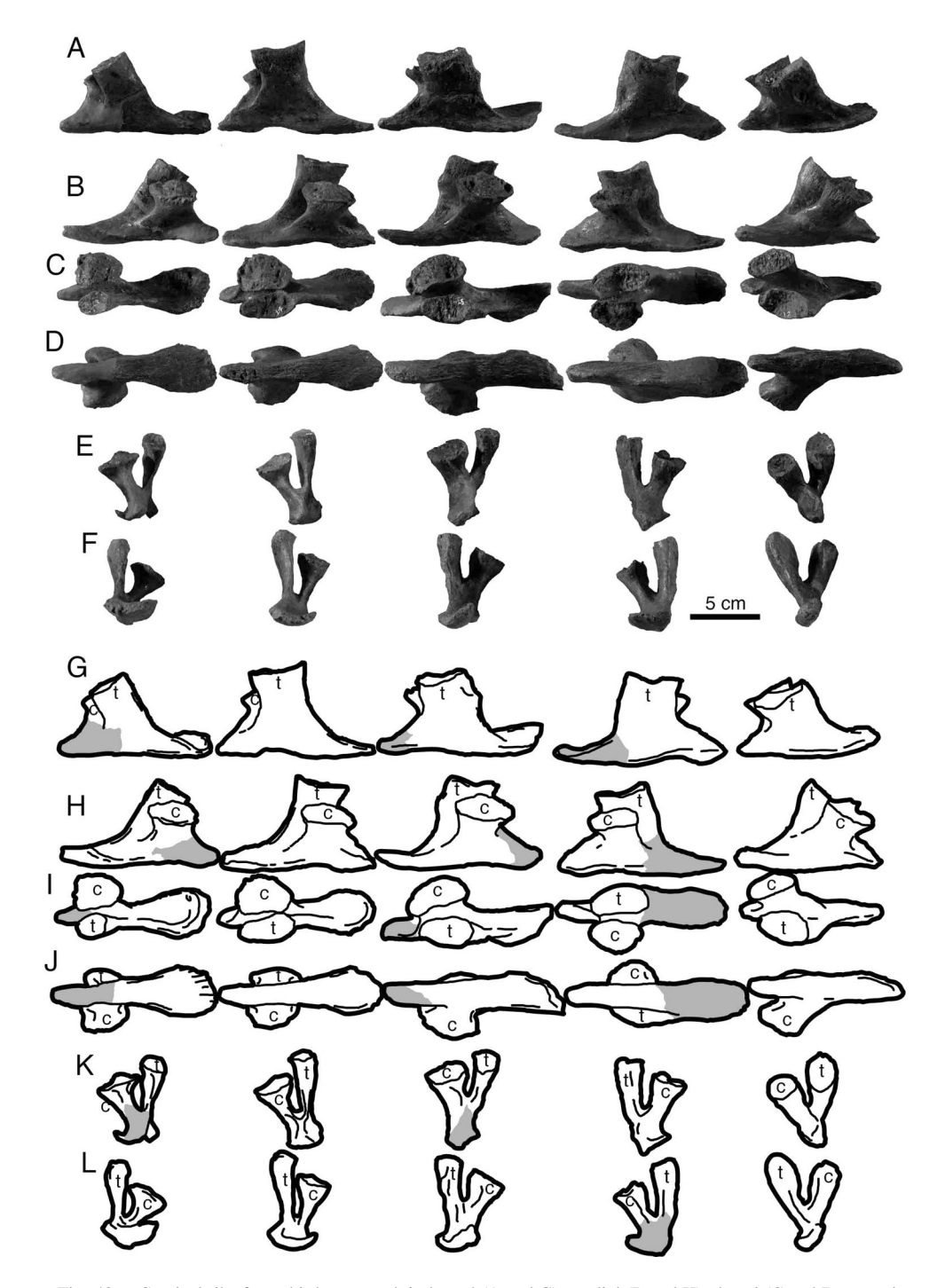


Fig. 48. Cervical ribs from third to seventh in lateral (A and G), medial (B and H), dorsal (C and I), ventral (D and J), anterior (E and K), and posterior (F and L) views. All except the left sixth cervical rib are from right side. Abbreviations: c, capitulum; t, tuberculum.

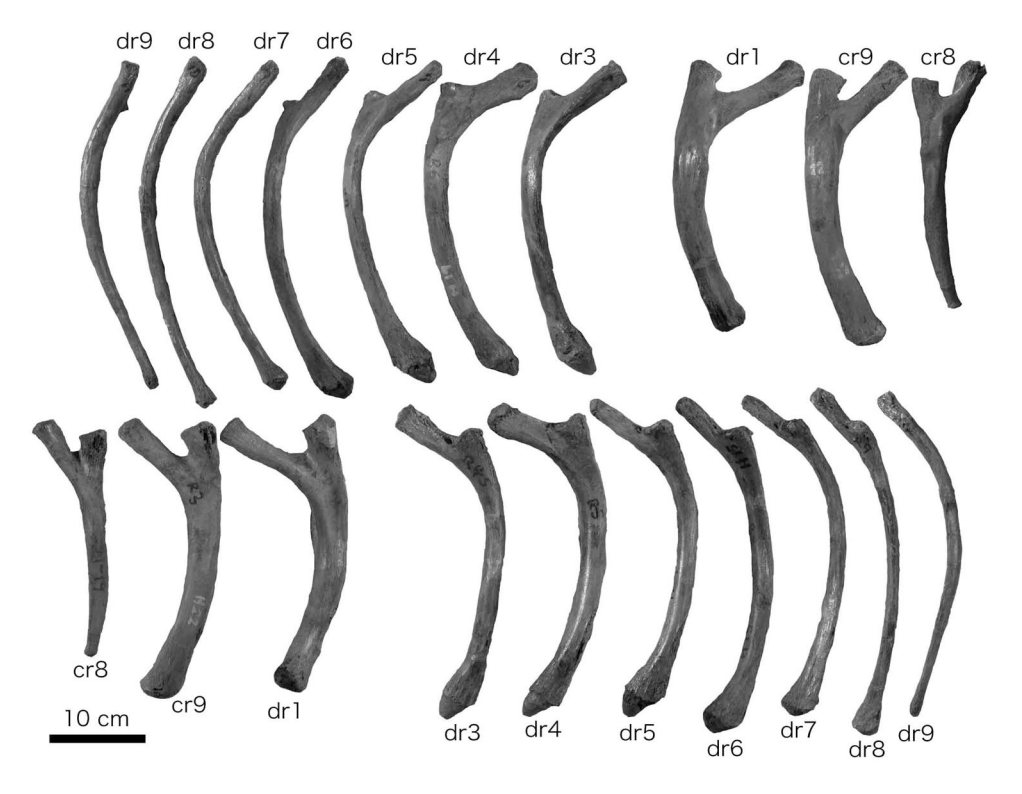


Fig. 49. Eighth and ninth cervical ribs and first and third to ninth dorsal ribs from left side (from left to right in upper row and from right to left in lower row) in lateral (upper row) and medial (lower row) views. Abbreviations: cr, cervical rib; dr, dorsal rib.

of the third cervical rib is more anteriorly positioned than the tuberculum. The shafts of the capitulum of the fourth to seventh cervical ribs are nearly covered by the tuberculum in lateral view because the capitulum is positioned medial to the tuberculum. Seen in lateral view, the shafts of the capitulum and tuberculum of the third cervical rib are thinner and more tilted anteriorly than those of the more posterior cervical ribs. The surfaces of capitulum and tuberculum that contact the centra are rugose. The surfaces of the capitulum are larger than the surfaces of the tuberculum of the third to fifth cervical ribs. In the sixth and seventh cervical ribs these surfaces are subequal in size. The horizontal rib shafts are slightly longer than the length of their corresponding centra. The anterior extension of the shaft is larger in more posterior cervical ribs. Anteriorly, the rib shafts are tapered into a pointed tip. The shafts are transversely expanded at posterior ends. The expansion of the third cervical rib is the largest and decreases posteriorly.

The eighth and ninth cervical ribs are similar to the **dorsal ribs** (Fig. 49). The eighth cervical rib is gracile and has a thinner shaft. The shaft thins distally. The tuberculum forms as a process at least up to the first dorsal rib. The capitulum is the longest in the first dorsal rib and becomes shorter posteriorly. On the lateral surface of the eighth and ninth cervical and first dorsal ribs the shaft of the rib has a strong crest. The crest is weak or absent in more posterior

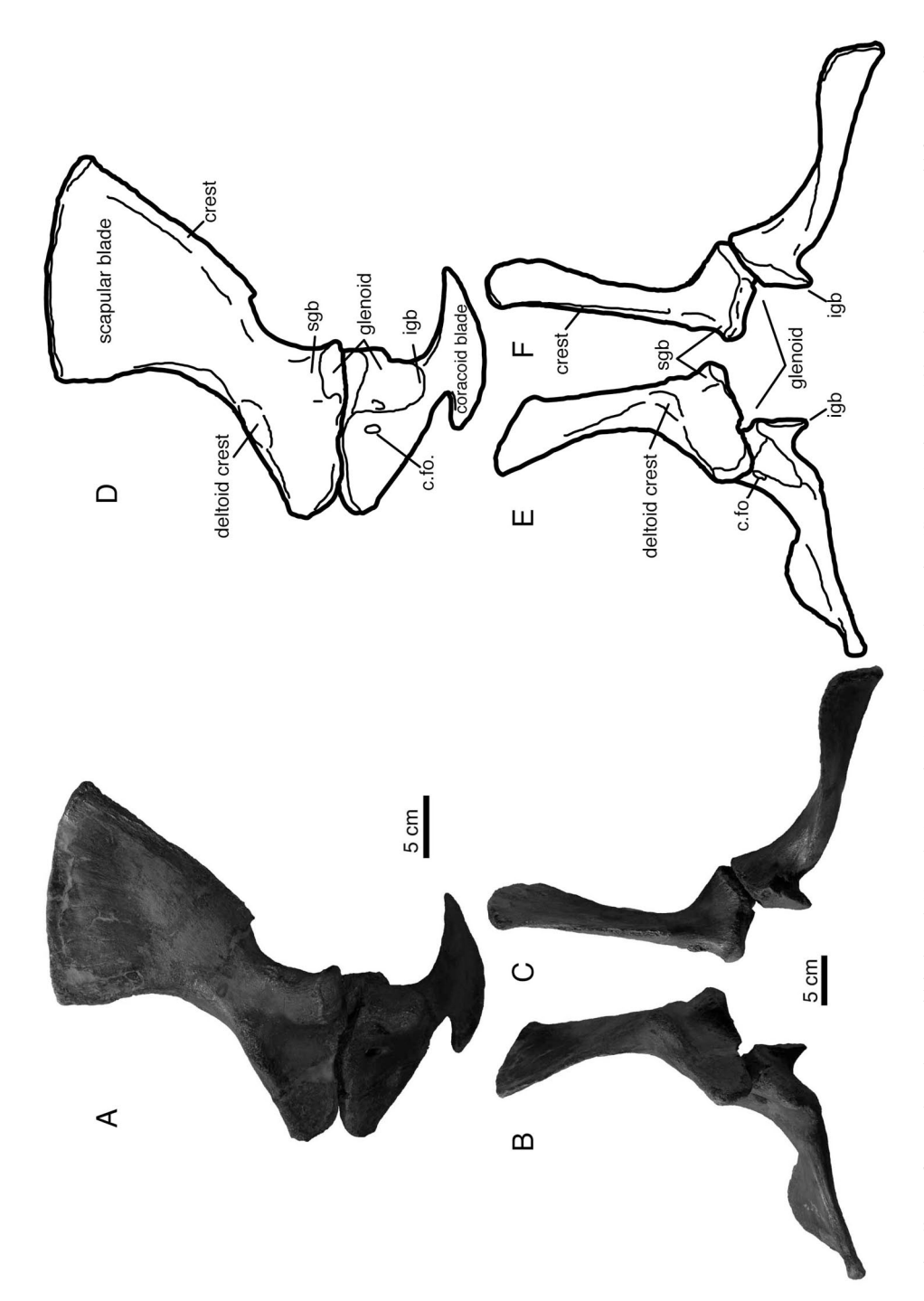


Fig. 50. Left scapula and coracoid in lateral (A and D), anterior (B and E), and posterior (C and F) views. Abbreviations: c.fo., coracoid foramen; igb, infraglenoid buttress; sgb, supraglenoid buttress.

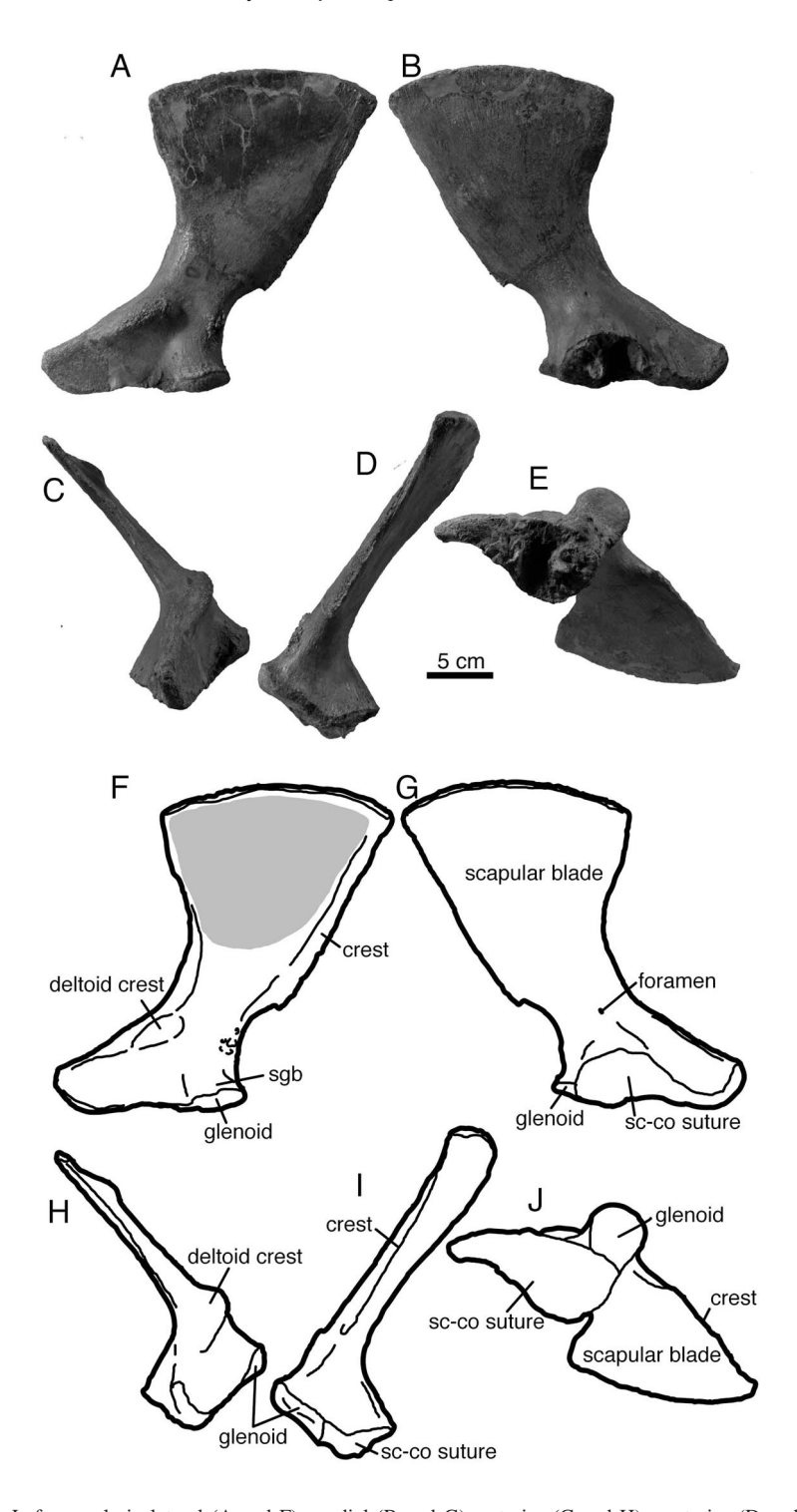


Fig. 51. Left scapula in lateral (A and F), medial (B and G), anterior (C and H), posterior (D and I), and ventral (E and J) views. Abbreviations: fo, foramen; sc-co suture, scapula-coracoid suture; sgb, supraglenoid buttress; 1, pathological area.

dorsal ribs. The distal tips of the third to seventh dorsal ribs have a process for the cartilaginous connection with the gastralia. The second dorsal rib, last dorsal rib, and gastralia are not preserved.

The **sacral ribs** are robust and become wider distally (Figs. 43–44). The sutures with the sacral vertebrae are not visible. The dorsal sides of the sacral ribs are flat and the proximal end is triangular in cross section. Distally, the sacral ribs have rugose surfaces for the iliac contacts. The first sacral rib is longer than the second sacral rib, and articulates to the anterior half of the lateral side of the centrum in dorsal view. In dorsal view, the first sacral rib angles posteriorly and the second sacral rib is nearly perpendicular to the sagittal plane. The posterior side of the first sacral rib has a depression. The distal end of the first sacral rib is higher than wide and is rectangular in distal view. The anterodorsal corner of the distal end has a laterally extending process. The second sacral rib articulates to the central part of the lateral side of the centrum in dorsal view. The distal end of this rib is longer anteroposteriorly than the first sacral rib and is roughly triangular seen in distal view.

Pectoral Girdle

The scapulae and coracoids from both sides and the interclavicle are preserved (Figs. 50–53). The scapula and coracoid remained unfused and would have fused late in ontogeny if at all. When the scapula and coracoid articulate, the glenoid faces posterolaterally.

Scapula (Figs. 50–51)

The dorsoventral length of the **scapula** is roughly twice as long as the anteroposterior width at the scapula-coracoid suture (122.4 mm) (Table 4). The scapular blade is posteriorly tilted in lateral view. It flares dorsally and its distal end (158.9 mm) is more than twice as anteroposteriorly wide as its base (60.7 mm). The lateral surface of the right scapula has a shallow depressed for the insertion of *M. dorsalis scapulae* and *M. teres major* (Cong et al., 1998). In lateral view, the anterior edge of the scapular blade is smooth and concave anteriorly, and the posterior edge is nearly straight. The posterior edge has a crest, and the lateral side of the crest is rugose (origin for *M. tricips brachii*: Cong et al., 1998). A small foramen is present on the medial surface at the base of the scapular blade. The deltoid crest is present on the anterior end

machikanensi	s in millimeters.												
Table 4.	Measurements	of	pectoral	girdle	and	forelimb	elements	of	the	holotype	of	Toyotamap	himeia

Element	Length	Width at prox end	Width at dist end
Scapula (left)	251.0	164.2	118.8
Coracoid (left)	252.7	123.0	149.3
Interclavicle	273.7	_	_
Humerus (left)	403.0	113.4	114.5
Ulan (left)	214.0	61.0	24.8
Radius (left)	182.3	52.7	27.9
Radiale (left)	46.1	48.2	41.8
Metacarpal I (left)	50.1	34.4	24.2
Metacarpal III (left)	68.3	22.0	18.6

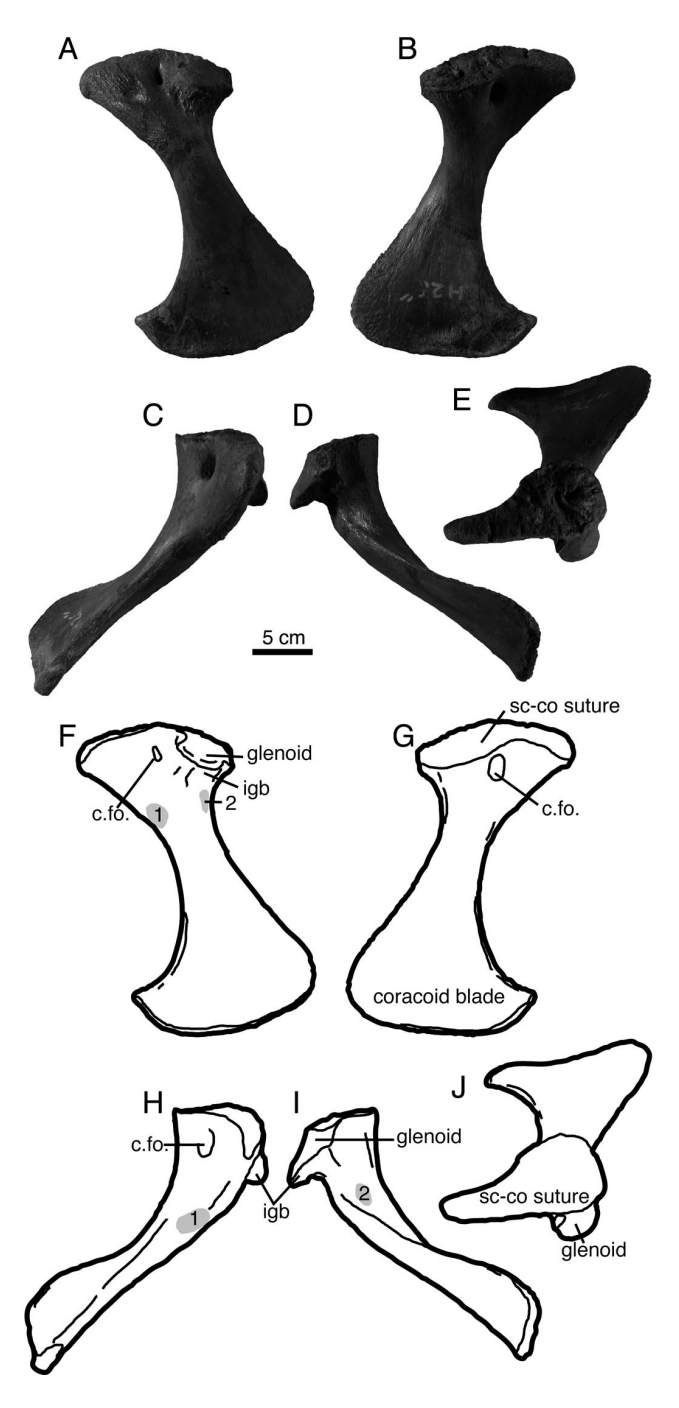


Fig. 52. Left coracoid in lateral (A and F), medial (B and G), anterior (C and H), posterior (D and I), dorsal (E and J) views. Abbreviations: c.fo., coracoid foramen; igb, infraglenoid buttress; sc-co suture, scapulacoracoid suture; sgb, supraglenoid buttress; 1, insertion area for *M. biceps brachii*; 2, insertion area for *M. triceps brachii*.

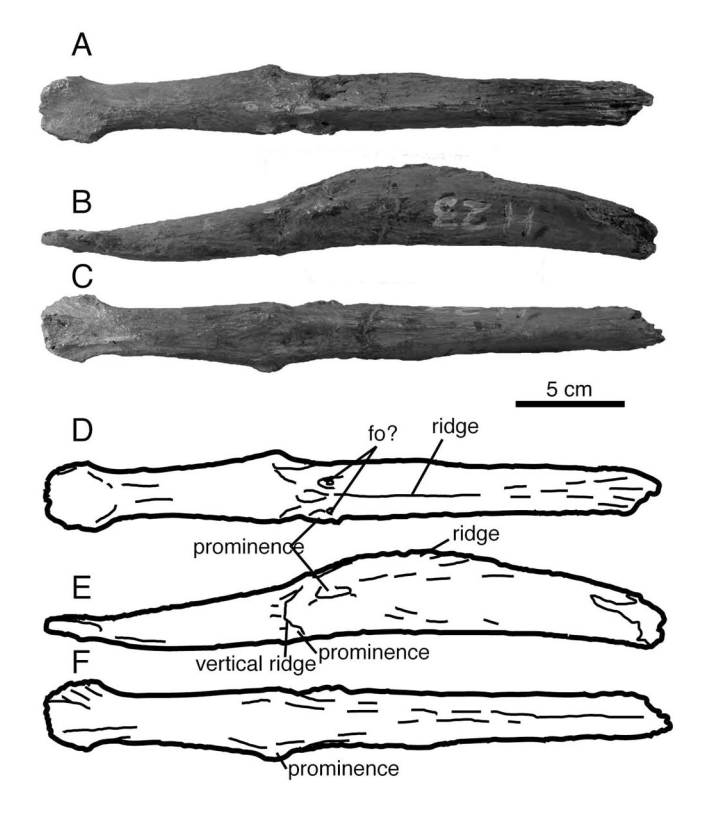


Fig. 53. Interclavicle in dorsal (A and D), left lateral (B and E), and ventral (C and F) views. Abbreviation: fo, foramen.

of lateral surface. This crest is wide in anterior view as in some species of *Alligator* and *Gavialosuchus ameicanus* (Brochu, 1999). The crest has a rough surface for the origin for *M. deltoideus* (Cong et al., 1998). The sutural surface with the coracoid is teardrop-shaped, and the transverse width at the posterior portion is much greater than the anterior portion.

Coracoid (Figs. 50, 52)

The **coracoid** is as long as the scapula (Table 4). The development of the infraglenoid buttress of the coracoid is equal to the developed of the supraglenoid buttress of the scapula. The coracoid foramen is located close to the scapula-coracoid suture. In ventral view, the coracoid blade is tilted posteriorly. The coracoid body is expanded medially and its anteroposterior length is more than three times as long as the length at the base (145. 39 and 40.72 mm). The base of the body has a rugose surface on the anterior side for the origin for *M. biceps brachii* and has a depression on the posterior side for *M. triceps brachii* (Cong et al., 1998). The ventral surface of the coracoid is flat. The dorsoventral thickness is nearly uniform along the medial edge of the coracoid blade, but posteriorly the distal edge of the blade becomes thin.

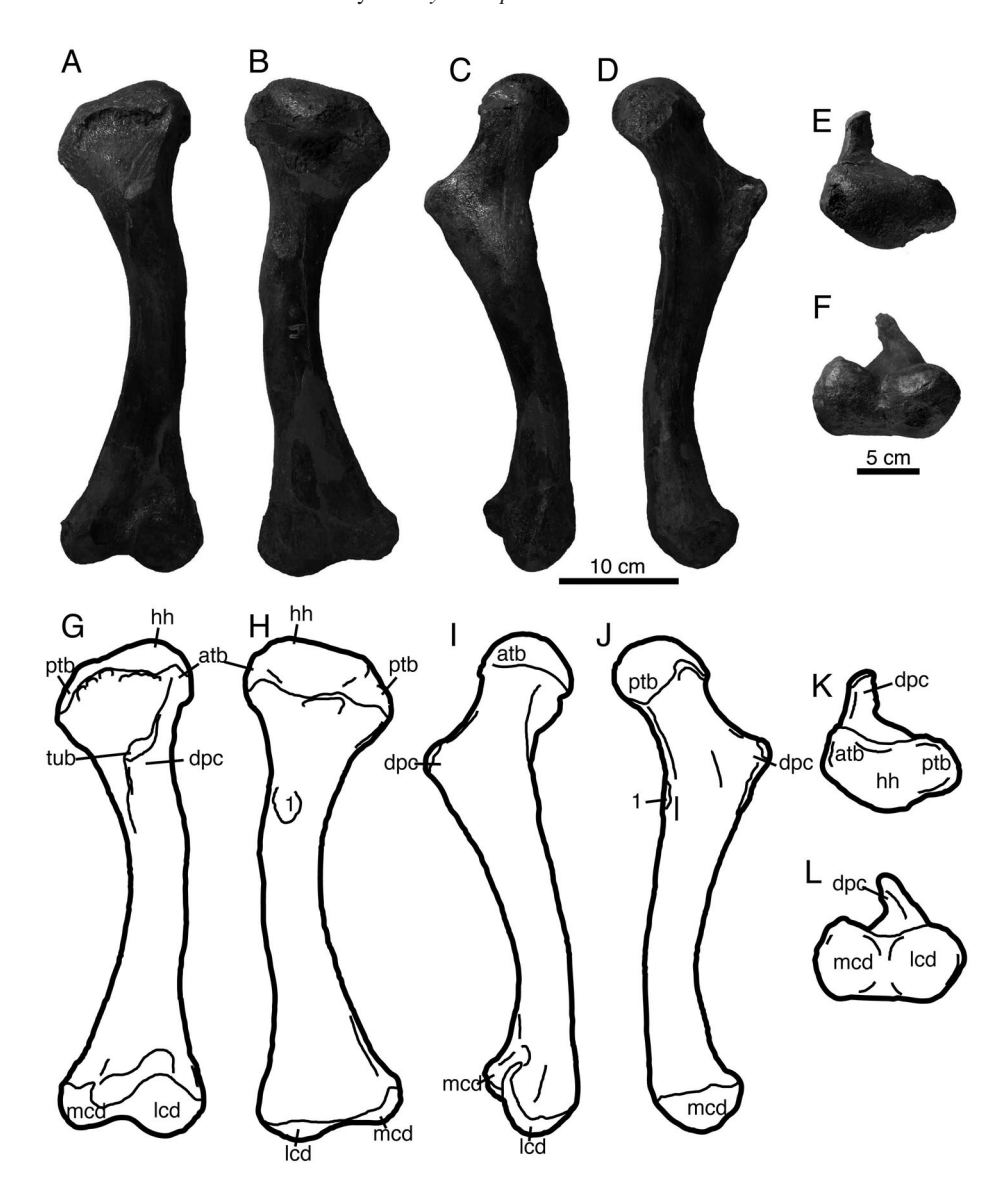


Fig. 54. Left humerus of *Toyotamaphimeia machikanensis* in ventral (A and G), dorsal (B and H), lateral (C and I), medial (D and J), proximal (E and K), and distal (F and L) views. Abbreviations: atb, anterior tuberosity; hh, humerus head; lat, lateral; lcd, lateral condyle; mcd. medial condyle; med, medial; ptb, posterior tuberocity; vent, ventral; 1, insertion scar for *M. teres major* and *M. dorsalis scapulae*.

Interclavicle

The **interclavicle** (Fig. 53) is missing the posterior end. It is rod-like throughout its length with circular cross section, except for the dorsoventrally flattened and laterally expanded anterior tip. The dorsal surface of the anterior tip is concave and smooth, but the ventral surface is rugose. The dorsal surface has a median ridge, and its anteroposterior length (94.3 mm) is

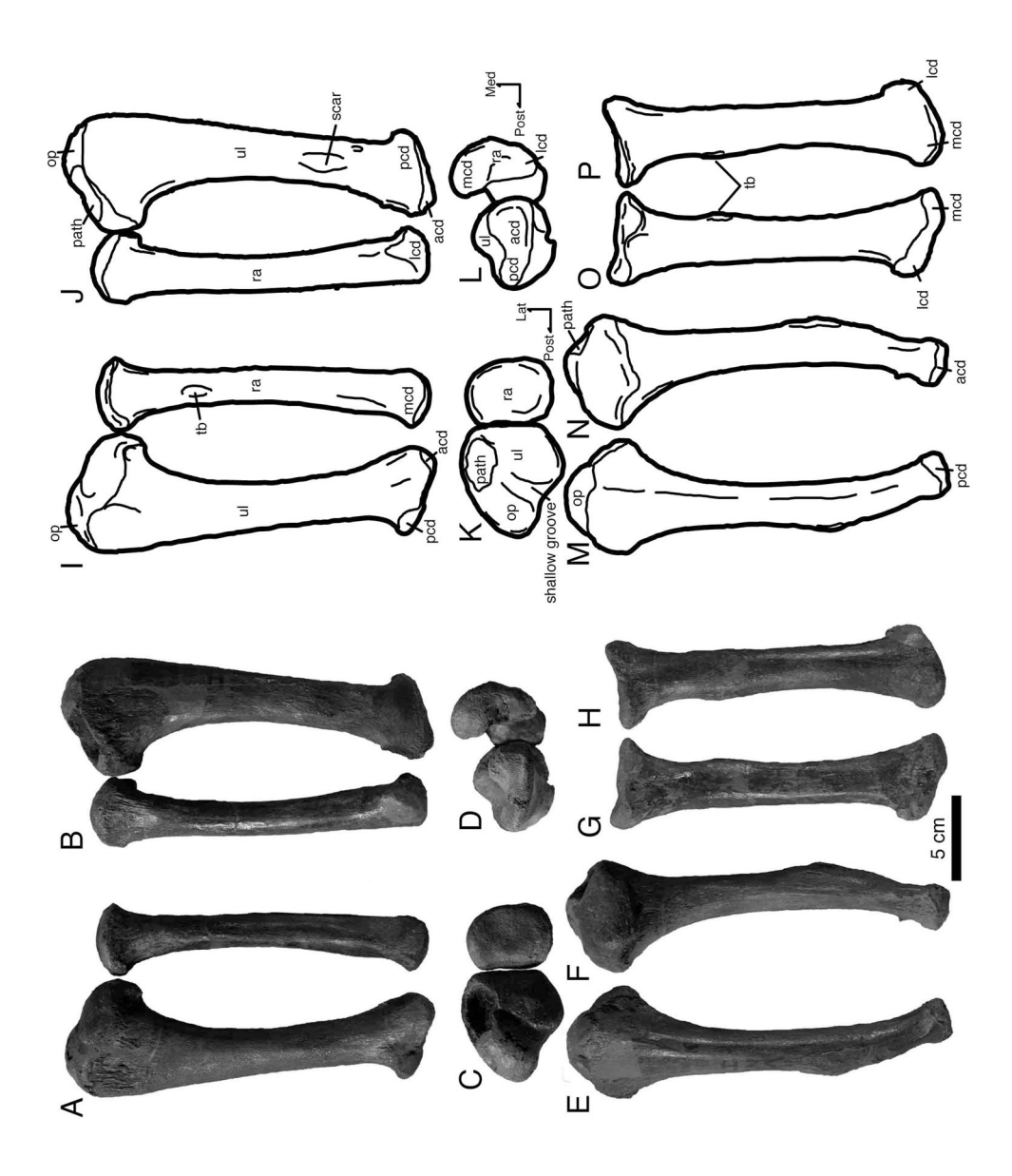


Fig. 55. Left ulna and radius of *Toyotamaphimeia machikanensis* in lateral (A and I), medial (B and J), proximal (C and K), and distal (D and L) views. Left ulna in posterior (E and M) and anterior (F and N) views. Left radius in posterior (G and O) and anterior (H and P) views. Abbreviations: acd, anterior condyle; lat, lateral; lcd, lateral condyle; mcd, medial condyle; med, medial; op, olecranon process; path, pathological feature; pcd, posterior condyle; post, posterior; ra, raduis; tb, tuberosity; ul, ulna.

roughly one-third of the total length of the interclavicle (Table 4). At the anterior end of the ridge, there is a pair of foramina and prominences lateral to the ridge, and the ventral surface of the main body is flat. There are prominences and vertical ridges on the lateral surface at the level of the flat ventral surface. In lateral view, the body of the interclavicle is weakly sinuous.

Forelimb

Humurus

The left **humerus** (Fig. 54) has a posteriorly curved shaft. In posterior view, the anterior tuberosity is as high as the humeral head, and the posterior tuberosity is slightly distally positioned. In proximal view, the anteroposterior length of the humerus is roughly half of the lateromedial length (50%: 56.7 and 113.4 mm). The humeral head and anterior tuberosity are continuous. The deltopectoral crest projects distally and is connected to the anterior tuberosity by a ridge. In lateral view, the ridge is distally concave. The distal tip of the deltopectoral crest

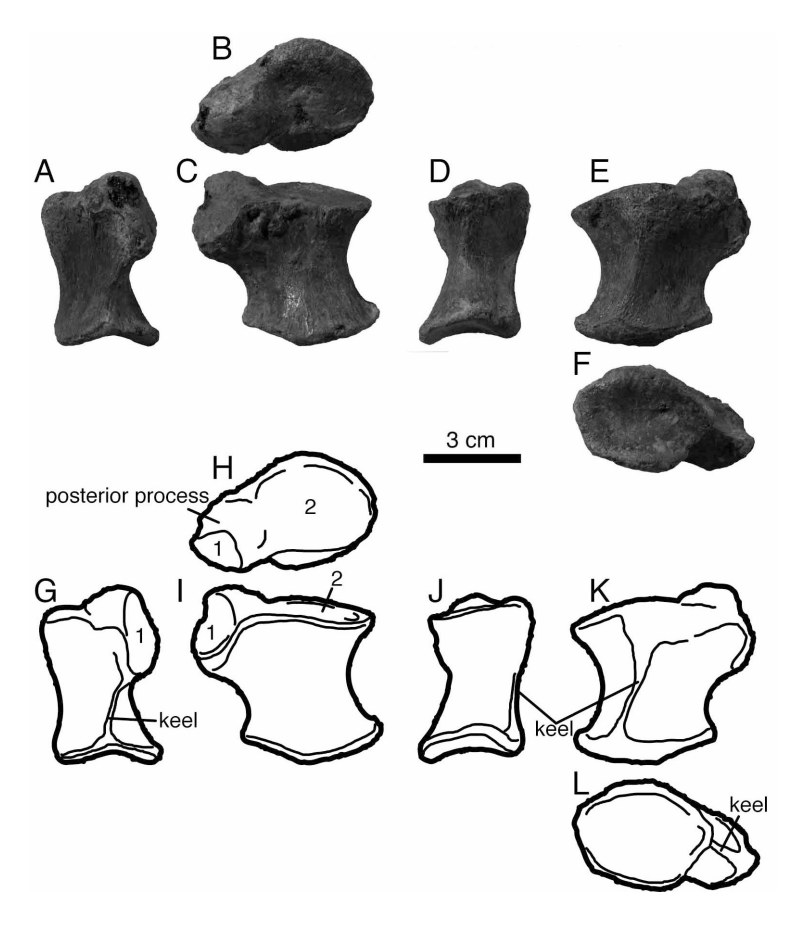


Fig. 56. Left radiale in posterior (A and G), proximal (B and H), medial (C and I), anterior (D and J), lateral (E and K), and distal (F and L) views. 1, articular surface for ulna; 2, articular surface for radius.

has a tubercle for the origin of *M. pectoralis* and *M. deltoides scapuilaris inferior* (Brochu, 1997; Brochu, 1999). The posterior surface of the humeral shaft, proximal to the deltopectoral crest, has a single insertion scar for *M. teres major* and *M. dorsalis scapulae* (Brochu, 1997; Brochu, 1999). The lateromedial axis of the distal end of the left humerus is twisted clockwise with respect to the proximal end in distal view. The lateral and medial condyles at the distal end are equally developed and well separated by the intercondylar groove. The articular surface of the lateral condyle, which articulates with the ulna, is larger than the medial condyle.

Ulna and Radius

The left **ulna** and **radius** are preserved (Fig. 55). These are subequal in length and are approximately half the length of the humerus (Table 4). The proximal end of the ulna is expanded more than twice as much as the ulnar shaft (26.7 mm). In proximal view, the proximal end is triangular. The olecranon process is spherical. It is slightly higher than the main articular surface for the humerus and is separated from the articular surface by a shallow groove. The lateral portion of the proximal surface is excavated, and the distal portion of the lateral surface of the shaft has a rugose surface. These features may be pathological features. The distal end is transversely flattened and has anterior and posterior condyles. The anterior condyle is much wider transversely than the posterior condyle. The radius is straight. The proximal end is oval in proximal view. The medial surface of the shaft at one-third of the radial length from the proxi-

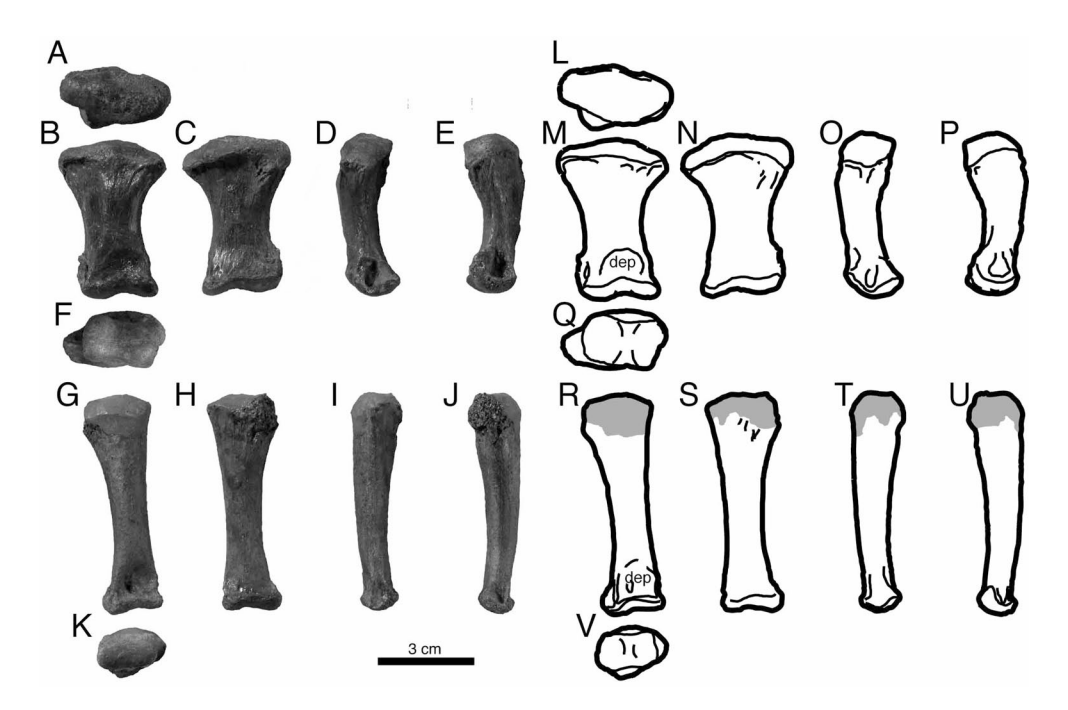


Fig. 57. Metacarpals of *Toyotamaphimeia machikanensis*. Left metacarpal I in proximal (A and L), anterior (B and M), posterior (C and N), medial (D and O), lateral (E and P), and distal (F and Q) views. Left metacarpal III in anterior (G and R), posterior (H and S), medial (I and T), lateral (J and U), and distal (K and V) views. Abbreviation: dep, depression. Gray area is missing or filled with plaster.

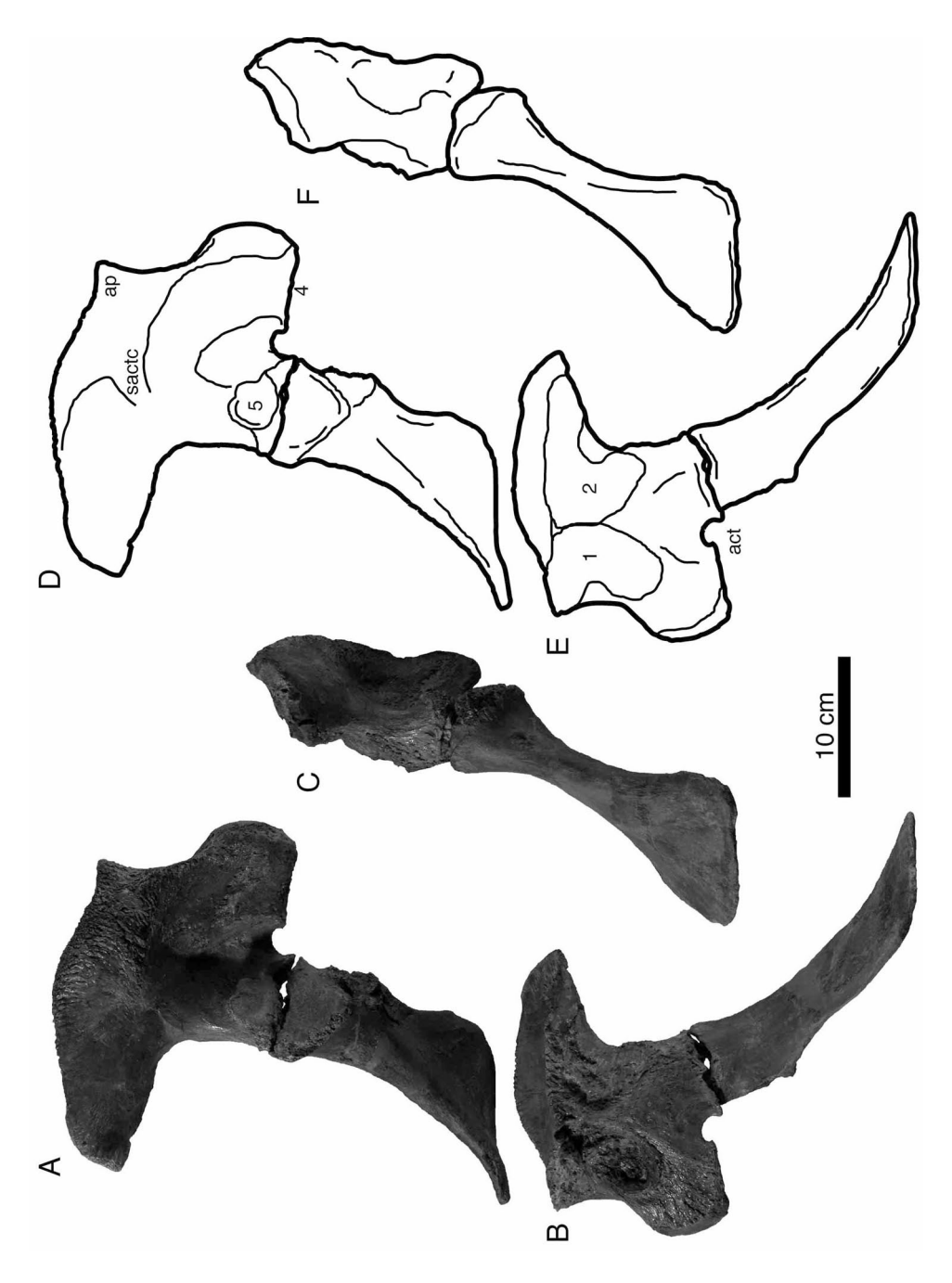


Fig. 58. Right ilium and ischium in lateral (A and D), medial (B and E), and posterior (C and F) views. Abbreviation: act, accetabulum; ap, anterior process; sactc supraaccetabular crest; 1, sutural surface for first sacral rib; 2, sutural surface for second sacral rib; 4, sutural surface for pubis; 5, articular surface for femur.

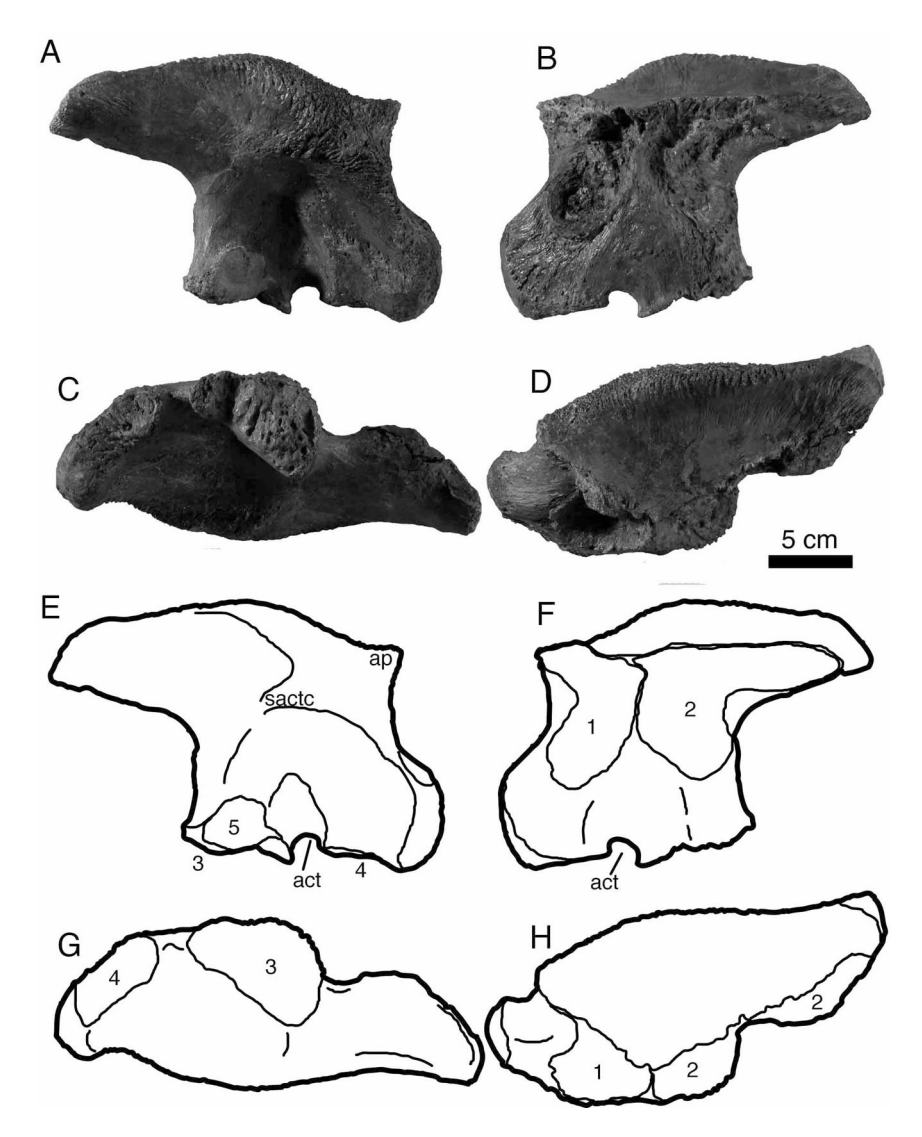


Fig. 59. Right ilium of *Toyotamaphimeia machikanensis* in lateral (A and E), medial (B and F), ventral (C and G), and dorsal (D and H) views. Abbreviation: act, accetabulum; ap, anterior process; sacte supraaccetabular crest; 1, sutural surface for first sacral rib; 2, sutural surface for second sacral rib; 3, sutural surface for ishchium; 4, sutural surface for pubis; 5, articular surface for femur.

mal end had a small tubercle with rugose surface. The distal end is anteroposteriorly flattened and has lateral and medial condyles, with the medial condyle being larger and extending more distally than the lateral one.

Carpus and Metacarpus

The left radiale is preserved (Fig. 56). The articular surface for the radius is circular in

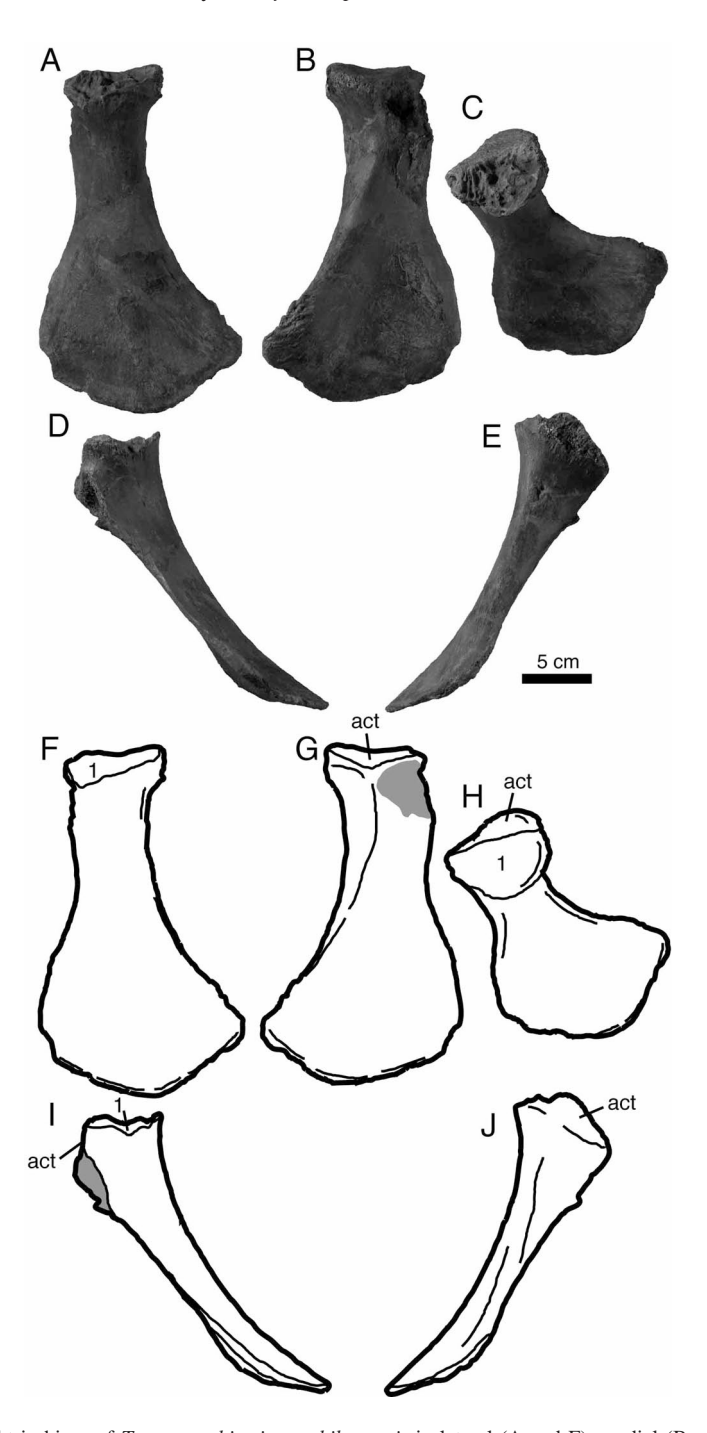


Fig. 60. Right ischium of *Toyotamaphimeia machikanensis* in lateral (A and F), medial (B and G), dorsal (C and H), anterior (D and I), and posterior (E and J) views. Abbreviation: act, accetabulum; 1, sutural surface with ilium. Grey areas are missing.

 Element
 Length
 Width
 Height

 Ilium (left)
 210.6
 87.7
 142.6

 Ischium (left)
 153.8
 73.5
 235.6

Table 5. Measurements of pelvic girdle and hindlimb elements of the holotype of *Toyotamaphimeia machikanensis* in millimeters. *Tibia and fibula have pathological features.

	M: 1	M:
	Maximum length	Maximum width
Femur (prox. end only)	_	105.5
Tibia* (right)	265.8	81.2
Fibula* (right)	261.9	33.3
Astragalus (left)	56.1	67.9
Calcaneum (left)	79.7	65.2
Distal tarsal 4 (left)	39.3	48.2
Metatarsal I (right)	185.5	42.9
Metatarsal III (right)	171.9	45.6
Metatarsal IV (right)	157.1	26.3
Metatarsal V (right)	50.3	39.5
Pedal phalanx II-1	58.7	30.0
Pedal ungula phalanx II-3	49.6	18.2
Pedal phalanx II-2 or III-2	40.1	24.0
Pedal phalanx III-3 or IV-2	33.2	23.5
Pedal ungula phalanx IV-4	29.5	22.0

shape and is slightly concave. The posterior process at the proximal end has a small articular surface with the anterior condyle of the ulna. The lateral and posterior surfaces of the element, distal to the posterior process, have a keel. The distal surface is oval shaped and concave.

Metacarpals I and III from left side are preserved (Fig. 57) but manual phalanges are missing. Metacarpal I is short and thick. The proximal surface is dorsoventrally flat and is convex. The proximal end is twisted clockwise by roughly 30 degrees with respect to the distal end in proximal view so that, in articulation, it imbricates with the proximal end of metacarpal II. The distal end has a dorsal depression and deep collateral ligament fossae. The distal condyles are separated by an intercondylar groove and are equally developed. Metacarpal III is thin and long. The transverse width is two-thirds of the width of metacarpal I (Table 4). The dorsal depression at the distal end is large and deep. The collateral ligament fossae are shallow. The distal condyles are weakly separated by the intercondylar groove. The proximal end is twisted clockwise by approximately 30 degrees, as in metacarpal I.

Pelvic Girdle

Ilium

Both **ilia** (Figs. 58–59) are preserved and are anteroposteriorly longer than high (Table 5). The dorsal edge of the iliac blade is heavily scarred. The anterodorsal part of the iliac blade has a small process (anterior process) like *Borealosuchus* (*Leidyosuchus* in Erickson, 1976) and *Gavialis gangeticus* (Brochu, 1997, 1999). The dorsal margin of the iliac blade is gently convex anteriorly and has a moderate indentation of its posterior region. The posterior end of the iliac blade is shallow. The pubic peduncle is transversely narrower than the ischial peduncle. Both

pubic and ischial peduncles have rough surfaces. The lateral surface of the ischial peduncle has an articular surface for the femur. The accetabulum, which is 20 mm in diameter, is small. Dorsal to the accetabulum between the pubic and ischial peduncles is a dorso-ventrally elongate depression. The supraacetabular crest dorsal to a depression for accetabulum is very weak. Medially, there are two rugose articular surfaces for the sacral ribs. The boundary between these surfaces is located dorsal to the accetabulum.

Pubis and Ischium

The pubes are not preserved. Both **ischia** (Figs. 58, 60) are preserved and their dorsoventral heights are as long as the anteroposterior lengths (Table 5). The proximal end is circular in proximal view and has a sutural surface for the ilium medially and a smooth surface for the accetabulum laterally. The shaft is triangular in cross section and is much thicker posteriorly than anteriorly. The distal expansion of the ischum is 153.1 mm wide, more than half of its dorsoventral height, and is three times as wide as the shaft thickness (53.7 mm). The lateral surface of the distal part is convex, whereas the medial surface is concave. The distal edge of the distal expansion is convex in lateral view.

Hindlimb

Femur, Tibia, and Fibula

The right **femur** (Fig. 61) is incomplete and its proximal end is preserved. The transverse width of the femur is 106.07 mm. The femur length is estimated as 450 mm. The femur head is rounded in posterior view.

The right **tibula** and **fibula** (Figs. 62–63) are preserved but both have pathological features of the shafts as described in detail by Katsura (2004). The shafts of these bones were fractured and regrown together before the animal's death. The posterior portions of both elements are

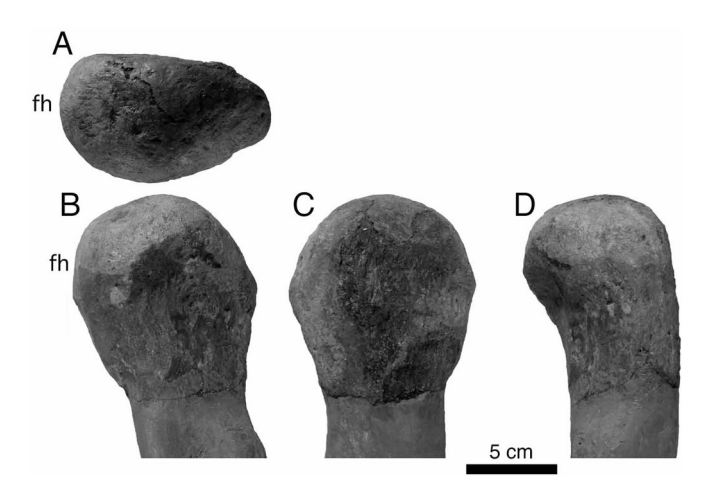


Fig. 61. Proximal end of femur of *Toyotamaphimeia machikanensis* in proximal (A), medial (B), lateral (C), and posterior (D) views. Abbreviation: fh, femur head.

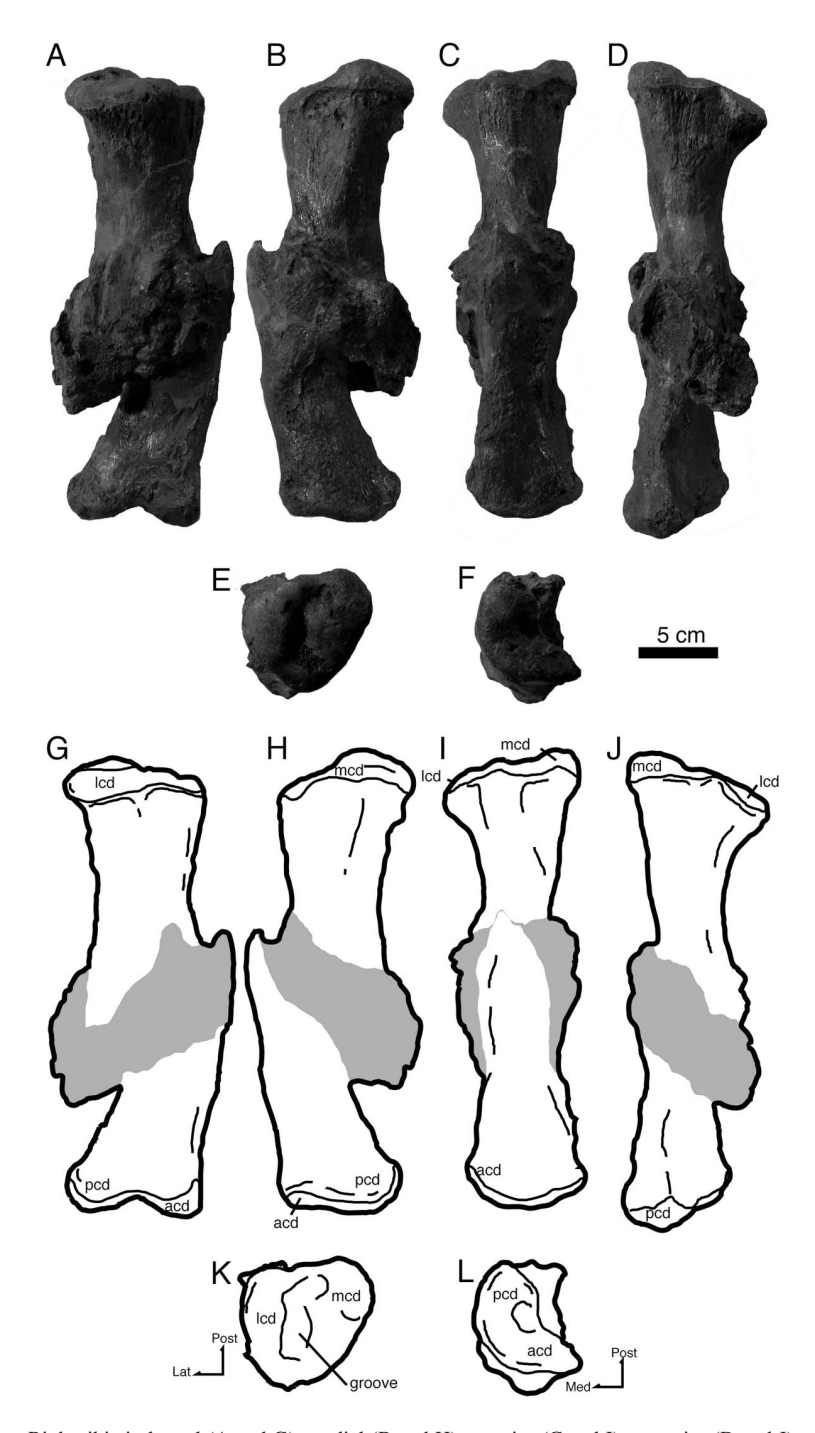


Fig. 62. Right tibia in lateral (A and G), medial (B and H), anterior (C and I), posterior (D and J), proximal (E and K), and distal (F and L) views. Abbreviations: acd, anterior condyle; Lat, lateral; lcd, lateral condyle; Med, medial; mcd, medial condyle; Post, posterior; pcd, posterior condyle. Gray areas show pathological features.

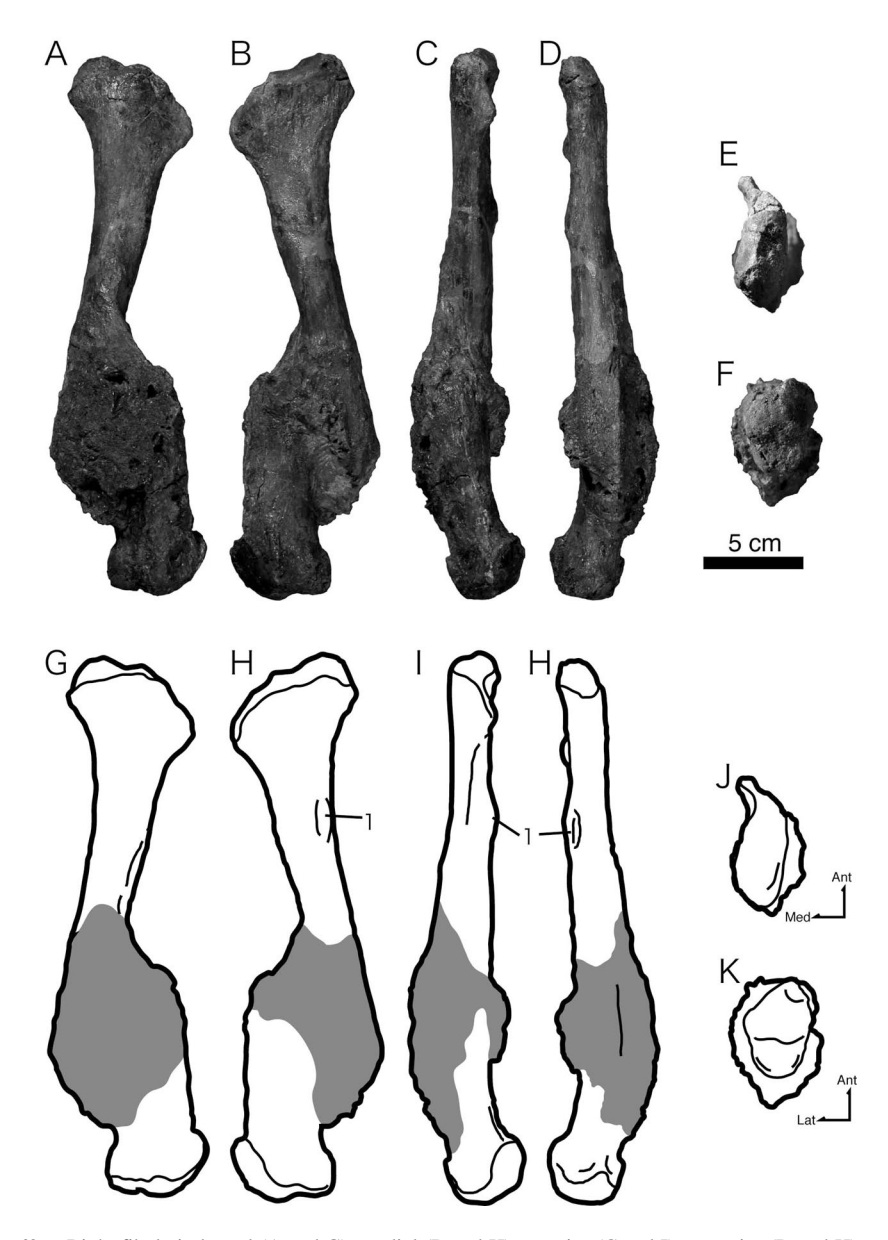


Fig. 63. Right fibula in lateral (A and G), medial (B and H), anterior (C and I), posterior (D and H), proximal (E and J), and distal (F and K) views. Abrreviations: Ant, anterior; Lat, lateral; Med, medial. 1 is for the origin for *M. iliofibularis*.

shifted to the right with respect to the distal portion, and the fractures are diagonal to their main axis. When the tibia and fubula are in articulation, the fractures are aligned on the same plane, suggesting that these fractures occurred at the same time (Fig. 64).

The proximal surface of the tibia has lateral and medial condyles, separated by a groove

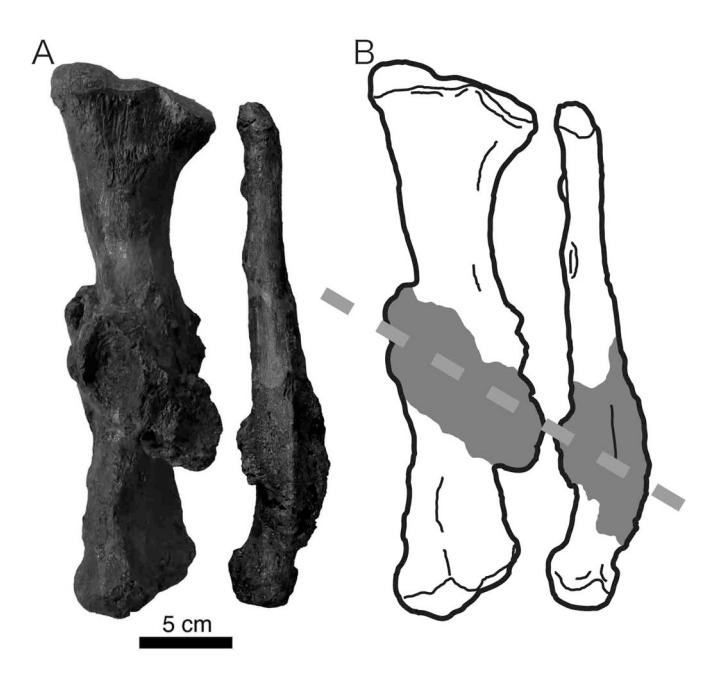


Fig. 64. Right tibia and fibula in posterior view, showing fractured areas are aligned on the same plane.

(Fig. 62). Both condyles are equally developed, and the medial condyle is more proximally extended than the lateral one in anterior view. The distal end is transversely flattened and has anterior and posterior condyles. These condyles are separated by a weak intercondylar groove. The posterior condyle is more ventrally extended than the anterior condyle.

Proximally, the fibula is transversely flat (Fig. 63). The posterior portion of the proximal end is thicker and extends more proximally than anterior portion. A small prominence for the origin for *M. iliofibularis* is present 77 mm from the proximal end. The distal end has a rounded articular surface for the tarsal articulation is thicker than the proximal end.

Tarsus

The astragalus, calcaneum and distal tarsal IV are preserved (Fig. 65). When the astragalus and calcanuem are articulated, the ankle joints of *Toyotamaphimeia* are similar those of *Alligator* and *Crocodylus* (Parrish, 1987). The distal ankle joint (between the astragalus-calcanuem complex and distal tarsals) is slightly angled from the proximal ankle joint (between the tibia-fibula and the astragalus-calcanuem complex) in anterior view. Ankle joint between the astragalus and calcanuem is unlike *Alligator* in being steeper than 45 degrees. The astragalus has articular surfaces dorsally for the tibia and fibula. The tibial articular surface is elongated and the fibular articular surface is squared. The main body of the astragalus has a depression on the anterior surface but lacks a depression on the posterior surface, in contrast to the condition in *Alligator* and *Crocodylus*. The peg-like process for the articulation with the calcaneum is constricted by a depression from the main body and fits into the socket on the medial side of the calcaneum (Parrish, 1987). The dorsal half of the wheel-shaped articular surface

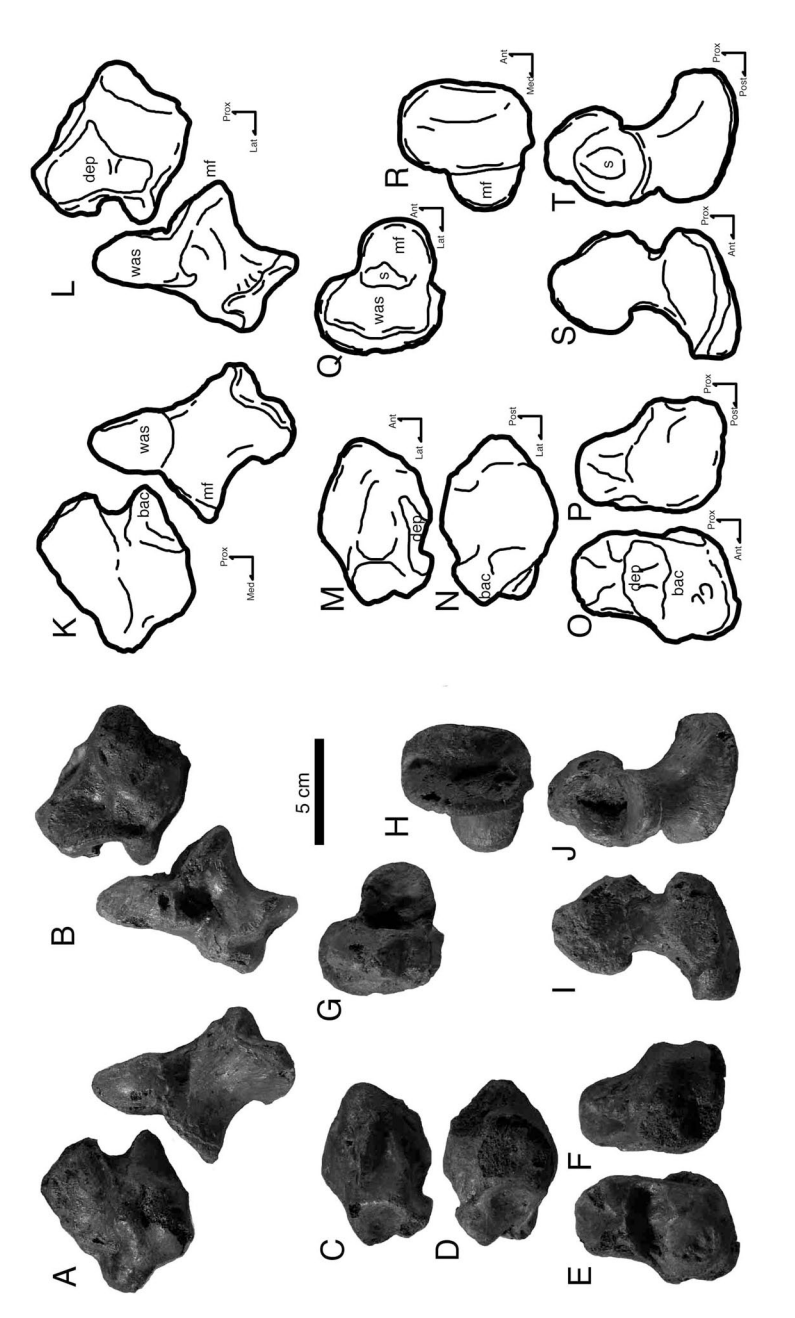


Fig. 65. Right astragalus and calcaneum of Toyotamaphimeia machikanensis in posterior (A and K) and anterior (B and L) views. Right astragalus in proximal (C and M), distal (D and N), lateral (E and O), and medial (F and P) views. Right calcaneum in proximal (G and Q), distal (H and R), lateral (I and S), and medial (J and T) views. Abbreviations: Ant, anterior; ast, astragalus; bac, ball-shaped articulation for calcaneum; cal, calcaneum; ct, calcaneal tuber; dep. depression; fas, fibular articular surface; Lat, lateral; Med, medial; mf, medial flange; Post, posterior, Prox, proximal; s, socket for astragalus; tas, tibual articular surface; was, wheel-shaped articular surface.

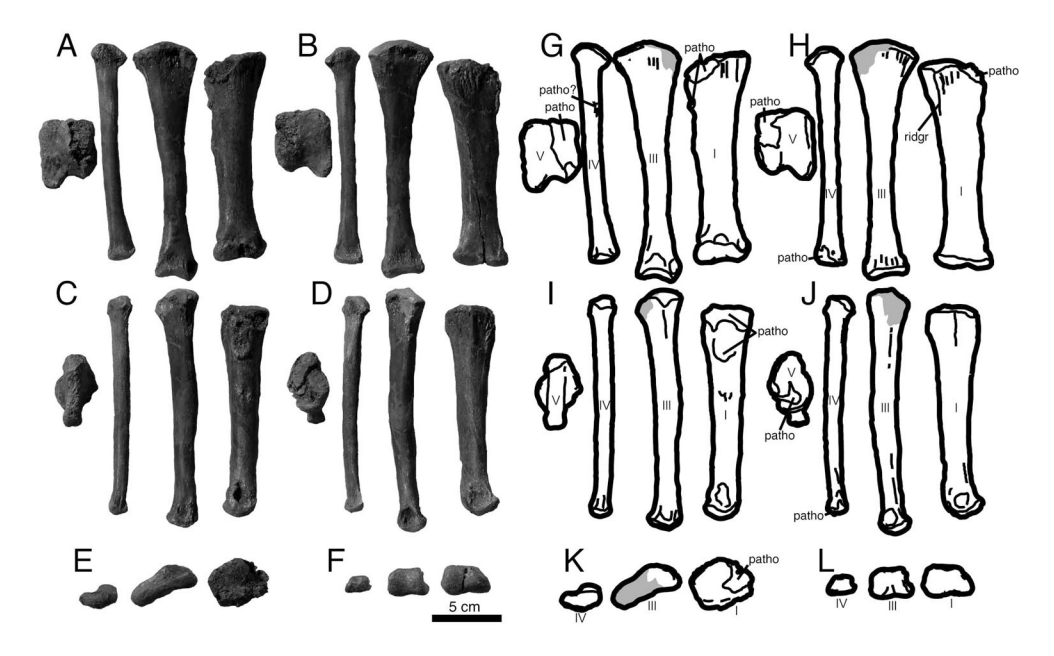


Fig. 66. Right metatarsals I, III, IV, and V of *Toyotamaphimeia machikanensis* in dorsal (A and G), ventral (B and H), lateral (C and I), medial (D and J), proximal (E and K), and distal (F and L) views. Abbreviation: patho, pathological area. Gray areas are missing parts, fillied by plasters.

of the calcaneum is for the fibula. Posteriorly, the calcaneum is dorsoventrally higher than wide and has a calcaneal tuber. Distal tarsal IV is simple in shape and triangular in proximal view.

Metatarsus and Pedal Phalanges

Metatarsals I, III, IV, and V from right side are preserved (Fig. 66). Except for the highly modified metatarsal V, metarasal I is the thickest and the shortest of the metatarsals. The proximal end has an excavation and a rugose surface, which are pathological features. The main axis of the proximal end of metatarsal I is twisted counterclockwise, which is also true in metatarsals III and IV, and results in the proximal end of these metatarsals being imbricated when in articulation. The distal condyles are weakly separated. The dorsal fossa at the distal end is small and shallow. In distal view, the main axis of the lateral condyle is perpendicular to the ventral border of the distal end while the medial condyle is laterally tilted. The fossa for the collateral ligament is deeper on the lateral surface than the medial surface. Metatarsals III and IV are subequal in length (Table 5) and are similar in shape but metatarsal IV is thinner. The proximal end is transversely expanded and dorsoventrally flat. The distal end of metatarsal III has deeper dorsal fossa than metatarsal I. The dorsal fossa of metatarsal IV is diminished. The distal condyles of metatarsal III are well separated by an intercondylar groove. The distal end of metatarsal IV has a single condyle. The fossae for the collateral ligaments on metatarsal III are deep (deeper on the lateral side). The fossae on metatarsal IV are shallow. Metatarsal V is short, less than one-third of metatarsal IV in length (Table 5) and rectangular in dorsal view. Its lateral edge has an anterior process, which extends more anteriorly than the anterior edge of metatarsal

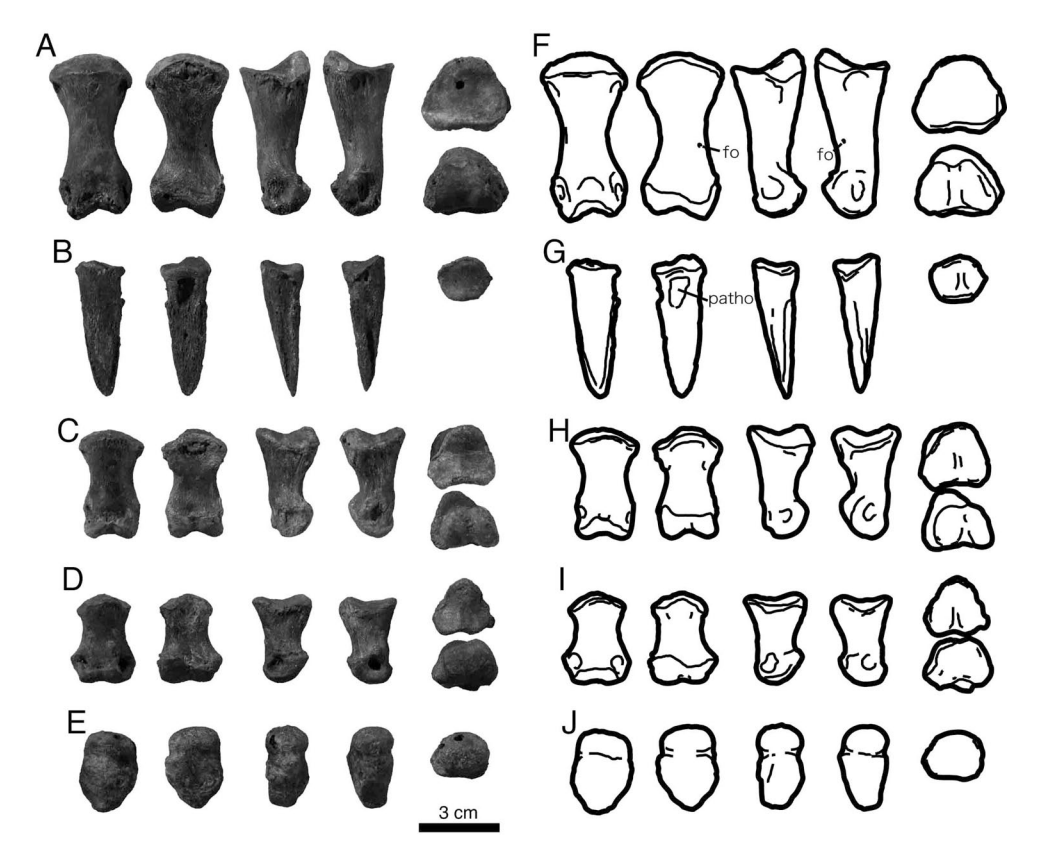


Fig. 67. Pedal phalanges of *Toyotamaphimeia machikanensis*; pedal phalanges II-1 (A and F), II-3 (B and G), II-2 or III-2 (C and H), III-3 or IV-2 (D and J), and IV-4 (E and J) in dorsal, ventral, left or right lateral, proximal, and distal views (no distal view in B, E, G and J). Abbreviations: fo, foramen; patho, pathological feature.

V main body unlike *Crocodylus*. Medially, metatarsal V is thick and has an oval-shaped surface for articulation with metatarsal IV. The medial portion of this element shows pathological features.

Five **pedal phalanges** are preserved (Fig. 67). The exact positions of these phalanges are not clear, but include a most proximal and two ungual phalanges. Referring to the ratios of pedal phalanges of *Alligator sinensis* (Cong et al., 1998), the most proximal phalanx is II-1 and one of the unguals is II-3. The other ungual may be IV-4. The other two are II-2 or III-2 and III-3 or IV-2. The most proximal phalanx is long and has an undivided proximal articular surface. The dorsal extensor tubercle is weak. The distal end has a small dorsal fossa and moderately deep collateral ligament fossae. The distal condyles are well separated by the intercondylar groove. The ungual II-3 is approximately three times as long as its transverse width at the proximal end (Table 5). The proximal surface has a weak median ridge. The ventral surface is excavated, which is interpreted as a pathology. Ungual phalanx IV-4 is short and rounded. The other two phalanges are similar in shape. The proximal end is triangular in

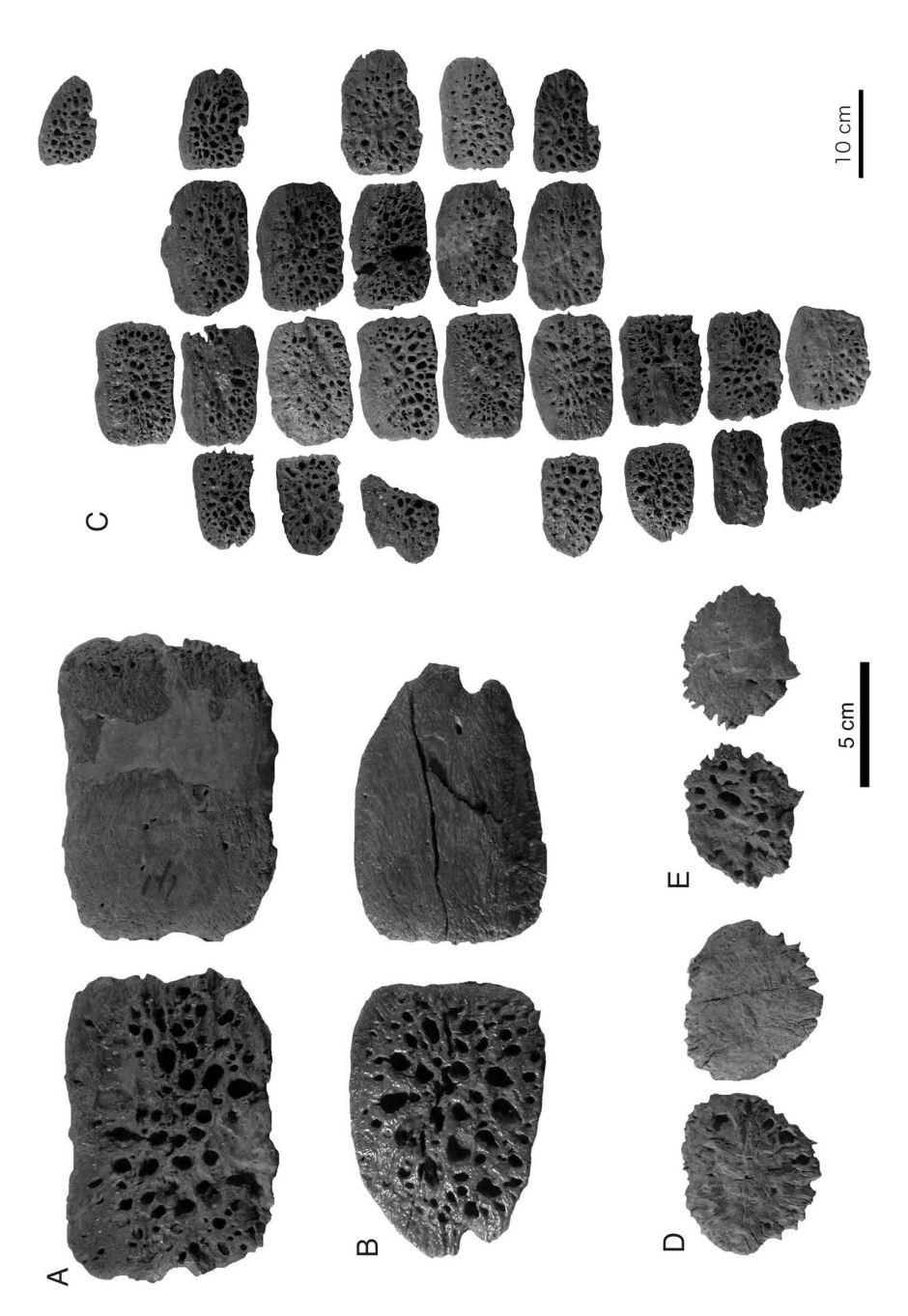


Fig. 68. Three different types of osteoderms of Toyotamaphimeia machikanensis. A median dorsal osteoderm in dorsal and ventral view (A), and a lateral dorsal osteoderm in dorsal and ventral view (B). Dorsal osteoderms in dorsal view (left lateral dorsal osteoderms, left median dorsal osteoderms, right median dorsal osteoderms, and right lateral dorsal osteoderms from left row to right) (E). Ventral osteoderms in ventral (left) and dorsal (right) views (D and E). Note: Exact anteroposterior position of each osteoderm is not clear.

proximal view and is divided by a weak median ridge. The ventral surfaces of the proximal ends have stronger flexor tubercles than pedal phalanx II-1. The dorsal fossa at the distal end is small. The distal end has deep collateral ligament fossae and equally developed condyles.

Osteoderms

Thirty three osteoderms (Fig. 68) are preserved. There are three types; median dorsal, lateral dorsal, and ventral osteoderms. Because all of the other osteoderms were disarticulated when discovered, the number of dorsal osteoderms in each row has been uncertain. However, there would have been four osteoderms in each transverse row because the width of median osteoderms is nearly consistent and the width of each row with four osteoderms is approximately the same as the body width in the reconstructed skeleton (Fig. 68C). Those osteoderms all have an anterior facet on the dorsal surfaces and a posterior facet on the ventral surface, which indicate dorsal osteoderms overlapped each other in life (i.e., the anterior row covers the anterior margion of the posterior row). The median and lateral dorsal osteoderms are rectangular, but the median dorsal osteoderms are transversely longer than lateral dorsal osteoderms (Fig. 68A, B). These osteoderms lack an anterior process at thier lateral edges or a keel on their dorsal surfaces. In median dorsal osteoderms, the ratios between the anteroposterior lengths and transverse widths are roughly half of the transverse width. The median dorsal osteoderms have sutures along their lateral and medial sides. The anteroposterior lengths of the dorsal overlap area reachs 20 mm in some osteoderms. In anterior view, the medial dorsal osteoderms are straight. The medial portion of the osteoderms is thicker than the lateral portion. One of these median dorsal osteoderms has cavities, interpreted as a pathological feature by Katsura (2004). The lateral dorsal osteoderms have sutural facets only on their medial sides. Laterally, these osteoderms become thin. The anterior facet is anteroposteriorly narrower than the ones in the medial dorsal osteoderms. In anterior view, the lateral dorsal osteoderms are curved, in some cases strongly so. These strongly curved osteoderms are probably from anterior or posterior parts of the dorsal armor. The ventral surfaces of the median and lateral dorsal osteoderms have nutrient foramina. Two pieces of ventral osteoderms, characterized by irregular edges and convex ventral surface, were recovered (Fig. 68D, E). These are much smaller than the other two types and are nearly circular in shape. The dorsal surface of a larger ventral osteoderm lacks any neutrient foramen, but a foramen is present in the smaller piece.

DISCUSSION

Phylogenetic Analyses

To test the phylognetic status of *Toyotamaphimeia machikanensis* within Crocodylia, the data matrix, based on previous studies (Brochu, 1999, 2004, 2006; Brochu and Gingerich, 2000; Brochu and Rincón, 2004; Delfino et al., 2005,) was used. In addition to *Toyotamaphimeia machikanensis*, five taxa are used for Alligatoroidea (*Leidyosuchus canadensis*, *Diplocynodon darwini*, *Brachychampsa montana*, *Stangerochampsa mccabei*, *Alligator mississippiensis*, and *Caiman yacare*), and four are used for gavialoids (*Thoracosaurus neocesariensis*, *Argochampsa krebsi*, *Piscogavialis jugaliperforatus* and *Siquisiquesuchus venezuelensis*). Two basal crocodyloids (*Prodiplocynodon langi* and *Asiatosuchus grangeri*) are excluded in order to reduce the number of polytomies in these clades. *Bernissertia fagesii* and *Hylaeochampsa vectiana* are used as outgroup taxa. Characters in this study follow the data matrix of Brochu (2006).

A phylogenetic analysis was performed utilizing 165 characters and including 46 ingroup taxa and two outgroup taxa (Appendices 1 and 2). All characters are equally weighted and unordered. This phylogenetic analysis was carried out using PAUP 4.0Beta (Swofford, 2000). Heuristic searches produced 323 equally most parsimonious trees with a tree length of 420 steps (C.I. excluding uninformative characters = 0.425, R.I. = 0.756, R.C. = 0.349). As suggested by Brochu and Gingerich (2000), all nodes within Tominstominae are not strongly supported and collapse in trees one step longer because of the low number of apomorphies per node.

A strict consensus tree of 323 equally most parsimonious trees is shown in Figure 69, and *Toyotamaphimeia machikanensis* is placed as a derived Tomistominae and a sister taxon of a modern genus *Tomistoma schlegelii*. The relationships among *Dollosuchus dixoni*, *Gavialosuchus americanus*, and the calde of *Tomistoma cairense* and higher taxa and among *Gavialosuchus eggenbergensis*, *Tomistoma lusitanica*, and the clade including *Tomistoma schlengelii* and *Toyotamaphimeia machikanensis* is unresolved. The general tree topology of the strict consensus tree is almost same as the one proposed by Brochu (2006). Six different tree topologies for the clade of Tomistominae are suggested from 323 equally most parsimonious trees (Fig. 70). Character status of some important characters for the relationships of the members of Tomistominae are shown in Table 6.

The monophyly of Tomistominae is supported by two unambiguous synapomorphies (deep splenial symphysis longer than five dentary alveoli, forming narrow "V", and thin-wedged palatine process; characters 43 and 118) in all tree topologies (Fig. 70). These unambiguous synapomorphies are related to the elongation of the rostrum (Brochu and Gingerich, 2000). The deep splenial symphysis is seen in both Tomistominae and Gavialoidea but narrow splenial is characteristic to the members of Tomistominae. The thin-wedged palatine process is common

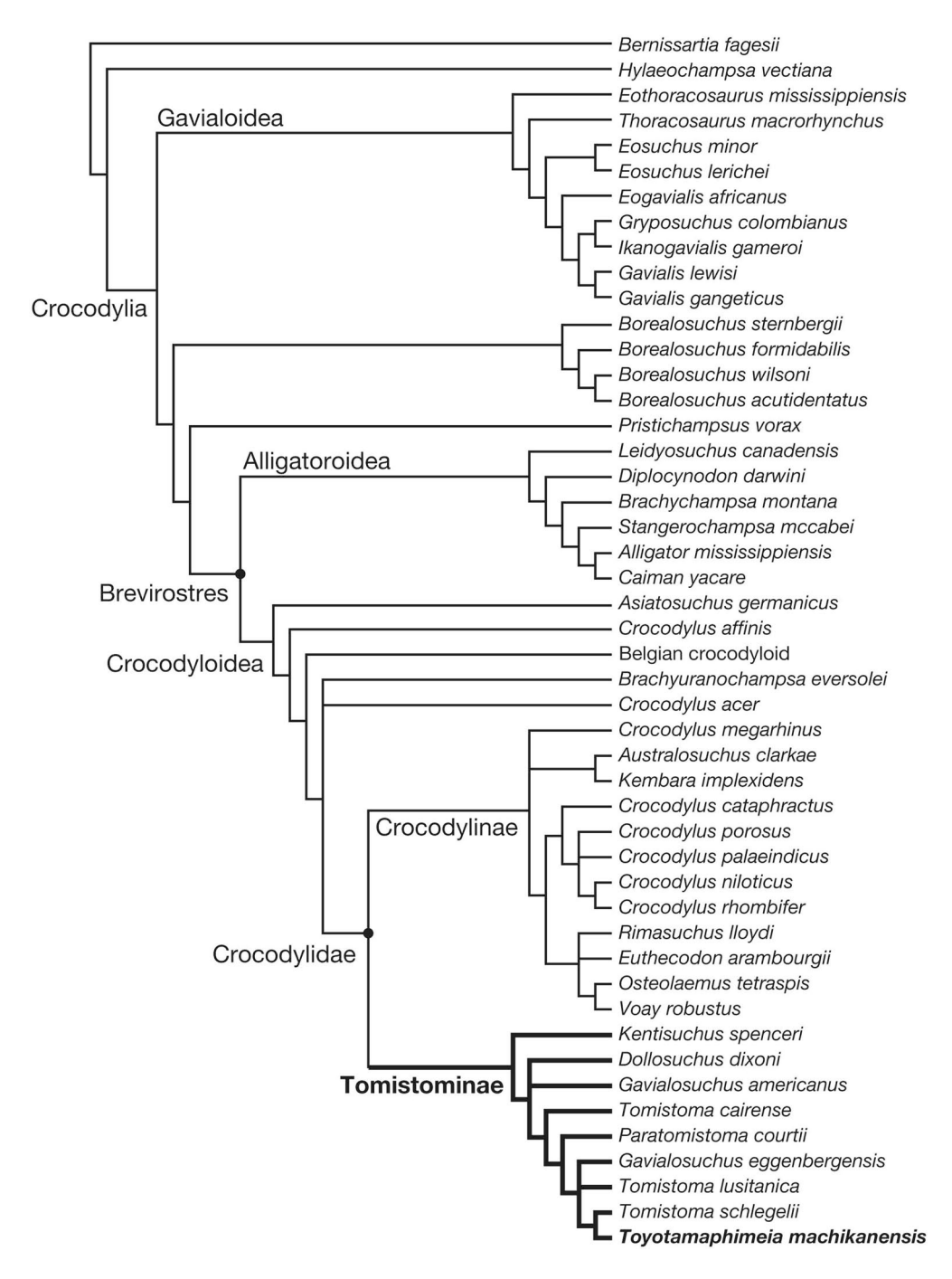


Fig. 69. Strict consensus tree of 323 equally most parsimonious trees of 420 steps.

Character number	43	88	93	92	118	84	95	68	44	45	86	47	18
Bernissartia fagesii	0	0	?	?	0	0	?	0	0	?	1	?	?
Hylaeochampsa vectiana	?	0	1	1	0	0	?	?	?	?	1	?	?
Brachyuranochampsa eversolei	?	1	0	1	?	0	1	?	?	?	1	?	?
Crocodylus acer	?	1	0	1	0	0	1	?	?	?	0	?	?
Australosuchus clarkae	1	?	0	1	0	0	1	0	1	1	0	0	?
Kembara implexidens	1	0	0	1	0	0	1	0	1	1	0	0	?
Crocodylus megarhinus	1	1	2	1	0	0	1	0	?	?	?	0	?
Kentisuchus spenceri	4	0	1	1	1	0	1	?	1	1	0	0	?
Dollosuchus dixoni	4	0	1	1	1	1	2	0	?	?	0	0	0
Gavialosuchus americanus	4	?	1	?	1	1	2	2	1	2	0	?	0
Tomistoma cairense	4	0	0	1	1	1	2	2	0	2	0	?	?
Paratomistoma courtii	?	?	0	1	?	1	?	?	0	0	0	0	?
Gavialosuchus eggenbergensis	?	0	2	1	1	1	2	?	?	?	1	?	?
Tomistoma lusitanica	4	0	0	1	1	1	2	2	?	?	1	0	?
Tomistoma schlegelii	4	0	1	1	0	0	2	2	0	0	1	1	1
Tovotamanhimeia machikanensis	4	0	0	1	0	2	2	2	0	0	1	1	1

Table 6. Character status for characters, suggested as unambiguous synapomorphies of all nodes in the clade of Tomistominae by the phylogenetic analysis in this study. Character descriptions are shown in Appendix 1.

in Tomistominae and Gavialoidea as well as other lineages (derived forms of Borealosuchus and Crocodylus cataphractus). In derived tomistomines (Tomistoma schlegelii and Toyotamaphimeia machikanensis), the palatine process is broad anteriorly. One additional character (posterior process of the maxilla extending within the lacrimal; character 93) appears as an unambiguous synapomorphy of Tomistominae when Dollosuchus dixoni and Gavialosuchus americanus are paraphyletic (Fig. 70A-C). This condition is seen in basal tomistomines (Kentisuchus spenceri, Dollosuchus dixoni, and Gavialosuchus americanus) and Tomistoma schlegelii and occurs in other lineages (e.g., Rimasuchus lloydi, Crocodylus niloticus, Crocodylus rhombifer, and some gavialoids and alligatoroids) as well. Another additional character (suborbital fenestra without posterior notch; character 88) becomes an unambiguous synapomorphy of Tomistominae when Crocodylus megarhinus is placed as a basal taxon of Crocodylinae and is basal to Kembara implexidens. This character is common in Tomistominae and is not seen in other crocodyloids, used in this analysis, except for one of basal taxa of Crocodylinae, Kembara implexidens. To clarify whether suborbital fenestra without posterior notch is an unambiguous synapomorphy or not, the relationships of basal crocodylines need to be better understood.

Kentisuchus spenceri is a sister taxon to the clade of *Dollosuchus dixoni* + *Gavialosuchus americanus* + higher taxa, which is supported by two unambiguous synapomorphies (squamosal groove flaring anteriorly and nasals excluded from external naris with the premaxillae and nasals in contact; characters 84 and 95) in all tree topologies (Fig. 70). When *Dollosuchus dixoni* and *Gavialosuchus americanus* form a monophyly with a single unambiguous synapomorphy (amphicoelous presacral centra; character 18), character 45 (lingual foramen for articular artery and alveolar nerve on angular entirely) becomes an additional unambiguous synapomorphy of the clade of *Dollosuchus dixoni* + *Gavialosuchus americanus* + higher taxa. The presence of amphicoelous presacral centra is known in *Dollosuchus dixoni* and *Gavialosuchus americanus* but unkown in other basal tomistomines (*Kentisuchus spenceri*,

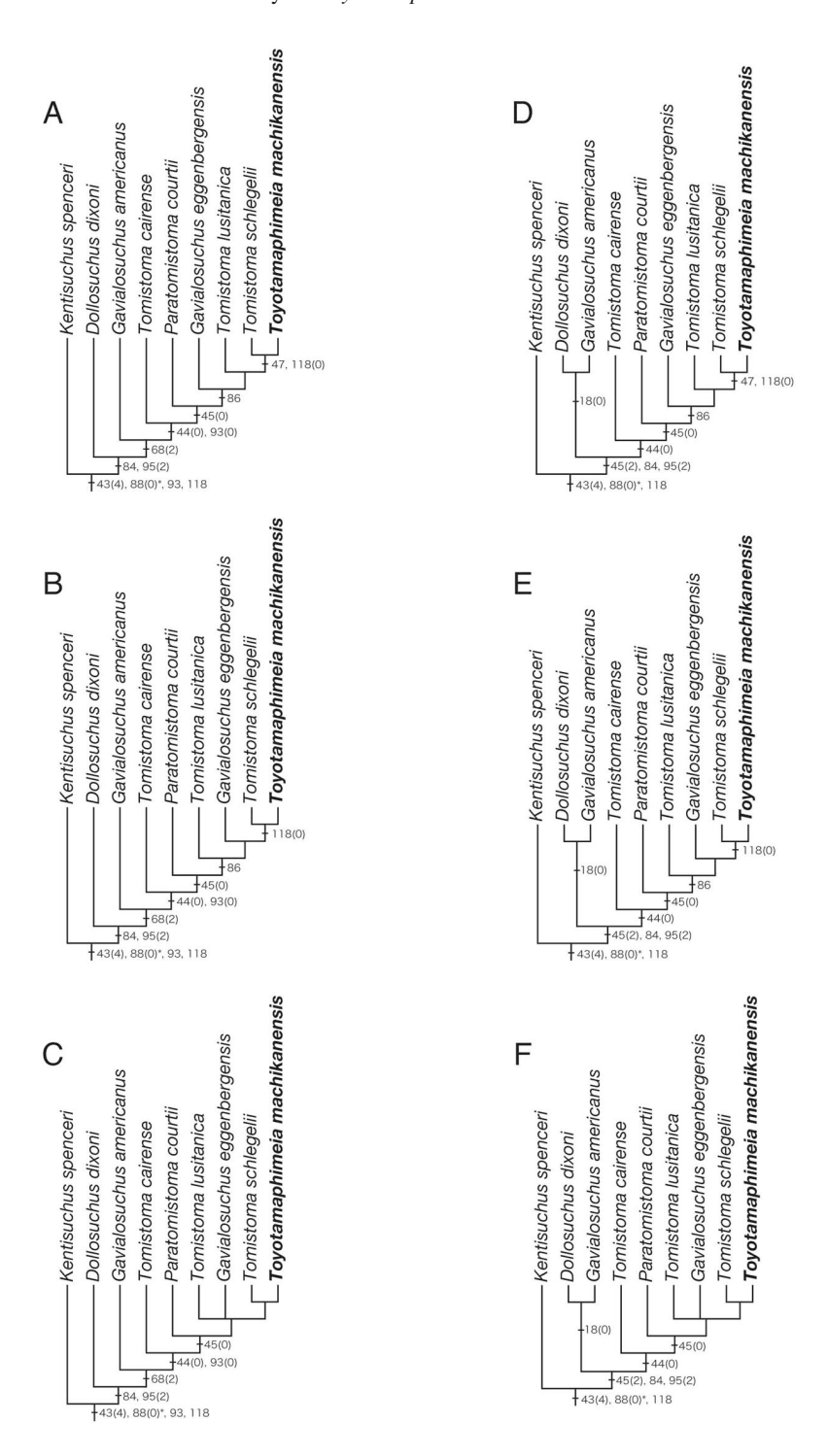


Fig. 70. Six different tree topologies, showing the relationships of the members of Tomistominae.

Tomistoma cairense, Paratomistoma courtii, Gavialosuchus eggenbergensis and Tomistoma lusitanica). Derived tomistomines (Tomistoma schlegelii and Toyotamaphimeia machikanensis) has procoelous presacral centra. The evolutionary trend of the position of the lingual foramen for articular artery and alveolar nerve within Tomistominae is complex. Primitively, crocodylids have this foramen on surangular-angular suture. A basal tomistomine, Kentisuchus spenceri, retains the primitive condition, but more derived forms such as Gavialosuchus americanus and Tomistoma lusitanica shift the position of the foramen onto the angular. In tomistomines more derived than Paratomistoma courtii, the foramen is positioned on the surangular.

The clade of *Tomistoma cairense* and higher taxa is supported by two unambiguous synapomorphies (simple articular-surangular suture on the medial surface and absence of posterior process of the maxilla; characters 44 and 93) when *Dollosuchus dixoni* and *Gavialosuchus americanus* are paraphyletic and by a single character (character 44) when *Dollosuchus dixoni* and *Gavialosuchus americanus* are monophyletic. A similar result is shown by Brochu and Gingerich (2000) (the clade of *Tomistoma cairense* and higher taxa united by a single unambiguous synapomorphy; character 44). The simple articular-surangular suture on the medial surface is common in non-crocodylid crocodylians as well as *Tomistoma cairense* and higher taxa, and most members of Crocodylidae have the anterior process of the articular along the articular-surangular suture, suggesting that derived tomistomines secondarily lost the anterior process of the articular. The absence of the posterior process of the maxilla is a plesiomorphic condition for Crocodylia and is lost in derived tomistomines as a reversal.

Paratomistoma courtii and the clade of Gavialosuchus eggenbergensis + Tomistoma lusitanica + higher taxa share a single unambiguous synapomorphy (lingual foramen for articular artery and alveolar nerve on surangular entirely; character 45). This agrees with the results of Brochu and Gingerich (2000). This condition is known in Paratomistoma courtii, Tomistoma schlengelii, and Toyotamaphimeia machikanensis (unknown in Gavialosuchus eggenbergensis and Tomistoma lusitanica).

The clade of *Gavialosuchus eggenbergensis* + *Tomistoma lusitanica* + higher taxa is supported by one unambiguous synapomorphy (linear frontoparietal suture; character 86). This condition is known in *Gavialosuchus eggenbergensis*, *Tomistoma lusitanica*, *Toyotamaphimeia machikanensis*, and *Tomistoma schlengelii* among tomistomines and occurs in other lineages (e.g., some species of *Borealosuchus* and derived gavialoids).

Phylogenetic relationships of Gavialosuchus eggenbergensis, Tomistoma lusitanica, and the clade of Tomistoma schlengelii and Toyotamaphimeia machikanensis are poorly resolved. The phylogenetic analysis in this study shows three different topologies for the relationships of these clades (Fig. 70). The clade of Tomistoma lusitanica, Tomistoma schlengelii, and Toyotamaphimeia machikanensis is supported by only one ambiguous synapomorphy (vomer exposed on palate between palatines; character 126) by DELTRAN optimization. This condition is characteristic of derived tomistomines because it is only known in Tomistoma lusitanica and Tomistoma schlengelii. A close relationship between Gavialosuchus eggenbergensis, the clade of Tomistoma schlengelii and Toyotamaphimeia machikanensis is supported only by one ambiguous character (angular-surangular suture passing broadly along ventral margin of external mandibular fenestra; character 47) (Fig. 70B, E) by ACTRAN optimization, but this condition is unkown in Gavialosuchus eggenbergensis.

Toyotamaphimeia machikanensis and Tomistoma schlengelii form a monophyly, sharing two unambiguous synapomorphies (angular-surangular suture passing broadly along ventral margin of external mandibular fenestra and palatine process generally broad anteriorly; characters 47 and 118) when Tomistoma lusitanica is a sister taxon to the clade of Tomistoma schlengelii and Toyotamaphimeia machikanensis but only one unambiguous synapomorphy (character 118) when Gavialosuchus eggenbergensis is a sister taxon to the clade. As discussed earlier, the thin-wedged palatine process is one of unambiguous synapomorphies for Tomistominae, but the broad palatine process occurs in derived tomistomines (Tomistoma schlegelii and Toyotamaphimeia machikanensis) as a reversal. The condition of angular-surangular suture seen in Tomistoma schlegelii and Toyotamaphimeia machikanensis is derived condition in Tomistominae and is also known in other lineages of Crocodylia (e.g., Eogavialis africanus, Caiman yacare, and some species of Crocodylus).

Fifteen characters are suggested as autapomorphies of *Toyotamaphimeia machiakanensis*: axis neural arch with a lateral process ("diapophysis") (character 4); axial hypapophysis toward the center of centrum (character 6); axis neural spine without crest (character 12); dorsal margin of atlantal rib with prominent process (character 14); prominent iliac anterior process (character 34); dorsal osteoderms without keel (character 35); four dorsal osteoderms per row (character 37); splenial with anterior perforation for mandibular ramus of cranial nerve V (character 41); absence of a sulcus between articular and surangular (character 60); massive postorbital bar (character 70); all dentary teeth occlude lingual to maxillary teeth (character 78); ectpterygoid separated from maxillary toothrow (character 91); smooth posterior margin of otic aperture (character 102); lateral eustachian canal positioned lateral to medial eustachian canal (character 147); and internal choana not septate (character 152).

Some characters are the plesiomorphic condition for Crocodylia and reversal from the derived state seen in *Borealosuchus* and higher taxa (characters 4 and 70), Brevirostres (characters 34, 35, 37, and 102), the clade of *Crocodylus affinis* and higher taxa (character 41), and Crocodyloidea (character 12). Some characters are independently acquired by other forms of Tomistominae: massive postorbital bar in *Dollosuchus dixoni* and *Tomistoma cairense*, and non-crested axis neural spine in *Dollosuchus dixoni*. Two other characters are plesiomorphic condition for Breviostres and a reversal from the derived state seen in the clade of *Tomistoma cairense* and higher taxa (character 60) and the clade of *Brachyuranochampsa eversolei*, *Crocodylus acer*, and higher taxa (character 78).

Similar conditions of five characters in *Toyotamaphimeia machikanensis* are seen in other non-tomistomine groups: axial hypapophysis toward the center of centrum (character 6) seen in *Diplocynodon* and Belgian crocodyloid; dorsal margin of atlantal rib with prominent process (character 14) seen in Alligatoroidea and *Crocodylus affinis*; ectpterygoid separated from maxillary toothrow (character 91) seen in Alligatoroidea; lateral eustachian canal positioned lateral to medial eustachian canal (character 147) seen in some species of *Crocodylus*; and internal choana not septate (character 152) seen in *Euthecodon arambougii* and gavialoids.

Among the autopomorphies for *Toyotamaphimeia machikanensis*, twelve characters (characters 4, 6, 14, 34, 35, 37, 41, 78, 91, 102, 147, and 152) can be used as diagnostic of this taxon because these are seen only in *Toyotamaphimeia machikanensis* among tomistomine crocodylians. Also, as suggested by Aoki (1983), a large seventh maxillary teeth is diagnostic of *Toyotamaphimeia machikanensis*

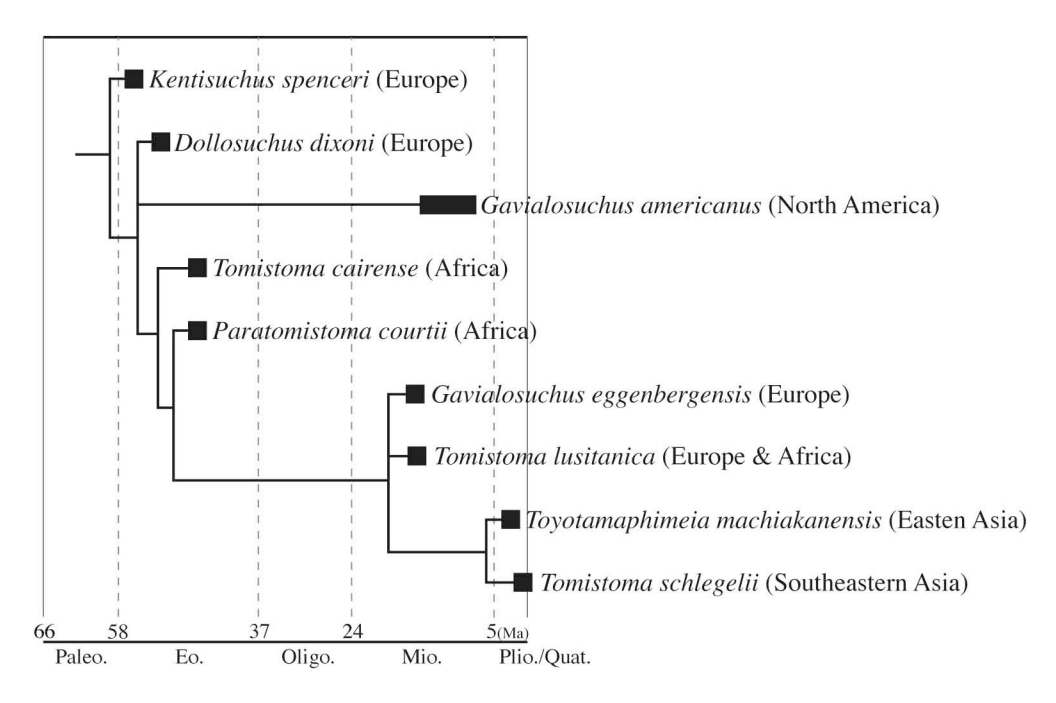


Fig. 71. Phylogenetic tree of Tomistominae with time scale, modified from Brochu (2001b)

The phylogenetic tree shown in Figure 71 suggests that tomistomines first appeared in Europe during the early Eocene and dispersed to other parts of Europe and Africa with a migration of *Gavialosuchus americanus* to North America prior to the Middle Eocene (Brochu, 2001a and b). The migration of tomistomines to eastern Asia occurred during or prior to the middle Miocene. However, possible tomistomines are known from the Eocene of Asia (*Tomistoma petrolica* from China, Yeh, 1958; *Ferganosuchus planus* from Russia, Yefimov, 1982), suggesting that tomistomines migrated into Asia during or prior to the Eocene and the dispersal pattern of tomistomines maybe more complex than the phylogenetic tree shows.

Comments on "Toyotamaphimeia machikanensis", Another Tomistomine from the Osaka Group, from Kishiwada City of Osaka Prefecture

A partial skeleton of a tomistomine, the Kishiwada tomistomine, was found from the sediments near the lower boundary of Ma5 (approximately 6 million years ago) of the Osaka Group in Kishiwada City of Osaka Prefecture and was described by Taruno (1999) (Fig. 72). Taruno (1999) discussed similarities and differences between the Kishiwada tomistomine and *Toyotamaphimeia machikanensis* (Fig. 73). Based on his study, the Kishiwada tomistomine shows similarities with *Toyotamaphimeia machikanensis* in having a narrow snout, sub-circular orbits, supratemporal fenestra equal in size to the orbit, nasal excluded from external naris, and large seventh maxillary teeth, although the latter two can not be confirmed because of poor preservation of the specimen. However, the similarities discussed by Taruno maybe

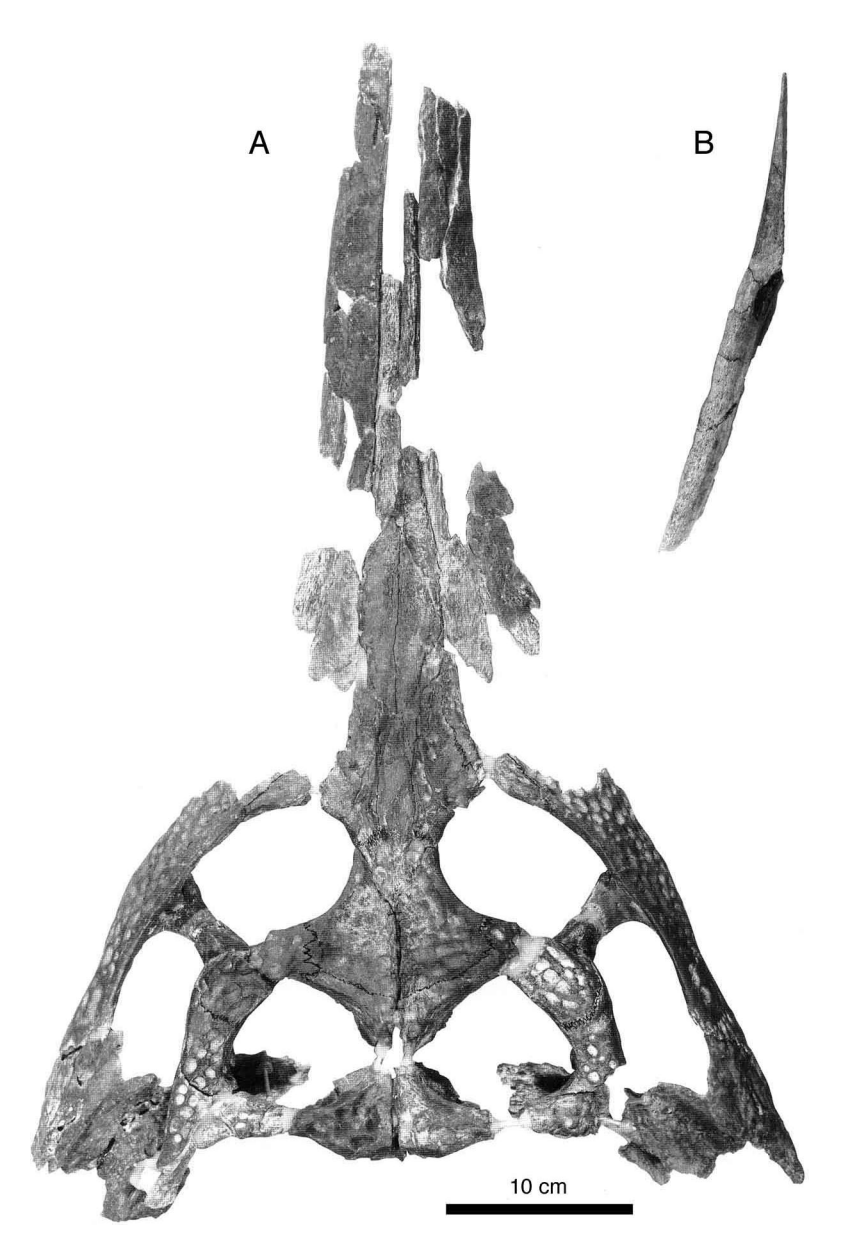


Fig. 72. Photographs of a tomistomine crocodylian from the Kishiwada town from Taruno (1999). Skull in dorsal view (A) and splenial in ventral view (B).

synplesiomorphies except for the large seventh maxillary teeth, which is characteristic to *Toyotamaphimeia machikanensis*. Until the size of the seventh maxillary teeth relative to the more anterior teeth is known, whether or not the Kishiwada tomistomine is *Toyotamaphimeia machikanensis* is uncertain.

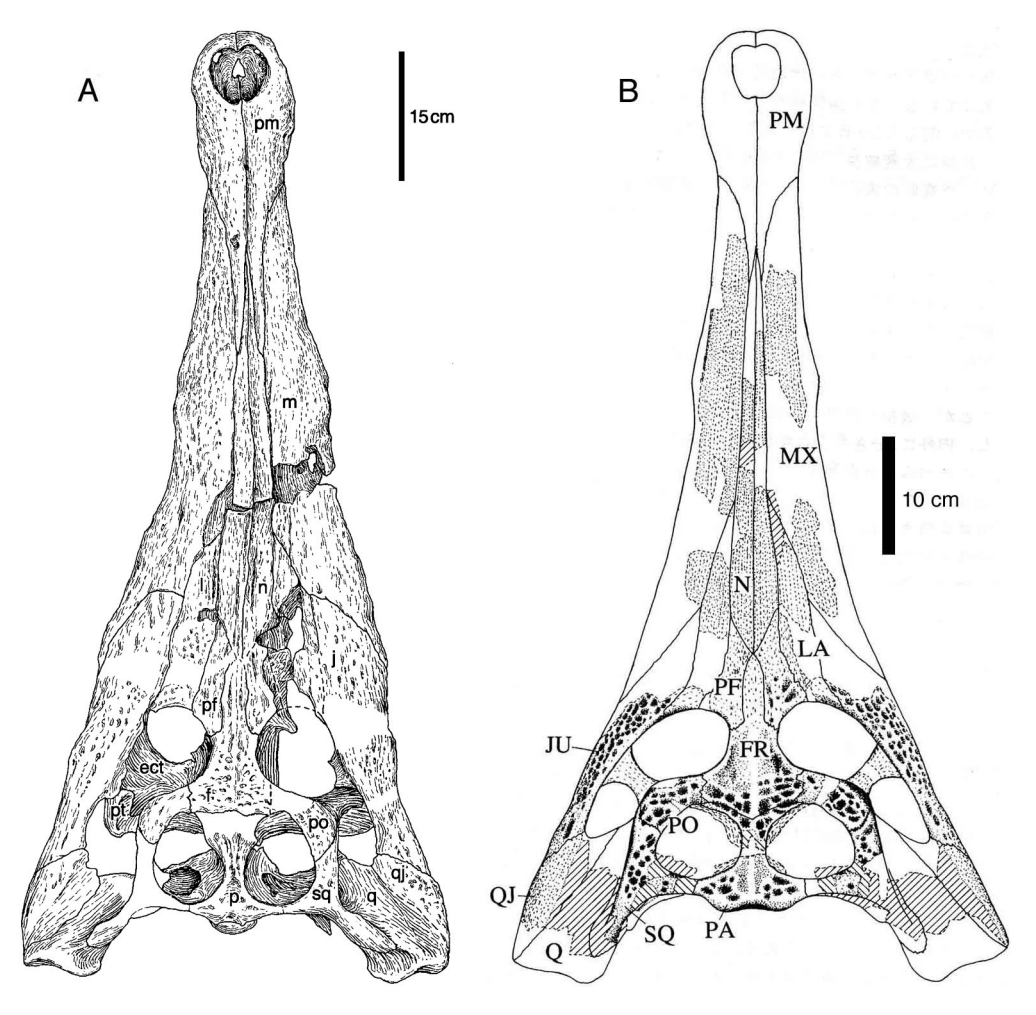


Fig. 73. Comparisons of *Toyotamaphimeia machikanensis* (A) and a tomistomine crocodylian from the Kishiwada town (B) (Taruno, 1999).

Taruno (1999) also pointed out that the Kishiwada tomistomine is different from *Toyotamaphimeia machikanensis* in having more slender snout and wide postorbital region of the skull but considered the taxonomic significance of differences to be unclear (Fig. 73). From drawings and photographs in published by Taruno (1999), some additional differences can be observed. Some preorbital elements, especially the nasals and lacrimals, are narrower than in *Toyotamaphimeia machikanensis*, which is probably because of the more slender snout of the Kishiwada tomistomine. The skull table is relative broader than in *Toyotamaphimeia machikanensis*. The supratemporal fenestra is circular in the Kishiwada tomistomine, but oval-shaped in *Toyotamaphimeia machikanensis*. The frontal-parietal suture is anteriorly concave, whereas the suture is straight in *Toyotamaphimeia machikanensis*. Taruno (1999) described the articular of the Kishiwada tomistomine as probably having an anterior process dorsal to the

lingual foramen along the articular-surangular suture on the medial surface of the mandible. This process is absent in *Toyotamaphimeia machikanensis*.

The Kishiwada specimen is probably a tomistomine because it has deep splenial symphysis and the anterior portion of the splenial is narrow and V-shaped as in other tomistomines (Fig. 72). Although Taruno (1999) suggested that the Kishiwada tomistomine is *Toyotamaphimeia machikanensis*, some of the aforementioned differences between these forms may indicate that the Kishiwada tomistomine is a distinct taxon, more primitive than *Toyotamaphimeia machikanensis*. The concave frontal parietal suture may place the Kishiwada tomistimine more basal to the clade including *Gavialosuchus eggenbergensis* and *Tomistoma lusitanica* plus two more crown taxa. Furthermore, if the anterior process of the articular is present in the Kishiwada tomistomine, this form is placed more basal to the clade of *Tomistoma cairense* and higher taxa. If the Kishiwada tomistomine is more primitive than the clade of *Gavialosuchus eggenbergensis* + *Tomistoma lusitanica* + higher taxa or the clade of *Tomistoma cairense* and higher taxa, the dispersal of tomistomines to the eastern edge of Asia may have occurred during or prior to the Eocene, which is also suggested by the occurrence of *Tomistoma petrolica* from the Eocene of China. However, additional material is needed to clarify the taxonomic status and establish the phylogenetic relationships of the Kishiwada tomistomine.

ACKNOWLEDGMENTS

Authors are grateful to Christopher A. Brochu and Massimo Delfine for providing their data matrices and discussions for phylogenetic analyses, and Ryosuke Aoki for sharing unpublished information and discussions. Donald B. Brinkman, Xiao-chun Wu, and Christopher A. Brochu reviewed the paper and improved its quality. We would like to thank Makoto Manabe for organizing loans of modern crocodylian specimens from the National Science Museum in Tokyo, Hiroyuki Taruno for allowing us to use photographs from his paper, Masakazu Kitade for making line drawings, Yasuko Okamoto for detailed line drawings of skull and jaws, Shinichi Sano for providing information on the geology of the Osaka Group, Katsuhiro Kubota for providing us photocopies of some papers, and Kazunori Miyata for his help in many ways. We are thankful to Drs. Kojiro Nakaseko and Tsuguo Sunamura for their help in loaning the original specimen to the National Science Museum in Tokyo, and Y. K. is thankful to the staff of Museum of Osaka University for their hospitality during his study at the museum.

REFERENCES CITED

- Aoki, R., 1983. A new generic allocation of *Tomistoma machikanense*, a fossil crocodilian from the Pleistocene of Japan. *Copeia*, 1: 89–95.
- Aoki, R., 1992. Fossil crocodilians from the late Tertiary strata in the Sinda Basin, eastern Zaire. African Study Monographs, 17: 67–85.
- Benton, M. and J. M. Clark., 1988. Archosaur phylogeny and the relationships of the Crocodylia. *In M. J. Benton (ed.), The Phylogeny and Classification of the Tetrapods, Vol. 1.* Clarendon Press, Oxford: 295–338.
- Brochu, C. A., 1996. Closure of neurocentral sutures during crocodilian ontogeny: implications for maturity assessment in fossil archosaurs. *Journal of Vertebrate Paleontology*, **16**: 49–62.
- Brochu, C. A., 1997. Phylogenetic systematics and taxonomy of Crocodylia. Ph. D. dissertation, University of Texas at Austin, Austin, Texas.
- Brochu, C. A., 1999. Phylogenetic, taxonomy, and historical biogeography of Alligatoroidea. *Society of Vertebrate Paleontology Memoir*, **6**: 9–97.
- Brochu, C. A., 2001a. Crocodylian snouts in space and time: phylogenetic approaches toward adaptive radiation. American Zoologists, 41: 564–585.
- Brochu, C. A., 2001b. Congruence between physiology, phylogenetics and the fossil record on crocodylian historical biogeography. *In* G. C. Grigg, F. Seebacher, and C. E. Franklin (eds.), *Crocodilian biology and evolution*, Surrey Betty and Sons, Chopping Norton: 9–28.
- Brochu, C. A., 2004. A new Late Cretaceous gavialoid crocodylian from eastern North America and the phylogenetic relationships of thoracosaurs. *Journal of Vertebrate Paleontology*, **24**: 610–633.
- Brochu, C. A., 2006. Osteology and phylogenetic significance of *Eosuchus minor* (Marsh, 1870) new combination, a longirostrine crocodylian from the Late Paleocene of North America. *Journal of Paleontology*, **80**: 162–186.
- Brochu, C. A. and P. D. Gingerich., 2000. New tomistomine crocodylian from the middle Eocene (Bartonian) of Wadi Hitan, Fayum Province, Egypt. Contributions from the Museum of Paleontology, University of Michigan, 30: 251–268.
- Brochu, C. A. and A. D. Rincón., 2004. A gavialoid crocodylian from the Lower Miocene of Venezuela. *In M. Sánc hez-Villagra and J. Clack (eds.)*, Fossils of the Castillo Formation, Venezuela: Contributios in Neotropical Palaeontology. *Special Papers in Palaeontology*, **71**: 61–79.
- Buscalioni, A. D., J. L. Sanz, and M. L. Casanovas., 1992. A new species of the eusuchian crocodile *Diplocynodon* from the Eocence of Spain. *Neues Jahrbuch für Geologie und Palaontologie Abandlungen* 187: 1–29.
- Clark, J. M., 1994. Patterns of evolution in Mesozoic crocodyliformes. In N. C. Fraser and H.-D. Sues (eds.), In the Shadow of the Dinosaurs, Cambridge University Press, New York: 84–97.
- Cong, L., L. Hou, X. Wu, and J. Hou., 1998. The gross anatomy of Alligator sinensis Fauvel. Science Publishing Co. Beijing, China.
- Delfino, M, P. Piras, and T. Smith., 2005. Anatomy and phylogeny of the gavialoid crocodylian *Eosuchus lerichei* from the Paleocene of Europe. *Acta Palaeontologica Polonica*, **50**: 565–580.
- Erickson, B. R. 1976., Osteology of the early eusuchian crocodile *Leidyosuchus formidabilis*, sp. nov. *Monographs of the Science Museum of Minnesota (Paleontology)*, 2: 1–61.
- Frey, E. 1988., Anatomie des Körperstammes von Alligator mississippiensis Daudin. Stuttgarter Beiträge zur Naturkunde, Ser. A, 426: 1–60.
- Frey, E., J. Reiss, and S. F. Tarsitano., 1989. The axial tail musculature of recent crocodilians and its phylogenetic implications. *American Zoologist*, **29**: 857–862.
- Gmelin, J. F., 1789. Linnei Systema Naturae. G. E. Beer, Leipzig. 1057p.
- Hayashi, T. and T. Kawabe., 1993. The Kobiwako Group, terrace deposits and alluvium. *In M. Itihara* (ed.), *The Osaka Group*. Sougensha Inc., Osaka: 158–168.
- Itihara, M. 1993., Introduction geology and geomorphology, and a historical review of researches. *In M. Itihara* (ed.), *The Osaka Group.* Sougensha Inc., Osaka: 3–11.

- Itihara, M. and K. Inoue., 1993. The northern part of the Osaka Basin. In M. Itihara (ed.), The Osaka Group. Sougensha Inc., Osaka: 13–32.
- Kagemori, N., 1993. Chemical constituent of fossil wood. In M. Itihara (ed.), The Osaka Group. Sougensha Inc., Osaka: 283–289.
- Kälin, J. A., 1955. Crocodilia. In J. Piveteau (ed.), Traite de Palaeontologie, Vol. 5. Masson, Paris: 695-784.
- Kamei, T., 1971. Pleistocene crocodile from Kinki District, central Japan. In Editorial Committee by Tsukiji Shokan Publishing Co. Ltd. (ed.), Atlas of Japanese Fossils. Tsukiji Shokan Publishing Co. Ltd., Tokyo: no. 17, Q–20.
- Kamei, T. and E. Matsumoto., 1965. in Kobatake, N., M. Chiji, N. Ikebe, S. Ishida, T. Kamei, K. Nakaseko, and E. Matsumoto., 1965. Discovery of crocodile fossil from the Osaka Group. *Quaternary Research*, 4: 49–58.
- Kamei, T., Y. Kawamura, and H. Taruno., 1988. Mammalian stratigraphy of the Late Neogene and Quaternary in the Japanese Islands. *Memoir Geological Society of Japan* 30: 181–204.
- Katsura, Y. 2004., Paleopathology of *Toyotamaphimeia machikanensis* (Diapsida, Crocodylia) from the middle Pleistocene of central Japan. *Historical Biology*, **16**: 93–97.
- Kawamura, Y., 1991. Quaternary mammalian faunas in the Japanese Islands. *The Quaternary Research* (Daiyonki Kenkyu) **30**: 213–220.
- Kobatake, N. and T. Kamei., 1966. The first discovery of fossil crocodile from central Honshu, Japan. *Proceedings of Japan Academy*, **42**: 264–269.
- Kobatake, N., M. Chiji, N. Ikebe, S. Ishida, T. Kamei, K. Nakaseko, and E. Matsumoto., 1965. Discovery of crocodile fossil from the Osaka Group. *Quaternary Research*, **4**: 49–58.
- Momohara, A., 1993. Plant megafossils in Kinki District and adjacent areas. *In M. Itihara* (ed.), *The Osaka Group*. Sougensha Inc., Osaka: 256–270.
- Mook, C.C. 1921., Notes on the postcranial skeleton in the Crocodilia. *Bulletin of the American Museum of Natural History*, **44**: 67–100.
- Nishimura, S. and S. Sasajima., 1970. Age measurements of tuff layers of the Osaka Group and its equivalent deposits by fission track method. *Chikyukagaku*, **24**: 222–224.
- Norell, M. A., 1988. Cladistic approaches to paleobiology as applied to the phylogeny of alligatorids. Ph.D. dissertation, Yale University, New Heaven, Connecticut.
- Norell, M. A., 1989. The higher level relationships of the extant Crocodylia. Journal of Herpetology, 23: 325-335.
- Norell, M. A. and J. M. Clark., 1990. A reanalysis of *Bernissartia fagesii*, with comments on its phylogenetic position and its bearing on the origin and diagnosis of the Eusuchia. *Bulletin de l'Institut Royal des Sciences Naturelles de Belgique*, 60: 115–128.
- Parrish, M. J., 1987. The origin of crocodilian locomotion. *Paleobiology*, 13: 396-414.
- Poe, S., 1996. Data set incongruence and the phylogeny of crocodilians. Systematic Biology, 45: 393–414.
- Shikama, T., 1972. Fossil Crocodilia from Tsochin, southwestern Taiwan. Science Reports of the Yokohama National University, Section II, Biological and Geological Sciences, 19: 125–131.
- Suzuki, S., 1988. Fission track ages of tuff layers of Quaternary. Memoir Geological Society of Japan, 29: 37-58.
- Swofford, D. L. 2000. PAUP*. Phylogenetic analysis using parsimony (*and other methods). Version 4. Sinauer and Associates, Sunderland, Massachusetts.
- Taplin, L. E. and G. C. Grigg., 1989. Historical zoogeography of the eusuchian crocodilians: a physiological perspective. American Zoologist, 29: 885–901.
- Taruno, H. and T. Kamei., 1993. Mammalian fossils of the Pliocene and Plistocene in the Kinki District. *In M. Itihara* (ed.), *The Osaka Group*. Sougensha Inc., Osaka: 216–231.
- Taruno, H., 1999. A fossil crocodile from Nagareki Town, Kishiwada City. In Kishiwada City Board of Education (ed.), Excavation report on a fossil crocodile from Nagareki Town, Kishiwada City. Natural History Museum of Kishiwada City, Kishiwada, Osaka: 1–36.
- Willis, P. M. A., 1993. *Trilophosuchus rackhami* gen. et sp. nov., a new crocodilian from the early Miocene limestone of Riversleigh, northwestern Queensland. *Journal of Vertebrate Paleontology*, **13**: 90–98.
- Witmer, L. M., 1995. Homology of facial structures in extant archosaurs (birds and crocodilians), with special reference to paranasal pneumaticity and nasal conchae. *Journal of Morphology*, **225**: 269–327.
- Witmer, L. M., 1997. The evolution of the antorbital cavity of archosaurs: a study in soft-tissue reconstruction in the fossil record with an analysis of the function of pneumaticity. *Society of Vertebrate Paleontology Memoir*, 3: 1–73
- Yefimov, M. B., 1982. New fossil crocodiles from the USSR. Paleontological Journal, 2: 140-145.
- Yeh, H., 1958. A new crocodiles from Maoming Kwangtung. Vertebrata Palasiatica, 2: 237-242.
- Yoshikawa, S., 1993. Volcanic ash layers in the Kinki District. *In M. Itihara* (ed.), *The Osaka Group*. Sougensha Inc., Osaka: 190–200.

APPENDICES

Appendix 1

Character Descriptions, Used for the Phylogenetic Analyses in This Study. All descriptions are from Brochu (1999) and Brochu (2006).

- 1. Ventral tubercle of proatlas at least one half (0) or less than one half (1) the width of the dorsal crest.
- 2. Proatlas boomerang-shaped (0), strap-shaped (1), or massive and block-shaped (2).
- 3. Posterior half of axis neural spine wide (0) of narrow (1).
- 4. Axis neural arch lacks (0) or possesses (1) a lateral process ("diapophysis"). (Adapted from Norell, 1989, character 7.)
- 5. Atlas intercentrum wedge-shaped in lateral view, with insignificant parapophyseal processes (0), or plate-shaped in lateral view, with prominent parapophyseal processes at maturity (1). (Modified from Clark, 1994, character 89.)
- 6. Axial hypapophysis located toward the center of centrum (0) or toward the anterior end of centrum (1).
- 7. Hypapophyseal keels extend to eleventh vertebra behind atlas (0), twelfth vertebra behind atlas (1), or tenth vertebra behind atlas (2).
- 8. First postaxial cervical vertebra with prominent hypapophysis (0) or lacks prominent hypapophysis (1). (Adapted from Norell, 1989, character 12; Norell and Clark, 1990, character 11; Clark, 1994, character 91.)
- 9. Neural spine on first postaxial cervical wide, dorsal tip at least half the length of the centrum without the cotyle (0) or narrow, dorsal tip acute and less than half the length of the centrum without the cotyle (1).
- 10. Proatlas with prominent anterior process (0) or lacks anterior process (1).
- 11. Anterior half of axis neural spine oriented horizontally (0) or slopes anteriorly (1).
- 12. Axis neural spine crested (0) or not crested (1).
- 13. Anterior sacral capitulum projects far anteriorly of tuberculum and is broadly visible in dorsal view (0), or anterior margins of tuberculum and capitulum nearly in same plane, and capitulum largely obscured dorsally (1).
- 14. Dorsal margin of atlantal rib generally smooth with modest dorsal process (0) or with prominent process (1).
- 15. Atlantal ribs lack (0) or possess (1) large articular facets at anterior ends for each other.
- 16. Atlantal ribs without (0) or with (1) very thin medial laminae at anterior end.
- 17. Proatlas has tall dorsal keel (0) or lacks tall dorsal keel; dorsal side smooth (1).
- 18. Presacral centra amphicoelous (0) or procoelous (1). (Adapted from several previous

- analyses, e.g. Benton and Clark, 1988; Norell and Clark, 1990, characters 8 and 10; Clark, 1994, characters 92 and 93.)
- 19. Axial hypapophysis with (0) or without (1) deep fork.
- 20. Axial rib tuberculum wide, with broad dorsal tip (0) or narrow, with acute dorsal tip (1).
- 21. Axial rib tuberculum contacts diapophysis late in ontogeny, if at all (0) or early in ontogeny (1).
- 22. Scapular blade flares dorsally at maturity (0) or sides of scapular blade subparallel; minimal dorsal flare at maturity (1). (Adapted from Benton and Clark, 1988.)
- 23. Deltoid crest of scapula very thin at maturity, with sharp margin (0) or very wide at maturity, with broad margin (1).
- 24. Scapulocoracoid synchondrosis closes very late in ontogeny (0) relatively early in ontogeny (1).
- 25. Scapulocoracoid facet anterior to glenoid fossa uniformly narrow (0) or broad immediately anterior to glenoid fossa, and tapering anteriorly (1).
- 26. Proximal edge of deltopectoral crest emerges smoothly from proximal end of humerus and is not obviously concave (0) or emerges abruptly from proximal end of humerus and is obviously concave (1).
- 27. Olecranon process of ulna narrow and subangular (0) or wide and rounded (1).
- 28. Dorsal margin of iliac blade rounded with smooth border (0) or rounded, with modest dorsal indentation (1) or rounded, with strong dorsal indentation ("wasp-waisted;" 2) or narrow, with dorsal indentation (3) or rounded with smooth border; posterior tip of blade very deep (4).
- 29. *M. teres major* and *M. dorsalis scapulae* insert separately on humerus; scars can be distinguished dorsal to deltopectoral crest (0) or insert with common tendon; single insertion scar (1).
- 30. Interclavicle flat along length, without dorsoventral flexure (0) or with moderate dorsoventral flexure (1) or with severe dorsoventral flexure (2).
- 31. Anterior end of interclavicle flat (0) or rodlike (1).
- 32. Supraacetabular crest narrow (0) or broad (1).
- 33. Limb bones relatively robust, and hindlimb much longer than forelimb at maturity (0) or limb bones very long and slender, and forelimb and hindlimb more equal in length at maturity (1).
- 34. Iliac anterior process prominent (0) or virtually absent (1). (Adapted from Benton and Clark, 1988; Clark, 1994, character 84; although the transformation recorded here is different.)
- 35. Dorsal osteoderms not keeled (0) or keeled (1). (Adapted from Buscalioni et al., 1992, character 22.)
- 36. Dorsal midline osteoderms rectangular (0) or square or equant (1). (Adapted from Norell and Clark, 1990, character 16; Clark, 1994, character 95.)
- 37. Four (0), six (1), eight (2), or ten (3) contiguous dorsal osteoderms per row at maturity. (Adapted from Norell and Clark, 1990, character 12; Clark, 1994, character 97.)
- 38. Nuchal shield grades continuously into dorsal shield (0) or differentiated from dorsal shield; four nuchal osteoderms (1) or differentiated from dorsal shield; six nuchal osteoderms with four central and two lateral (2) or differentiated from dorsal shield; eight nuchal osteoderms

- in two parallel rows (3).
- 39. Ventral armor absent (0) or present; osteoderms single (1) or present; osteoderms consist of paired ossifications that suture together (2). (Adapted from Buscalioni et al., 1992, character 21.)
- 40. Anterior margin of dorsal midline osteoderms with anterior process (0) or smooth, without process (1). (Adapted from Norell and Clark, 1990, character 13; Clark, 1994, character 96.)
- 41. Splenial with anterior perforation for mandibular ramus of cranial nerve V (0) or lacks anterior perforation for mandibular ramus of cranial nerve V (1).
- 42. Mandibular ramus of cranial nerve V exits splenial anteriorly only (0) or splenial has singular perforation for mandibular ramus of cranial nerve V posteriorly (1) or splenial has double perforation for mandibular ramus of cranial nerve V posteriorly (2). (Characters 41 and 42 adapted from Norell, 1988, character 15 and 1989, character 8.)
- 43. Splenial participates in mandibular symphysis; splenial symphysis adjacent to no more than five dentary alveoli (0) or splenial excluded from mandibular symphysis; anterior tip of splenial passes ventral to Meckelian groove (1) or splenial excluded from mandibular symphysis; anterior tip of splenial passes dorsal to Meckelian groove (2) or deep splenial symphysis, longer than five dentary alveoli; splenial forms wide "V" within symphysis (3) or deep splenial symphysis, longer than five dentary alveoli; splenial constricted within symphysis and forms narrow "V" (4). (Adapted from Clark, 1994, character 77.)
- 44. Articular-surangular suture simple (0) or with anterior process dorsal to lingual foramen ("crocodyline process" of Aoki, 1992) (1) or with anterior process ventral to lingual foramen (2).
- 45. Lingual foramen for articular artery and alveolar nerve on surangular entirely (0) or on surangular-angular suture (1) or on angular entirely (2).
- 46. Coronoid bounds posterior half of foramen intermandibularis medius (0) or completely surrounds foramen intermandibularis medius at maturity (1) or obliterates foramen intermandibularis medius at maturity (2). (Adapted from Norell, 1988, character 12.)
- 47. Angular-surangular suture contacts external mandibular fenestra at posterior angle at maturity (0) or passes broadly along ventral margin of external mandibular fenestra late in ontogeny (1). (Adapted from Norell, 1988, character 40.)
- 48. Anterior processes of surangular unequal (0) or subequal to equal (1).
- 49. Foramen aerum at extreme lingual margin of retroarticular process (0) or set in from margin of retroarticular process (1). (Adapted from Norell, 1988, character 16.)
- 50. Retroarticular process projects posteriorly (0) or projects posterodorsally (1). (Adapted from Benton and Clark, 1988; Clark, 1994, character 71; Norell and Clark, 1990, character 7.)
- 51. Surangular extends to posterior end of retroarticular process (0) or pinched off anterior to tip of retroarticular process (1). (Adapted from Norell, 1988, character 42.)
- 52. Alveoli for dentary teeth 3 and 4 nearly same size and confluent (0) or fourth alveolus larger than third, and alveoli are separated (1).
- 53. Anterior dentary teeth strongly procumbent (0) or project anterodorsally (1).
- 54. Superior edge of coronoid slopes strongly anteriorly (0) or almost horizontal (1).
- 55. Inferior process of coronoid laps strongly over inner surface of Meckelian fossa (0) or

- remains largely on medial surface of mandible (1).
- 56. Coronoid imperforate (0) or with perforation posterior to foramen intermandibularis medius (1).
- 57. Dorsal projection of hyoid cornu flat (0) or rodlike (1).
- 58. Dorsal projection of hyoid cornu narrow, with parallel sides (0) or flared (1).
- 59. Process of splenial separates angular and coronoid (0) or no splenial process between angular and coronoid (1).
- 60. Sulcus between articular and surangular (0) or articular flush against surangular (1).
- 61. Surangular with spur bordering the dentary toothrow lingually for at least one alveolus length (0) or lacking such spur (1).
- 62. External mandibular fenestra absent (0) or present (1). (Clark, 1994, character 75.)
- 63. Dorsal anterior projection of coronoid longer than ventral (0) or ventral projection longer than dorsal (1).
- 64. External mandibular fenestra small; foramen intermandibularis caudalis not visible laterally (0) or external mandibular fenestra large; foramen intermandibularis caudalis visible laterally (1). (Adapted from Norell, 1988, character 14.)
- 65. Surangular-dentary suture intersects external mandibular fenestra anterior to posterodorsal corner (0) or at posterodorsal corner (1).
- 66. Angular extends dorsally toward or beyond anterior end of foramen intermandibularis caudalis; anterior tip acute (0) or does not extend dorsally beyond anterior end of foramen intermandibularis caudalis; anterior tip very blunt (1).
- 67. Surangular-angular suture lingually meets articular at ventral tip (0) or dorsal to ventral tip (1).
- 68. Dentary gently curved (0), deeply curved (1), or linear (2) between fourth and tenth alveoli.
- 69. Spina quadratojugalis prominent at maturity (0) or greatly reduced or absent at maturity (1). (Adapted from Norell, 1989, character 1.)
- 70. Postorbital bar massive (0) or slender (1). (Norell, 1989, character 3.)
- 71. Anterior border of the internal choana is comprised of the palatines (0) or choana entirely surrounded by pterygoids (1). (Benton and Clark, 1988; Clark, 1994, character 43; Norell and Clark, 1990, character 1.)
- 72. Choana projects posteroventrally (0) or anteroventrally (1) at maturity.
- 73. Pterygoid surface lateral and anterior to internal choana flush with choanal margin (0) or pushed inward to form "neck" (1).
- 74. Extensive exposure of prootic on external braincase wall (0) or prootic largely obscured by quadrate and laterosphenoid externally (1). (Adapted from Norell, 1989, character 5.)
- 75. Quadratojugal forms posterior angle of infratemporal fenestra (0) or jugal forms posterior angle of infratemporal fenestra (1) or quadratojugal-jugal suture lies at posterior angle of infratemporal fenestra (2) (Adapted from Norell, 1989, character 10.)
- 76. Postorbital neither contacts quadrate nor quadratojugal medially (0) or contacts quadratojugal, but not quadrate, medially (1) or contacts quadrate and quadratojugal at dorsal angle of infratemporal fenestra (2) or contacts quadratojugal with significant descending process (3).
- 77. Dentary tooth 4 occludes in notch between premaxilla and maxilla early in ontogeny (0) or occludes in a pit between premaxilla and maxilla; no notch early in ontogeny (1). (Norell,

- 1988, character 29.)
- 78. All dentary teeth occlude lingual to maxillary teeth (0) or occlusion pit between seventh and eighth maxillary teeth; all other dentary teeth occlude lingually (1) or dentary teeth occlude in line with maxillary toothrow (2). (Adapted from Norell, 1988, character 5; Willis, 1993, character 1.)
- 79. Naris projects anterodorsally (0) or dorsally (1).
- 80. Quadratojugal extends to superior angle of infratemporal fenestra (0) or does not extend to superior angle of infratemporal fenestra; quadrate participates in fenestra (1). (Adapted from Buscalioni et al., 1992, character 6.)
- 81. Frontoparietal suture deeply within supratemporal fenestra; frontal prevents broad contact between postorbital and parietal (0) or suture makes modest entry into supratemporal fenestra at maturity; postorbital and parietal in broad contact (1) or suture on skull table entirely (2).
- 82. Supraoccipital exposure on dorsal skull table small (0), absent (1), large (2), or large such that parietal is excluded from posterior edge of table (3). (Norell, 1988, character 11.)
- 83. Quadratojugal sends long anterior process along lower temporal bar (0) or sends modest process, or none at all, along lower temporal bar (1).
- 84. Dorsal and ventral rims of squamosal groove for external ear valve musculature parallel (0) or squamosal groove flares anteriorly (1).
- 85. Palatine-pterygoid suture nearly at (0) or far from (1) posterior angle of suborbital fenestra.
- 86. Frontoparietal suture concavoconvex (0) or linear (1).
- 87. Supratemporal fenestra with fossa; dermal bones of skull roof do not overhang rim at maturity (0) or dermal bones of skull roof overhang rim of supratemporal fenestra near maturity (1) or supratemporal fenestra closes during ontogeny (2). (Adapted from Norell, 1988, character 9.)
- 88. Suborbital fenestra without (0) or with (1) posterior notch.
- 89. Largest maxillary alveolus is #3 (0), #5 (1), #4 (2), #4 and #5 are same size (3), or maxillary teeth homodont (4). (Adapted from Norell, 1988, character 1.)
- 90. Lateral edges of palatines parallel posteriorly (0) or flare posterioly, producing "shelf" (1). (Adapted from Norell, 1988, character 2.)
- 91. Ectopterygoid abuts maxillary toothrow (0) or maxilla broadly separates ectopterygoid from maxillary toothrow (1). (Norell, 1988, character 19.)
- 92. Shallow fossa at anteromedical corner of supratemporal fenestra (0) or no such fossa; anteromedial corner of supratemporal fenestra smooth (1).
- 93. Lacrimal makes broad contact with nasal; no posterior process of maxilla (0) or maxilla sends posterior process within lacrimal (1) or maxilla sends posterior process between lacrimal and prefrontal (2).
- 94. Lateral edges of palatines smooth anteriorly (0) or with lateral process projecting from palatines into suborbital fenestrae (1).
- 95. External naris bisected by nasals (0) or nasals contact external naris, but do not bisect it (1) or nasals excluded, at least externally, from naris; nasals and premaxillae still in contact (2) or nasals and premaxillae not in contact (3). (Adapted from Norell, 1988, character 3; Clark, 1994, characters 13 and 14.)
- 96. Palpebral forms from single ossification (0) or from multiple ossifications (1). (Adapted

- from Norell, 1988, characer 8; Clark, 1994, character 65.)
- 97. Premaxilla has five teeth (0) or four teeth (1) early in posthatching ontogeny. (Norell, 1988, character 17.)
- 98. Posterior pterygoid processes tall and prominent (0) or small and project posteroventrally (1) or small and project posteriorly (2).
- 99. Prefrontal pillar solid (0) or with large pneumatic sinus (prefrontal recess of Witmer, 1997) (1).
- 100. Prefrontals separated by frontals and nasals (0) or prefrontals meet medially (1). (Norell, 1988, character 27.)
- 101. Dorsal surface of rostrum curves smoothly (0) or bears medial dorsal boss (1).
- 102. Posterior margin of otic aperture smooth (0) or invaginate (1).
- 103. Margin of orbit flush with skull surface (0) or dorsal edges of orbit upturned (1) or orbital margin telescoped (2).
- 104. Medial parietal wall of supratemporal fenestra imperforate (0) or bearing foramina (1). (Norell, 1988, character 51.)
- 105. Lateral edge of suborbital fenestra straight (0) or bowed medially (1).
- 106. Surangular continues to dorsal tip of lateral wall of glenoid fossa (0) or truncated and not continuing dorsally (1).
- 107. Posterior rim of internal choana not deeply notched (0) or deeply notched (1).
- 108. Anterior face of palatine process rounded or pointed anteriorly (0) or invaginate (1).
- 109. Anterior ectopterygoid process tapers to a point (0) or forked (1).
- 110. Palatine process extends (0) or does not extend (1) significantly beyond anterior end of suborbital fenestra. (Adapted from Willis, 1993, character 2.)
- 111. Maxillary foramen for palatine ramus of CN-V small or not present (0) or very large (1).
- 112. Quadrate with small, ventrally-reflected medial hemicondyle (0) or with small medial hemicondyle; dorsal notch for foramen aerum (1) or with prominent dorsal projection between hemicondyles (2) or with expanded medial hemicondyle (3).
- 113. Basisphenoid thin (0) or anteroposteriorly wide (1) vental to basioccipital.
- 114. Spina quadratojugalis low, near posterior angle of infratemporal fenestra (0) or high, between posterior and superior angles of infratemporal fenestra (1).
- 115. Laterosphenoid bridge comprised entirely of laterosphenoid (0) or with ascending process or palatine (1).
- 116. Ectopterygoid-pterygoid flexure disappears during ontogeny (0) or remains throughout ontogeny (1).
- 117. Lacrimal longer than prefrontal (0), prefrontal longer than lacrimal (1), or lacrimal and prefrontal both elongate and nearly the same length (2). (Modified from Norell, 1988, character 7.)
- 118. Palatine process generally broad anteriorly (0) or in form of thin wedge (1).
- 119. Basisphenoid not broadly exposed ventral to basioccipital at maturity; pterygoid short ventral to median eustachian opening (0) or basisphenoid exposed as broad sheet ventral to basioccipital at maturity; pterygoid tall ventral to median eustachian opening (1).
- 120. Medial jugal foramen small (0) or very large (1).
- 121. Quadrate foramen aerum on mediodorsal angle (0) or on dorsal surface (1) of quadrate.
- 122. Sulcus on anterior braincase wall lateral to basisphenoid rostrum (0) or braincase wall

- lateral to basisphenoid rostrum smooth; no sulcus (1).
- 123. Skull table surface slopes ventrally from sagittal axis (0) or planar (1) at maturity.
- 124. Incisive foramen small, less than half the greatest width of premaxillae (0) or large, more than half the greatest width of premaxillae (1) or large, and intersects premaxillary-maxillary suture (2).
- 125. Vomer entirely obscured by premaxilla and maxilla (0) or exposed on palate at premaxillary-maxillary suture (1). (Adapted from Norell, 1988, character 22.)
- 126. Vomer entirely obscured by maxillae and palatines (0) or exposed on palate between palatines (1).
- 127. Significant ventral quadrate process on lateral braincase wall (0) or quadrate-pterygoid suture linear from basisphenoid exposure to foramen ovale (1).
- 128. Lateral carotid foramen opens lateral (0) or dorsal (1) to basisphenoid lateral exposure at maturity.
- 129. Basisphenoid not exposed extensively (0) or exposed extensively (1) on braincase wall anterior to foramen ovale. (Adapted from Norell, 1989, character 5.)
- 130. Capitate process of laterosphenoid oriented laterally (0) or anteroposteriorly (1) toward midline.
- 131. Pariental and squamosal widely separated by quadrate on posterior wall of supratemporal fenestra (0) or pariental and squamosal approach each other on posterior wall of supratemporal fenestra without actually making contact (1) or pariental and squamosal meet along posterior wall of supratemporal fenestra (2).
- 132. Squamosal-quadrate suture extends dorsally along posterior margin of external auditory meatus (0) or extends only to posteroventral corner of external auditory meatus (1).
- 133. Ectopterygoid extends along medial face of postorbital bar (0) or stops abruptly ventral to postorbital bar (1).
- 134. Two prominent projections (0) or single projection, generally not prominent, on postorbital bar (1). (Adapted from Norell, 1989, character 2.)
- 135. Maxillary toothrow curved medially or linear (0) or curves laterally broadly (1) posterior to first six maxillary alveoli. (Adapted from Clark, 1994, character 79.)
- 136. Medial process of prefrontal pillar expanded dorsoventrally (0) or anteroposteriorly (1).
- 137. Dorsal half of prefrontal pillar narrow (0) or expanded anteroposteriorly in dorsal half (1). (Adapted from Norell, 1988, character 41.)
- 138. Medial process of prefrontal pillar wide (0) or constricted (1) at base.
- 139. Ventral margin of orbit gently circular (0) or with prominent notch (1).
- 140. Mature skull table with broad curvature; short squamosal prongs (0) or with nearly horizontal sides; significant squamosal prongs (1).
- 141. Exoccipital with very prominent boss on paroccipital process; process lateral to cranioquadrate opening short (0) or exoccipital with small or no boss on paroccipital process; process lateral to cranioquadrate opening long (1).
- 142. Premaxillary surface lateral to naris smooth (0) or with deep notch lateral to naris (1).
- 143. Canthi rostralii absent or very modest (0) or very prominent (1) at maturity. (Norell, 1988, character 34.)
- 144. Preorbital ridges absent or very modest (0) or very prominent (1) at maturity.
- 145. Dorsal premaxillary processes short, not extending beyond third maxillary alveolus (0) or

- long, extending beyond third maxillary alveolus (1).
- 146. Ventral margin of postorbital bar flush with lateral jugal surface (0) or inset from lateral jugal surface (1). (Adapted from Benton and Clark, 1988; Norell and Clark, 1990, character 3.)
- 147. Lateral eustachian canals open dorsal (0) or lateral (1) to medial eustachian canal. (Adapted from Norell, 1988, character 46.)
- 148. Surface of maxilla within narial canal imperforate (0) or with multiple cecal recesses (1). (See Witmer, 1995.)
- 149. Ectopterygoid extends (0) or does not extend (1) to posterior tip of lateral pterygoid flange at maturity. (Adapted from Norell, 1988, character 32.)
- 150. Squamosal does not extend (0) or extends (1) ventrolaterally to lateral extent of exoccipital and quadrate.
- 151. Otoccipitals terminate dorsal to basioccipital tubera (0) or send robust process ventrally and participate in basioccipital tubera (1) or send slender process ventrally to basioccipital tubera (2). (Adapted from Norell, 1988, character 20; Clark, 1994, character 57 and 60.)
- 152. Internal choana not septate (0) or with septum that remains recessed within choana (1) or with septum that projects out of choana (2).
- 153. Incisive foramen completely situated far from premaxillary toothrow, at the level of the second or third alveolus (0) or abuts premaxillary toothrow (1) or projects between first premaxillary teeth (2).
- 154. Parietal with sinus communicating with pneumatic system (0) or solid, without sinus (1).
- 155. Ventral scales have (0) or lack (1) follicle gland pores. (Poe, 1996.)
- 156. Ventral collar scales not enlarged relative to other ventral scales (0) or in a single enlarged row (1) or in two parallel enlarged rows (2). (Poe, 1996.)
- 157. Median pelvic keel scales form two parallel rows along most of tail length (0) or form single row along tail (1) or merge with lateral keel scales to form Y-shaped keel (2). (Poe, 1996.)
- 158. Lingual osmoregulatory pores small (0) or large (1). (See Taplin and Grigg, 1989.)
- 159. Tongue with (0) or without (1) keratinized surface. (See Taplin and Grigg, 1989.)
- 160. *M. caudofemoralis* with single head (0) or with double head (*longus* and *brevis*; 1). (See Frey et al., 1989.)
- 161. Naris circular or keyhole-shaped (0) or wider than long (1).
- 162. Surangular-articular suture oriented anteroposteriorly (0) or bowed strongly laterally (1) within glenoid fossa.
- 163. Postorbital-squamosal suture oriented ventrally (0) or passes medially (1) ventral to skull table.
- 164. Anterior foramen for palatine ramus of cranial nerve VII ventrolateral (0) or ventral (1) to basisphenoid rostrum.
- 165. Quadrate foramen aereum small or absent (0) or comparatively large (1). (Brochu, 2006)

Appendix 2

Data Matrix Used for the Phylogenetic Analysis in This Study. Characters are described in Appendix 1.

Bernissartia fagesii

??11? 1210? 010?0 ???0? ?0?0? 0000? ?0001 00010 0000? ???00 100?? ????1 10??? 0?000 0???0 ?0000 0??0? 10030 1??0? ?00?0 ?0001 00?00 ?00?? 0?0?? 0??0? ????? ????0 ???00 00000 00?0? 01??? ????0 0??0?

Hylaeochampsa vectiana

Eothoracosaurus mississippiensis

????? ????? ????? ????? ??000 ????? ?00?0 0???0 ??30? ??001 1?1?? ????0 ????? ??2?0 100?0 1021? 00?11 00040 01?02 ?00?0 00000 00000 000?? ?0100 0?0?0 ????? ?0?00 ???01 10001 00??? 0???? ????0 0??00

Thoracosaurus macrorhynchus

??11? 1?1?? 0???1 ???1? ????? 0??0? ???00 0???0 ??300 ??001 11??? ????0 ?1000 00200 100?0 10210 00011 10040 01002 ??000 00100 00000 0000? 1010? 00000 0?0?0 ?0000 ?0?01 10001 00?10 00??? ????0 00?00

Eosuchus minor

???1? 1???? 0???1 ???1? ?00?0 ?100? ?0000 00??0 ?0300 00001 1110? 0??00 ?1?00 ?02?0 100?0 10210 10011 00040 01002 ?0000 0?100 00000 031?? ?0100 00000 0??01 0000? 0?001 10001 00?1? 10??? ????0 00?10

Eosuchus lerichei

???0? 1???? ????1 ????? ????? ?1??? ????0 ????? ??3?? ????? ?11?? ????? ????? ??200 100?0 ?021? 2?011 00040 01002 ?00?0 0?100 ?0000 03?0? 00100 0?000 0???? 000?0 ?0?01 10001 0??10 10??? ????0 ?0?10

Eogavialis africanus

????? 1???? ??0?? ???11 ????? ????? ???0? ????0 ?030? ?10?1 111?? ????1 ?1?00 00200 10000 10210 11011 00040 01002 ?0000 00200 00000 00100 00100 000?0 0?0?0 0000? 00011 10001 00?10 100?? ????0 00?00

Gryposuchus colombianus

??1?0 ????? 00??1 ????? ??000 ????? ????? ????0 ?0300 00001 11110 0???0 01000 00200 10010 10210 10011 10040 01102 ?0200 00200 00000 ?0100 00100 00000 00000 00000 ????12 10001 00?10 10??? ????0 00?00

Ikanogavialis gameroi

Gavialis lewisi

????? ????? ??0?? ????? ????? ????? ????? ??30? ??0?1 ????? ????? ?1?00 00200 100?0 1?2?0 ?001? ?00?0 0??03 ??20? 00200 0?000 ?010? ???00 000?? 000?? 0000? ???11 1????

00?10 10??? ????0 00?00

Gavialis gangeticus

 $02110\ 10110\ 00001\ 00010\ 00000\ 01001\ 0000?\ 00000\ 00300\ 00001\ 11100\ 00100\ 01000\ 00200$ $10000\ 10210\ 10011\ 10040\ 01103\ 00200\ 00200\ 00000\ 00100\ 00100\ 00000\ 00000\ 00000\ 00000$ $00010\ 10000\ 00000\ 00000\ 00000$

Borealosuchus sternbergii

 $00000\ 1?100\ 11001\ 00110\ 00000\ 00010\ 00100\ 0???0\ 00000\ 00001\ 00100\ 000?0\ 01000\ 00001$ $10100\ 00001\ 00130\ 01012\ ?0000\ 00000\ 00000\ 0000?\ 00011\ 00100\ 00001\ 00011\ ?1?01$ $10000\ 10010\ 010??\ ????0\ 00?00$

Borealosuchus formidabilis

00000 10100 11001 ??0?0 00000 00010 00100 00?20 00000 00?01 0010? 00100 11000 00001 100?0 ?0200 00001 10030 01002 00000 00000 00000 0000? 02110 0?100 000?? 000?1 01001 10000 10?10 01??? ????0 00?00

Borealosuchus wilsoni

????? ??10? ??0?1 ????? ?0000 0001? ??100 00?20 ??102 00001 0010? 0???0 11?00 00001 10000 10200 100?1 10030 01002 ?0000 00000 00?00 ?0000 0211? ?01?? ??0?? 00001 ?1?01 1???? 1??10 01??? ????0 00?00

Borealosuchus acutidentatus

Pristichampsus vorax

??000 101?? 01??1 ???0? ?0000 0111? ?0001 0???1 00001 ?0??1 ?11?? ????? ?1?00 000?1 100?0 10000 20001 00030 01001 ?0000 00100 00000 020?0 00010 0?100 0?1?1 01010 ???01 10000 10?10 01??? ????0 10?00

Leidyosuchus canadensis

Diplocynodon darwini

10000 0?000 01011 00001 ?000? 1141? ?0011 01121 00101 00111 101?? 000?1 ?1?00 00011 1?0?0 11000 00001 10131 ?1002 ?0000 01000 00000 ?101? 00010 1?100 0?0?? 11?10 ???01 10000 10?10 01??? ????0 00?00

Brachychampsa montana

 $10001\ \ ??001\ \ 11?11\ \ 000?1\ \ 0?000\ \ 11010\ \ 000?1\ \ 03111\ \ 10100\ \ ?0111\ \ 111??\ \ ?00?1\ \ 11?00\ \ ?0011\ \ 11010\ \ 21010\ \ 12000\ \ 00111\ \ 11201\ \ ?0000\ \ 01000\ \ 00100\ \ 01010\ \ 00010\ \ 10120\ \ 00001\ \ 11110\ \ ?1?01\ \ 10001\ \ 10?10\ \ 01???\ \ ????0\ \ 00?01$

Stangerochampsa mccabei

??00? 1?00? 01011 ???1? ?0000 11010 00010 1??11 01000 001?1 111?? ????? 11?01 10011 11010 21010 10000 00121 11201 ?00?0 01000 00000 0101? 00010 1?120 0?0?1 2?110 ???01 10001 10?10 01??? ????0 00?01

Alligator mississippiensis

 $10001\ 10001\ 01011\ 00101\ 11101\ 11110\ 00011\ 12101\ 11201\ 00111\ 11110\ 00011\ 11010\ 00011$ $11010\ 21010\ 21010\ 21010\ 10121\ 11100\ 00010\ 01100\ 10000\ 01011\ 01010\ 10100\ 00001\ 21110\ 11001$

11000 10010 01011 00110 01102

Caiman yacare

10001 10001 10011 01101 11011 11110 00011 11221 11220 11111 01101 00111 01000 11011 11010 21111 23000 01121 11101 00001 01111 01000 01010 10010 10100 00001 21110 11001 10000 10010 22011 10110 01101

Asiatosuchus germanicus

00100 1?011 00??1 ??101 ?000? 11?1? ??01? ????1 000?? ?0001 011?? ?00?? 11?00 000?1 100?0 10000 1000? 10?10 010?1 ?0000 01000 00001 130?? 000?? 0?100 ??1?? 00?10 ???01 10000 10?10 01??? ????0 00?00

Crocodylus affinis

00000 10001 10111 00101 00000 11110 00011 0???1 10100 00001 01110 00001 11000 00001 100?0 1011? 20001 00110 01001 ?0000 01000 00001 130?0 00000 01100 0?1?? 00010 ???01 10000 10?10 011?? ????0 10?00

Belgian crocodyloid

??000 0100? 111?1 00?1? ?0000 1111? ?0011 0???1 10100 ?0001 011?? ????1 11?00 00001 10000 20110 20001 00?10 01?01 ?0000 01000 00001 13010 00001 01100 01111 00010 ?1?01 10001 10?10 01??? ????0 10?00

Brachyuranochampsa eversolei

Crocodylus acer

Crocodylus megarhinus

????? ???0? ????1 ????? ????? ????? ????? 101?? ?0001 011?? ????1 11?00 00001 10002 ?0211 2?101 ?0130 01201 ?0100 01100 00000 ?3000 00001 01100 0?11? 00010 ???01 10000 10?10 01??? ????0 10?00

Australosuchus clarkae

????? 170?? ????1 ????? ????? 1??1? ??0?1 0???1 10111 ?0001 011?? ????1 11?00 00001 ????2 00211 2010? 00?1? 01001 ?0?00 01100 0?000 0100? 00001 01100 0?111 01010 ?1?01 10001 10010 011?? ????0 10?0?

Kembara implexidens

????? ????? ????? ????? ????? 1?11? ?0011 0???1 10111 ?0001 011?? ????1 11?00 00001 10112 00211 20101 00010 01001 ?0100 01100 00000 01000 00001 01100 01111 00010 ?1101 10001 10010 011?? ????0 10?00

Crocodylus cataphractus

 $10000\ 1000?\ 00111\ 00?01\ 01001\ 11212\ 00011\ 11101\ 10111\ 01001\ 01110\ 0100?\ 01000\ 00001\ 10011\ 00211\ 20101\ 00110\ 01002\ 00100\ 01100\ 10010\ 03000\ 00101\ 01100\ 01111\ 00010\ 11101\ 10100$

Crocodylus porosus

 $11100\ 11011\ 00101\ 00101\ 01000\ 11212\ 00011\ 11201\ 10111\ 01001\ 01110\ 01001\ 11000\ 00001$ $10011\ 00211\ 20101\ 00110\ 01001\ 00100\ 01100\ 10010\ 03000\ 00001\ 01100\ 01111\ 00010\ 11101$

10010 11110 01101 01010 10100

Crocodylus palaeindicus

????? ????? ??1?1 ????? ????? ????? ????? 1011? 01001 ?111? 0??01 11000 00001 10011 00211 21100 00110 01001 ?0100 01100 1?010 0300? 00001 00100 01111 00010 11101 10000 11?10 01??? ????0 10?00

Crocodylus niloticus

 $10100\ 10011\ 10101\ 00101\ 01001\ 11212\ 00011\ 11201\ 10111\ 01001\ 01110\ 01001\ 11100\ 00001$ $10011\ 00211\ 20101\ 00110\ 01101\ 00100\ 01100\ 10010\ 03000\ 00001\ 01100\ 01111\ 00010\ 11101$ $10000\ 11110\ 01101\ 01010\ 10100$

Crocodylus rhombifer

00100 10011 10101 00101 01001 11112 00011 11201 10111 01001 01110 01001 11000 00001 10011 00211 20101 00110 01101 00100 11100 10010 03000 00001 01100 01111 00010 11101 10000 11110 01101 01010 10100

Rimasuchus lloydi

Euthecodon arambourgii

Osteolaemus tetraspis

??100 11001 00101 0?101 01001 11112 01011 11111 10111 01001 01110 01001 11000 00001 10111 00210 20101 11110 01010 11100 01101 00001 03000 00011 01100 01111 00010 11101 10010 10011 01101 01010 11100

Voay robustus

????? ????? ??1?1 ???0? ????? ?111? ?101? ????1 10111 00011 01110 0??01 11000 00001 10111 00211 21101 01110 01011 ?0100 01100 10001 03000 00001 0?100 01111 00010 11101 10010 1001? 01??? ????0 11100

Kentisuchus spenceri

Dollosuchus dixoni

0010? 1?001 11??1 ??00? ???00 11?1? ?001? ????? ??4?? ?0001 011?? ????? 01?00 0?0?0 100?? ?021? 20?11 00010 01102 ??0?0 0?100 001?0 03??? 0010? 01100 0???? ???10 ???01 10001 10?10 01??? ????0 10?0?

Gavialosuchus americanus

02100 1?000 00101 0000? ?0101 1?11? ??01? 0???1 ??412 ????1 01110 00??? ?1000 002?1 10000 1021? 21?11 00?10 0?102 ?0100 01100 00000 030?0 001?1 ??100 0?1?? 0001? ???01 10001 10?10 011?? ????0 10?00

Tomistoma cairense

1???0 01??? ????0 10?00

Paratomistoma courtii

7???? 7???? 7???? 7???? 7???? 7???? 7???? 7???? 7??00 0?01 0???? 7???0 71?00 70??1 7??0? 1?2?? 20?1? 00??? ?10?? ???00 0?10? 0???? ??0?0 ?0??? ??0?? ?1010 0???? ?1??1 1??0? ?0??0 0???? ????? 10?0?

Gavialosuchus eggenbergensis

Tomistoma lusitanica

Tomistoma schlegelii

 $02100\ 10011\ 00101\ 00101\ 00001\ 11111\ 00011\ 01301\ 10400\ 01001\ 01100\ 00000\ 01000\ 00201$ $10000\ 10210\ 20101\ 10010\ 01102\ 00100\ 01100\ 00001\ 03000\ 00001\ 01100\ 11111\ 00010\ 11101$ $10001\ 10010\ 01101\ 01010\ 10100$

Toyotamaphimeia machikanensis

00110 00011 11?1? 0010? ?0101 11111 00000 00??1 00400 ?10?1 0???? ?00?1 01?00 ?02?0 100?0 ?001? 2?1?1 100?0 11002 ?01?0 00100 00000 0300? ?000? ??100 ????? ??010 ???01 10001 11?10 ?01?? ????? ?0??0

National Science Museum Monographs

The National Science Museum has been publishing technical papers in the following series:

Bulletin of the National Science Museum

Series A: Zoology (Quarterly) Series B: Botany (Quarterly)

Series C: Geology & Paleontology (Annually)

Series D: Anthropology (Annually)

Series E: Physical Sciences & Engineering (Annually)

Memoirs of the National Science Museum (Annually)

In addition to the above, dozens monographic works have been published since 1984. They are originally published as independent publications, but the National Science Museum Editorial Board has decided to continue to publish such works on an irregular publication series, namely National Science Museum Monographs. Their titles and their corresponding numbers of the series are as follows:

- No. 1. Early Cretaceous marine and brackish-water Gastropoda from Japan. By Tomoki Kase, 199 pp., 31 pls., 1984.
- No. 2. A taxonomic study on the subfamily Herminiinae of Japan (Lepidoptera, Noctuidae). By Mamoru Owada, 208 pp., 1987.
- No. 3. Small mammal fossils and correlation of continental deposits, Safford and Duncan Basins, Arizona, USA. By Yukimitsu Tomida, 141 pp., 1987.
- No. 4. Late Miocene floras in northeast Honshu, Japan. By Kazuhiko Uemura, 174 pp., 11 pls., 1988.
- No. 5. A revisional study of the spider family Thomisidae (Arachnida, Araneae) of Japan. By Hirotsugu Ono, 252 pp., 1988.
- No. 6. The taxonomic study of Japanese dictyostelid cellular slime molds. By Hiromitsu Hagiwara, 131 pp., 1989.
- No. 7. A systematic study of the Japanese Chiroptera. By Mizuko Yoshiyuki, 242 pp., 1989.
- No. 8. Rodent and lagomorph families of Asian origins and diversification: Proceedings of Workshop WC-2 29th International Geological Congress, Kyoto, Japan. Edited by Yukimitsu Tomida, Chuankuei Li, and Takeshi Setoguchi, 195 pp., 1994.
- No. 9. A microevolutional history of the Japanese people as viewed from dental morphology. By Hirofumi Matsumura, 130 pp., 1995.
- No. 10. Studies on the human skeletal remains from Jiangnan, China. Edited by Bin Yamaguchi and Huan Xianghon, 108 pp., 3 pls., 1995.
- No. 11. Annotated checklist of the inshore fishes of the Ogasawara Islands. By John E. Randall, Hitoshi Ida, Kenji Kato, Richard L. Pyle, and John L. Earle, 74 pp., 19 pls., 1997.
- No. 12. Deep-sea fauna and pollutants in Suruga Bay. By Tsunemi Kubodera and Masaaki Machida, *et al.*, 336 pp., 12 pls., 1997.

- No. 13. Polychaetous annelids from Sagami Bay and Sagami Sea collected by the Emperor Showa of Japan and deposited at the Showa Memorial Institute, National Science Museum, Tokyo. Families Polynoidae and Acoetidae. By Minoru Imajima, 131 pp., 1997.
- No. 14. Advances in vertebrate paleontology and geochronology. Edited by Yukimitsu Tomida, Lawrence J. Flynn, and Louis L. Jacobs, 292 pp., 1998.
- No. 15. Proceedings of the second Gondwanan dinosaur symposium. Edited by Yukimitsu Tomida, Thomas H. Rich, and Patricia Vickers-Rich, 296 pp., 1999.
- No. 16. Onuphidae (Annelida, Polychaeta) from Japan, excluding the genus <u>Onuphis</u>. By Minoru Imajima, 115 pp., 1999.
- No. 17. Description of a new species of Anhangueridae (Pterodactyloidea) with comments on the pterosaur fauna from the Santana Formation (Aptian-Albian), northeastern Brazil.By Alexander W. A. Kellner and Yukimitsu Tomida, 135 pp., 2000.
- No. 18. Proceedings of the First and Second Symposia on Collection Building and Natural History Studies in Asia. Edited by Keiichi Matsuura, 188 pp., 2000.
- No. 19. A taxonomic revision of the marine species of <u>Cladophora</u> (Chlorophyta) along the coasts of Japan and the Russian Far-east. By Christiaan van den Hoek and Mitsuo Chihara, 242 pp., 2000.
- No. 20. Deep-sea fauna and pollutants in Tosa Bay. Edited by Toshihiko Fujita, Hiroshi Saito and Masatsune Takeda, 380 pp., 2001.
- No. 21. Marine fauna of the shallow waters around Hainan Island, South China Sea. Edited by Keiichi Matsuura, 126 pp., 2001.
- No. 22. Proceedings of the Third and Fourth Symposia on Collection Building and Natural History Studies in Asia and the Pacific Rim. Edited by Tsunemi Kubodera, Masanobu Higuchi, and Ritsuro Miyawaki, 193 pp., 2002.
- No. 23. Polychaetous annelids from Sagami Bay and Sagami Sea collected by the Emperor Showa of Japan and deposited at the Show Memorial Institute, National Science Museum, Tokyo (II). Orders included within the Phyllodocida, Amphinomida, Spintherida and Eunicida. By Minoru Imajima, 221 pp., 2003.
- No. 24. Proceedings of the Fifth and Sixth Symposia on Collection Building and Natural History Studies in Asia and the Pacific Rim. Edited by Shinobu Akiyama, Ritsuro Miyawaki, Tsunemi Kubodera and Masanobu Higuchi, 292 pp., 2004.
- No. 25. Revision of scydmaenid beetles of the genus <u>Syndicus</u> Motschulsky (Coleoptera, Scydmaenidae). By Pawel Jaloszynski, 108 pp., 2004.
- No. 26. A new specimen of <u>Apatosaurus ajax</u> (Sauropoda: Diplodocidae) from the Morrison Formation (Upper Jurassic) of Wyoming, USA. By Paul Upchurch, Yukimitsu Tomida, and Paul M. Barrett, 108 pp., 10 pls., 2004.
- No. 27. Leaf-rolling sawflies of the <u>Pamphilius vafer</u> complex (Hymenoptera, Pamphiliidae). By Akihiko Shinohara, 116 pp., 2005.
- No. 28. Types of Japanese bird. By Hiroyuki Morioka, Edward C. Dickinson, Takashi Hiraoka, Desmond Allen and Takashi Yamasaki, 154 pp., 2005.
- No. 29. Deep-sea fauna and pollutants in Nansei Islands. Edited by Kazunori Hasegawa, Gento Shinohara and Masatsune Takeda, 476 pp., 2005.
- No. 30. Phenology and growth habits of tropical trees: long-term observations in the Bogor

- and Cibodas Botanic Garden, Indonesia. Edited by Hiroaki Hatta and Dedy Darnaedi, 436 pp., 2005.
- No. 31. The Cretaceous System in the Kakarov area, southern Sakhalin, Russian Far East. Edited by Yasunari Shigeta and Haruyoshi Maeda, 136 pp., 2005.
- No. 32. Checklist of Japanese lichens and allied fungi. By Syo Kurokawa and Hiroyuki Kashiwadani, 257 pp., 2006.
- No. 33. Revision of the Palearctic Species of the Myrmecophilous Genus Pella (Coleoptera, Staphylinidae, Aleocharinae). By Munetoshi Maruyama, xxx pp., 2006.
- No. 34. Proceedings of the Seventh and Eighth Symposia on Collection Building and Natural History Studies in Asia and the Pacific Rim. Edited by Yukimitsu Tomida, Tsunemi Kubodera Shinobu Akiyama, and Taiju Kitayama, 294 pp., 2006.

All inquiries concerning the Monographs should be addressed to: Library National Science Museum (Natural History Institute) 3-23-1 Hyakunincho Shinjuku-ku, Tokyo 169-0073 Japan